

Topological Framework for Digital Image Analysis with Extended Interior and Closure Operators

by

Homa Fashandi

**A thesis submitted to the Faculty of Graduate Studies of
The University of Manitoba
in partial fulfilment of the requirements for the degree of**

DOCTOR OF PHILOSOPHY

Department of Electrical and Computer Engineering
University of Manitoba
Winnipeg

Copyright © 2012 by Homa Fashandi

Topological Framework for Digital Image Analysis with Extended Interior and Closure Operators

by

Homa Fashandi

**A thesis submitted to the Faculty of Graduate Studies of
The University of Manitoba
in partial fulfilment of the requirements for the degree of**

DOCTOR OF PHILOSOPHY

Department of Electrical and Computer Engineering
University of Manitoba
Winnipeg

Copyright © 2012 by Homa Fashandi

Permission has been granted to the Library of the University of Manitoba to lend or sell copies of this dissertation to the National Library of Canada to microfilm this dissertation and to lend or sell copies of the film, and University Microfilms to publish an abstract of this dissertation.

The author reserves other publication rights, and neither the dissertation nor extensive abstracts from it may be printed or otherwise reproduced without the author's permission.

Abstract

The focus of this research is the extension of topological operators with the addition of a inclusion measure. This extension is carried out in both crisp and fuzzy topological spaces. The mathematical properties of the new operators are discussed and compared with traditional operators. Ignoring small errors due to imperfections and noise in digital images is the main motivation in introducing the proposed operators. To show the effectiveness of the new operators, we demonstrate their utility in image database classification and shape classification. Each image (shape) category is modeled with a topological space and the interior of the query image is obtained with respect to different topologies. This novel way of looking at the image categories and classifying a query image shows some promising results. Moreover, the proposed interior and closure operators with inclusion degree is utilized in mathematical morphology area. The morphological operators with inclusion degree outperform traditional morphology in noise removal and edge detection in a noisy environment.

Keywords: Crisp topology, fuzzy topology, subethood measure, inclusion degree, interior and closure operators with inclusion degree, image database classification, shape classification, mathematical morphology.

Contributions

- Extended version of interior and closure operator are defined for both crisp and fuzzy topologies in chapter 3 section 3.2. The definition incorporates a relaxed version of subethood which is more applicable for digital space.
- Mathematical properties of newly defined topological operators are examined and compared with original operators (chapter 3-propositions 3, 4, 5 and 6).
- Building a fuzzy topology from a collection of fuzzy sets is proposed and proved in chapter 3-propositions 7 and 8.
- Three areas are considered to apply new operators and demonstrate their strength, namely, mathematical morphology, shape classification and image database classification.
- A topological framework to classify large image databases is introduced (chapter 4-section 4.1.4).
- Each image category is modeled with a subspace topology demonstrating the practical approach in a topological setting.
- An interior operator with inclusion degree is applied to a query image with respect to different subspace topologies (chapter 4-section 4.4).
- The same method used for image database classification is also used to solve the shape database classification problem (chapter 4-section 4.3).
- Morphological operators have been defined using the new topological operators. The properties have been discussed from topological point of view (chapter5-section 5.2). It should be mentioned that, there is a previous work that incorporated inclusion degree in the definition of morphological operators [108]. However, the work did not consider the topology underlying the morphological operators. This dissertation provides a mathematical foundation for such operators.
- Also, I proposed open-close-close-open sequence with inclusion degree for noise removal from binary images which outperformed traditional morphological filters and median filter in higher noise contamination (chapter 5-section 5.3).
- The morphological operators with inclusion degree showed a better performance in edge detection in noisy images in comparison to traditional morphological edge detectors in noisy environment (chapter 5-section 5.3).

Acknowledgments

It is a pleasure to thank those who made this thesis possible. I would like to take this opportunity to express my gratitude for their kindness and support.

I owe my deepest gratitude to my advisor, Dr. James F. Peters, who has supported me throughout my thesis with his encouragements, patience and knowledge. Without him, this thesis would not have been completed. I could not wish for a better supervisor.

I would like to show my gratitude to my advisory committee, Dr. Mirosław Pawlak, Dr. Pradeepa Yahampath, Dr. Stephen Pistorius and Dr. Lakhmi C. Jain who reviewed this manuscript and helped me throughout my studies with their suggestions and helpful discussions.

I would also like to thank Dr. Sheela Ramanna for collaborating on a coauthored paper.

I am grateful to the financial support of Natural Sciences and Engineering Research Council of Canada (NSERC), Canadian Arthritis Network and University of Manitoba International Graduate Students Scholarships.

I am indebted to the wonderful members of CILAB throughout these years, Christopher Henry, Amir H. Meghdadi, Daniel Lockery and Shabnam Shahfar for their friendships and helpful insights. I would like to thank my wonderful friends in Winnipeg for their friendships, encouragements and supports.

My deepest love and appreciation goes to my mother who left this world during my PhD studies. Her unconditional love for her children and her deep passion for learning and teaching were my greatest motivations throughout these years. I would like to express my gratitude to my father for his love, wisdom and support. I would like to thank my amazing sisters, Faeze and Maryam and my brother Hossein for their encouragements and love. My thanks goes to my grand moms, my aunt Shokoufeh and my uncle. Last but not least, I am deeply thankful to my husband, Babak, for his love, support, understanding and motivation in everything I do.

To the memory of my mom, Forough Mallak, for her unconditional love,

To my father, Reza Fashandi,

and

To my husband, Babak Seifi.

Contents

Abstract	i
Contributions	i
Acknowledgements	ii
List of Tables	vii
List of Figures	ix
List of Symbols	xvi
1 Introduction	1
I Theory	6
2 Background Information	8
2.1 Crisp Topological Space	8
2.2 Fuzzy Topological Space	14
2.2.1 Fuzzy Sets	14
2.2.2 Fuzzy Topology: Chang's Approach	21
2.3 Summary	25
3 New Topological Operators	26
3.1 Inclusion Measure	26
3.2 Interior and Closure with Inclusion Degree	29
3.3 Fuzzy Topology for a Collection of Fuzzy Sets	36

3.4	Summary	41
II	Applications	42
4	Interior Operator with Inclusion Degree Applied to Image Database Classification	44
4.1	Related Works	45
4.1.1	Image Database Classification	46
4.1.2	Shape Classification	47
4.1.3	Topological Approaches in Image Processing	48
4.1.4	Our proposed Classification Method	49
4.2	Feature Extraction	52
4.2.1	Shape Features	53
4.2.2	Color Features	58
4.3	Shape Classification	60
4.4	Color Image Database Classification	63
4.4.1	Image Segmentation	65
4.4.2	Cluster Validation and Initialization	67
4.4.3	Results	71
4.5	Summary	75
5	Application of Proposed Operators in Mathematical Morphology	81
5.1	Background Information on Mathematical Morphology	82
5.2	Mathematical Morphology Operators and Interior& Closure Operators with Inclusion Degree	87
5.3	Applications of Proposed Morphological Operators	92
5.3.1	Noise Reduction	92
5.3.2	Edge Detection	96

5.4 Summary	99
6 Conclusion	102
A Fuzzy Topological Space: Alternative Definitions	104
A.1 Lowen's Approach	104
A.2 Šostak's Approach	105
A.3 Goguen's Approach	107
A.4 Summery	108
B Gaussian Mixture Model and Expectation Maximization	109
B.1 Finite Mixture Model	109
B.2 Parametric Formulation of Mixture Model	110
B.3 Maximum Likelihood Estimation	111
B.4 Formulation of ML as an Incomplete-Data Problem	111
B.5 Expectation Maximization	112
References	114
Author Index	126
Subject Index	128

List of Tables

4.1	Results of our classification method on SIMPLicity images [58, 114]. The results are averages of 4 different runs. numbers inside the parantheses show the standard deviation. The results are reported in test images (67 images in each category). On-diagonal numbers shows the accuracy of the classification for the category of each row. Off diagonal numbers are the classification errors (¹ image category)	76
4.2	Classification results: Query images (taken from the test set) of the food category and three first choices of the system are shown. Inclusion degree is set to $\gamma = 0.6$, training set are 33 images. The accuracy of this run for this category is 71.6 and is calculated only on the first output of the system .	77
4.3	Classification results: Query images (taken from the test set) of the mountain category and three first choices of the system are shown. Inclusion degree is set to $\gamma = 0.5$, training set are 33 images. The accuracy of this run for this category is 53.7 and is calculated only on the first output of the system	78
4.4	Results of our classification method on a subset of COREL 10K image database. The number of images in each category range between 68 to 130.	79
5.1	Basic morphological operators	84
5.2	Some noise removal indicators. I is the reference image with $M \times N$ pixels, I' is the processed image (noise removed)	93

5.3 Noise Removal Evaluation- 3×3 median filter, Open-close (OC) and Open-close-close-open (OCCO) sequence of both traditional morphology and morphology with inclusion degree are tested. σ is set to 0.4 as the threshold of the inclusion degree. Best results are shaded in gray. Median filter is more efficient in lower probability noise contamination. For higher noise contamination (>30%) Open-close sequence with inclusion degree and Open-close-close-open sequence with inclusion degree perform better. 96

List of Figures

1.1	Chapter and Appendix Dependencies	5
2.1	A set A in the partitioned space of the form $[j, j + 1)^2$; (a) interior of A , (b) closure of A , (c) boundary of A	13
2.2	Fuzzy s-norms and t-norms (a) Memebreship function of fuzzy sets A and B are shown. (b) $\mu_{A \vee B}$ for different definitions of s-norms have been shown: Drastic sum (yellow), Einstein sum (dashed black), Algebraic sum (dotted black), Yager class $w = 2$ (red), Dombi class $\lambda = 2$ (solid black), Max operator (dashed green) and Dubois-Prade class $\alpha = 0.2$ (blue). (c) $\mu_{A \wedge B}$ for different definitions of t-norms have been shown: Drastic multiplication (yellow), Einstein multiplication (dashed black), Algebraic multiplication (dotted black), Yager class $w = 2$ (red), Dombi class $\lambda = 2$ (solid black), Min operator (dashed green) and Dubois-Prade class $\alpha = 0.2$ (blue).	19
2.3	Fuzzy Complements (a) Sugeno class of fuzzy complements are shown with different values of λ (b) Yager class of fuzzy complements are shown with different values of w	20
2.4	Fuzzy Complement. (a) Membership function of a fuzzy set A . (b) Membership functions of fuzzy complement of A , Yager class fuzzy complement with $w = 2$ is plotted in blue. Black lines are fuzzy complement of equation 2.7. Sugeno class complement is shown in green curves.	20

2.5	Open and closed fuzzy sets of a topology in example 2.2.6 are shown. The fuzzy topology is (X, δ) , where $X = [0, 1]$ and $\delta = \{B_1, B_2, B_1 \vee B_2, \mathbf{1}, \mathbf{0}\}$. Open (Closed) fuzzy sets are shown in first (second) row.	22
3.1	A set A in the partitioned space of the form $[j, j + 1)^2$; (a) interior of A , (b) closure of A , (c) boundary of A	30
3.2	Illustration of fuzzy interior operator with inclusion degree. Fuzzy Open sets B_1 and B_2 are shown with dashed lines. B_2 is shown with a thicker dashed line. Fuzzy set A is shown with solid line. The fuzzy topology is (X, δ) , where $\delta = \{B_1, B_2, B_1 \vee B_2, \mathbf{1}, \mathbf{0}\}$. Refer to example 3.2.5 for more details.	32
3.3	Illustration of fuzzy closure operator with inclusion degree. Fuzzy closed sets B'_1 and B'_2 are shown with dashed lines. B'_2 is shown with a thicker dashed line. Fuzzy set A is shown with solid line. The fuzzy topology is (X, δ) , where $\delta = \{B_1, B_2, B_1 \vee B_2, \mathbf{1}, \mathbf{0}\}$. Refer to example 3.2.7 for more details.	34
3.4	Fuzzy subsets U (solid line) and V (dashed line) of example 3.3.3 are shown.	40
3.5	Open fuzzy sets of the fuzzy topology (X, δ) defined in example 3.3.3 are shown.	40
3.6	Our proposed topological operators (fuzzy interior/closure operators with inclusion degree) have been applied in two different areas, namely: image/shape database classification and mathematical morphology	43
4.1	Training phase of our proposed classification method for concept $_i$	52

4.2	Distance histogram. (a) The process of obtaining a $n(n \rightarrow \infty)$ -bin distance histogram is shown. For each distance $d > 0$, a circle ($C(c, d)$) centering at the center of mass(c) of the object is considered. The value of the distance histogram at the corresponding bin to d is the number of pixels of the object that lie on $C(c, d)$. These pixels are shown with green colors on two depicted circle $C(c, d_1)$ and $C(c, d_2)$. (b) For coarser distance histogram, each bin represents a range of distances from center of mass shown in circular bands, the number of green colored pixels in each band is the value for the histogram's bin. Bird image is from Kimia image database [96] . . .	54
4.3	Normalized distance histograms - on each row an object (shown in white color on black background) and its normalized distance histogram are shown.	55
4.4	Normalized distance histograms- Images (from Kimia shape database [96]) and their corresponding normalized distance histograms.	55
4.5	Angle histogram. (a) The process of obtaining a $n(n \rightarrow \infty)$ -bin histogram is shown. For each angle $-\pi \leq \theta \leq \pi$, a vector ($c\vec{v}$) is considered, and the value of the histogram at the corresponding bin to θ is the number of pixels of the object that lie on $c\vec{v}$. These pixels are shown with green color. (b) For coarser angle histogram, each bin represents a range of angels, the number of green colored pixels are the value for the histogram's bin representing $0 \leq \theta \leq \theta_1$. Bird image is from Kimia image dataset [96]	56
4.6	Normalized angle histograms - on each row an object (shown in white color on black background) and its normalized angel histogram are shown.	57
4.7	Normalized angle histograms- Images (from Kimia shape database [96]) and their corresponding normalized angle histograms.	57

4.8	Chord Distribution- Point p on the boundary of the object is shown. Six other points ($b_i, i = 1, \dots, 6$) on the boundary are shown (a) Chord angle distribution- The angle between the \vec{px} and \vec{pb}_i 's are depicted. Angles are calculated for between all the points on the boundary of the object and an a histogram is obtained based on all the calculated angles. (b) Chord distance histogram- Distances between a point p on the boundary of the object and six other points on the boundary are shown (d_1, \dots, d_6). A histogram is obtained between all the points on the boundary of the object	58
4.9	Normalized Chord Distributions	59
4.10	Normalized chord distributions- Images (from Kimia shape database [96]) and their corresponding normalized angle histograms.	59
4.11	Image segments and red, green and blue color histograms. Images are from SIMPLIcity database [58, 114]	60
4.12	Shapes 216 or Kimia database [96]: 12 images in 18 different categories namely: bird, bone, brick, camel, car, children, classic, elephant, face, fork, fountain, glass, hammer, heart, key, misk, ray and turtle	62
4.13	Accuracy of the proposed shape classification method (inclusion measure is set to $\gamma = 0.7$) is shown for different number of training samples ($n = 1, 5, 6, 7, 8, 11$). The data set is Shapes 216 ([96]) and the training samples are selected randomly from each category. Results are shown on three random runs.	63
4.14	Classification results on the test set- Inclusion degree is set to $\gamma = 0.7$, angle and distance histograms are considered as fuzzy features to built subspace topologies for each category. Number of training sample in each category is set to 7. Accuracy of the results is 83% . Images are from Kimia iamge dataset [96]	64

4.15	Feature extraction process. Optimum number of cluster is obtained $k = 5$ for this particular image. RGB colors and position information have been considered for segmentation process. Each process is explained in detail in subsections 4.4.1, 4.4.2, 4.2	66
4.16	Windows [11] for initializing the EM: $k = 2, \dots, 5$. The best k is chosen based on the validation techniques described in subsection 4.4.2	70
4.17	Cluster validation indicators: EM segmentation algorithm has been run for 5 times. The cluster initialization are based on initial windows shown in figure 4.16. Davis Bouldin(DB), Calinski-Harabasz(CH), Dunn(D), Krzanowski-Lai(KL) and Hartigan(H) Indices are shown in green, gray, blue, black and yellow colors, respectively. Maximum values of CH and Dunn indexes are shown in red dots. Also, minimum values of KL, Han and DB indices are shown in red dots. Images are from SIMPLIcity image database [58, 114]	70
4.18	Application of median filter on an image(from SIMPLIcity image database [58, 114]) and the segmented result.	71
4.19	Results of the EM segmentation shown with white contours on images from the SIMPLIcity image database [58, 114]. Each row represents samples from a different category, namely, Africa, beach, buildings, buses, dinosaurs, elephants, flowers, horses, mountains and food.	72
4.20	Within class diversity in some image categories. Images are from SIMPLIcity image database [58, 114]	73
4.21	Between classes similarity: Some samples from the mountain and beach categories are shown . Images are from SIMPLIcity image database [58, 114]	73
4.22	Between classes similarity: Some samples from the elephant and Africa categories are shown . Images are from SIMPLIcity image database [58, 114]	74

4.23	Samples of our selected images from COREL database [58, 114]. Images are drawn and segmented from 8 categories, namely: sunset, flowers, cars, sailing, fall, forest, mountains, ocean.	79
5.1	Examples of structuring elements (B_1, B_2, B_3) and their reflections ($\hat{B}_1, \hat{B}_2, \hat{B}_3$). The dots denote the centers of SEs.	84
5.2	Structuring element is the 2×2 square shown in various positions on image plane. The origin of the structuring element is dotted.	84
5.3	Examples of mathematical dilation and erosion. Gray squares are members of the set and considered as the foreground color in these images. The dashed lines in (c),(d),(e) and (f) is the boundary of set A , shown only for reference.	85
5.4	Structuring element (B) is shown at various locations on the image plane. Based on location of B_i and $i \in \{w, x, y, z\}$, $Inc(B_i, A)$ varies between and one.	91
5.5	Noise Removal Evaluation Process	92
5.6	Salt and pepper noise. (a) Original image. (b) Noisy image has a 10% probability of being contaminated with noise, (c) Noisy image with 60% probability of contamination	93
5.7	Salt and pepper noise removal. (a) Noisy image has a 10% probability of being contaminated with noise, (b) Result of 3×3 Median filter, (c) Open-close sequence, (d) Open-Close-Close-Open sequence (e) Open-close sequence with inclusion degree $\sigma = 0.4$ (f) Open-Close-Close-Open sequence filtering with $\sigma = 0.4$. Structuring element is a 3 square in (c-f). .	97
5.8	Salt and pepper noise removal. (a) Noisy image has a 40% probability of being contaminated with noise, (b) Result of 3×3 Median filter, (c) Open-close sequence, (d) Open-Close-Close-Open sequence (e) Open-close sequence with inclusion degree $\sigma = 0.4$ (f) Open-Close-Close-Open sequence filtering with $\sigma = 0.4$. Structuring element is a 3 square in (c-f). .	97

5.9	Salt and pepper noise removal. (a) Noisy image has a 50% probability of being contaminated with noise, (b) Result of 3×3 Median filter, (c) Open-close sequence, (d) Open-Close-Close-Open sequence (e) Open-close sequence with inclusion degree $\sigma = 0.4$ (f) Open-Close-Close-Open sequence filtering with $\sigma = 0.4$. Structuring element is a 3 square in (c-f).	98
5.10	Salt and pepper noise removal. (a) Noisy image has a 70% probability of being contaminated with noise, (b) Result of 3×3 Median filter, (c) Open-close sequence, (d) Open-Close-Close-Open sequence (e) Open-close sequence with inclusion degree $\sigma = 0.4$ (f) Open-Close-Close-Open sequence filtering with $\sigma = 0.4$. Structuring element is a 3 square in (c-f).	98
5.11	Morphological Edge Detection	100
A.1	fuzzy sets G_n for $n \in \{2, 3, 4, 5, 10\}$ and the fuzzy set G of example A.2.2 are shown.	107
A.2	example of L-fuzzy sets. Figure is used with permission [50].	108

List of Symbols

(X, τ)	crisp topological space	8
$\mathcal{P}(X)$	power set of X	8
$\mathcal{F}(X)$	collection of all fuzzy sets on X	8
A, B	crisp sets	8
\mathbf{A}, \mathbf{B}	fuzzy sets	8
\emptyset	empty set	9
$X \setminus A$	set difference	10
\mathcal{B}	basis of a topology	11
(S, τ_S)	subspace topology	11
$\overset{\circ}{A}$	interior of set A	12
\overline{A}	closure of set A	12
∂A	boundary of set A	12
$\alpha(A)$	closure operator applied to set A	13
$\beta(A)$	interior operator applied to set A	14
A^c	complement of A	13
\cup	set union	13
\cap	set intersection	14
μ_A	membership function of the fuzzy set A	15
(X, δ)	fuzzy topological space	21
\vee	fuzzy union (supremum)	16

\wedge	fuzzy intersection (infimum)	16
\leq	fuzzy subsethood	16
$s[\mu_A, \mu_B]$	s-norm $(s_\lambda, s_\alpha, s_w, s_{ds}, s_{es}, s_{as})$	16
$t[\mu_A, \mu_B]$	t-norm $(t_\lambda, t_\alpha, t_w, t_{ds}, t_{es}, t_{as})$	17
$c[\mu_A]$	fuzzy complement	18
$\mathcal{N}_\delta(A)$	Chang's neighbourhood system of the fuzzy set A with respect to topology (X, δ)	22
\mathring{A}	fuzzy interior of the fuzzy set A with respect to fuzzy topology (X, δ) ...	23
\bar{A}	fuzzy closure of the fuzzy set A with respect to fuzzy topology (X, δ) ...	23
$\varphi(A)$	fuzzy closure operator applied to the set A	23
$\theta(A)$	fuzzy interior operator applied to the set A	23
$Inc(A, B)$	shows to what extends A is included in B, inclusion degree of A in B ..	27
$\Sigma Count(A)$	$\Sigma_i \mu_A(x_i)$	28
γ, σ	inclusion degrees	28
$Inc_{\{K\}}(A, B)$	inclusion measure for fuzzy sets: Kosko's method	28
$Inc_{\{G\}}(A, B)$	inclusion measure for fuzzy sets: Goguen method	28
$Inc_{\{\rightarrow\}}(A, B)$	inclusion measure for fuzzy sets: implication	28
\mathring{A}_γ	interior of set A with inclusion degree γ	29
\bar{A}_σ	closure of set A with inclusion degree σ	30
\mathring{A}_γ	fuzzy interior of fuzzy set A with inclusion degree γ	31
\bar{A}_δ	fuzzy closure of fuzzy set A with inclusion degree γ	32
\mathfrak{B}	basis of a fuzzy topology	38
\mathfrak{C}	a collection of fuzzy subsets of X	38
k	number of clusters	67
\mathcal{L}	likelihood	67
Ψ	parameters of finite mixture model	67

$DB(k)$	Davies Bouldin Index; k is the number of clusters	68
$D(k)$	Dunn Index; k is the number of clusters	68
$DH(k)$	Calinski-Harabasz Index; k is the number of clusters	68
$KL(k)$	Krzanowski-Lai Index; k is the number of clusters	68
$H(k)$	Hartigan Index; k is the number of clusters	69
$e_B(A)$	erosion of A by structuring element B	82
$d_B(A)$	dilation of A by structuring element B	82
$o_B(A)$	opening of A by structuring element B	83
$c_B(A)$	closing of A by structuring element B	83
\approx	approximately equal	87
$d_{B\sigma}(A)$	dilation of A with structuring element B and inclusion degree σ	89
$e_{B\sigma}(A)$	erosion of A with structuring element B and inclusion degree σ	89
$o_{B\sigma}(A)$	opening of A with structuring element B and inclusion degree σ	91
$c_{B\sigma}(A)$	closing of A with structuring element B and inclusion degree σ	91
L	completely distributive lattice	107
\perp	smallest element of a completely distributive lattice	107
\top	greatest element of a completely distributive lattice	107
$\kappa_i(y_j; \Psi)$	the posterior probability that the j th member of the sample with observed value y_j belongs to the i th component of the mixture.	113

Chapter 1

Introduction

Topological spaces are one of the primary areas in mathematics and have played a significant role in image processing. Many topological definitions have been adapted to image space, including but not limited to the concept of neighborhood, closure, interior and boundary. Although topological spaces and operators have affected the image processing society for a long time, the influence was mostly at the theoretical and abstract level. The general notations of topology are not often familiar to a non-mathematical society. Building a model based on topological notations in rich Euclidean space is often far from applying it directly to digital spaces. However, the introduction of Mathematical Morphology (MM) by Matheron and Serra [67,97] was directly stemmed from the topological operators. Serra discussed the topological foundation of MM comprehensively in chapter III and VII of his book on MM [97]. He addressed the notation of closure, interior, boundary, neighborhood, continuity, convergence and limits in Euclidean space and adapted them to the digital space. Moreover, the notation of neighborhood has been used intensively in digital image processing such as sliding filters, texture analysis and segmentation.

In this thesis, the concept of inclusion degree is introduced to the definition of topological interior and closure operators. The new operators with inclusion degree deal with imperfections in digital world including but are not limited to the presence of noise, imperfect boundaries and edges in images. Inclusion measures lead to a consideration of

subsethood in crisp and fuzzy spaces with values in $[0, 1]$ instead of $\{0, 1\}$. The motivation to relax the original view of a subset stemmed from the fact that we may want to talk about the inclusion degree or how much one (fuzzy or crisp) set is a subset of another (fuzzy or crisp) set. Introduction of this concept in the definition of topological interior and closure enabled us to ignore the minor imperfections with respect to the user defined threshold.

In this dissertation, it is argued that using a relaxed version of subsethood in the definition of fuzzy or crisp topological interior and closure operators, make them suitable for the image processing applications. The newly defined operators are equipped with inclusion degree to handle small errors due to noise and imperfections in digital images, while ordinary topological operators are unable to handle these imperfections. To evaluate the validity of the above statement, the new interior and closure operators with inclusion degree are incorporated in morphological operators, shape classification and image database classification. Morphological operators based on the new topological operators are defined and applied on noise removal and edge detection in noisy environment. The morphological operators with inclusion degree outperform median filters and traditional morphological operators in high noise contamination. I also proposed a new method for image database classification and shape classification which uses the topological subspaces to model image (shape) categories. The use of interior operator with inclusion degree with respect to different topological subspaces is proposed to classify a query image (shape). The method shows promising results.

This practical approach toward the topological notations and the extended version of topological operators make them more applicable in digital image processing as demonstrated in chapters 4 and 5. The main contributions presented in this dissertation are:

- Extended version of interior and closure operator are defined for both crisp and fuzzy topologies in chapter 3 section 3.2. The definition incorporates a relaxed version of subsethood which is more applicable for digital space.
- Mathematical properties of newly defined topological operators are examined and compared with original operators (chapter 3-propositions 3, 4, 5 and 6).

- Building a fuzzy topology from a collection of fuzzy sets is proposed and proved in chapter 3-propositions 7 and 8.
- Three areas are considered to apply new operators and demonstrate their strength, namely, mathematical morphology, shape classification and image database classification.
- A topological framework to classify large image databases is proposed (chapter 4-section 4.1.4).
- Each image category is modeled with a subspace topology demonstrating the practical approach in a topological setting.
- An interior operator with inclusion degree is applied to a query image with respect to different subspace topologies (chapter 4-section 4.4).
- The same method used for image database classification is also used to solve the shape database classification problem (chapter 4-section 4.3).
- Morphological operators have been defined using the new topological operators. The properties have been discussed from topological point of view (chapter5-section 5.2). It should be mentioned that, there is a previous work that incorporated inclusion degree in the definition of morphological operators [108]. However, the work did not consider the topology underlying the morphological operators. This dissertation provides a mathematical foundation for such operators.
- Also, I proposed open-close-close-open sequence with inclusion degree for noise removal from binary images which outperformed traditional morphological filters and median filter in higher noise contamination (chapter 5-section 5.3).
- The morphological operators with inclusion degree showed a better performance in edge detection in noisy images in comparison to traditional morphological edge detectors in noisy environment (chapter 5-section 5.3).

This thesis has been organized in two parts: Part I and Part II. Part I contains two theoretical chapters: Chapter 2 presents the basic background on crisp and fuzzy topological spaces. Chapter 3 contains information on inclusion measure for crisp and fuzzy sets and introduces the topological interior and closure operators with inclusion degree. This chapter presented the properties of the proposed operators. Part II contains two chapters for the applications of the new operators. Chapter 4 presents the proposed method for shape classification and image database classification. A literature review on image database classification techniques, shape classification and topological approaches on image processing is included in this chapter. Chapter 5 considered the application of the new topological operators in mathematical morphology. Background information on mathematical morphology is discussed in this chapter. Applications are considered in terms of noise removal and edge detection in noisy images. Chapter 6 is dedicated to concluding remarks and future works. Appendix A presents alternative definitions of a fuzzy topological space. Appendix B presents the details of the expectation maximization algorithm used in chapter 4. The diagram shown in figure 1.1 depicts the chapter and appendix dependencies.

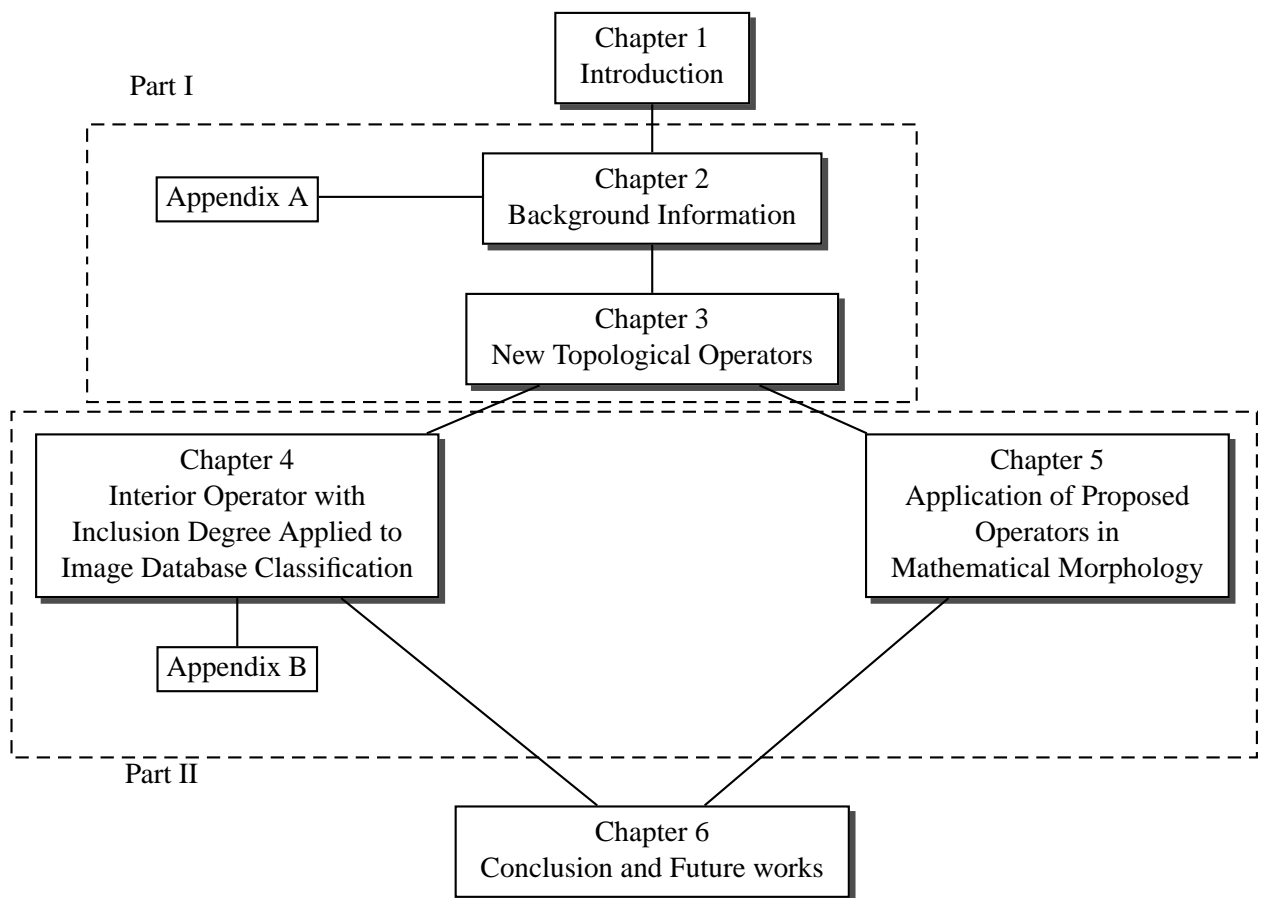


Figure 1.1: Chapter and Appendix Dependencies

Part I

Theory

This part of the thesis contains two chapters. Chapter 2 explains the background information on crisp and fuzzy topological structure. The chapter is self contained and has information on fuzzy sets as well. Chapter 3 gives the definition of our proposed interior and closure operators with inclusion degree. Moreover, it contains new propositions that establish the foundation for building a fuzzy topology on a collection of fuzzy sets.

Chapter 2

Background Information

This chapter presents the basic concepts of crisp topology (X, τ) and fuzzy topology (X, δ) , where X is a space, also known as a universe of discourse or universe for short. The term topology denotes a family of sets with certain properties that defines a topological space. Through out this document, we use A, B, \dots for crisp sets and A, B, \dots for fuzzy sets. The crisp power set of X is denoted by $\mathcal{P}(X)$ and the collection of all fuzzy sets on X is denoted by $\mathcal{F}(X)$. Crisp topologies are denoted by (X, τ) and fuzzy topologies shown by (X, δ) . We start this chapter with a brief overview of crisp topology in section 2.1. Section 2.2 considers the fuzzy space. Definition of fuzzy sets and basic fuzzy set theory operations are discussed in sub-section 2.2.1, followed by subsection 2.2.2 on fuzzy topological spaces based on C.L. Chang's seminal paper [13]. More information on alternative definitions of fuzzy topology is reported in appendeix B

2.1 Crisp Topological Space

This section presents the basic concepts of crisp topology, mainly based on the book by M.C. Gemignani [32].

Definition 2.1.1. *Let X be a non-empty set. A collection τ of subsets of X is said to be a topology on X if, and only if,*

cTop.1 X and \emptyset belongs to τ ,

cTop.2 The union of any finite or infinite number of sets in τ belongs to τ ,

cTop.3 The intersection of any two sets in τ belongs to τ .

The pair (X, τ) is called a topological space.

Depending on the cardinality of the space X , one or more topologies on the set X are possible.

Example 2.1.2. If $X = \{a, b\}$, then there are four possible topologies, namely, $\tau_1 = \{X, \emptyset\}$ (called an **indiscrete topology**), $\tau_2 = \{X, \{a\}, \emptyset\}$, $\tau_3 = \{X, \{b\}, \emptyset\}$, and $\tau_4 = \{X, \{a\}, \{b\}, \emptyset\}$ (called a **discrete topology**). In general, the collection of all subsets of X is called a discrete topology and the collection consisting only of X and the empty set \emptyset is called an indiscrete topology (cf., e.g., J.L. Kelley [52, p. 37]). Discrete and indiscrete topologies are two extremes among possible topologies on a non-empty set X .

Example 2.1.3. Let $X = \{a, b, c\}$. There are 29 possible topologies on X . However, only 9 of them are inequivalent topologies:

$$\tau_1 = \{X, \emptyset\}, (\text{indiscrete topology})$$

$$\tau_2 = \{\emptyset, \{a\}, X\},$$

$$\tau_3 = \{\emptyset, \{a, b\}, X\},$$

$$\tau_4 = \{\emptyset, \{a\}, \{a, b\}, X\},$$

$$\tau_5 = \{\emptyset, \{a\}, \{b, c\}, X\},$$

$$\tau_6 = \{\emptyset, \{a\}, \{a, b\}, \{a, c\}, X\},$$

$$\tau_7 = \{\emptyset, \{a\}, \{b\}, \{a, b\}, X\},$$

$$\tau_8 = \{\emptyset, \{a\}, \{b\}, \{a, b\}, \{a, c\}, X\},$$

$$\tau_9 = \{\emptyset, \{a\}, \{b\}, \{c\}, \{a, b\}, \{b, c\}, \{a, c\}, X\}, (\text{discrete topology}).$$

Not every collection of subsets of X is a topology on X . The following collections are not

topologies on X :

$$\kappa_1 = \{\emptyset, \{a\}, \{b\}, X\},$$

since $\{a\} \cup \{b\}$ is not the element of κ_1 . Also, κ_2 defined by:

$$\kappa_2 = \{\emptyset, \{a, b\}, \{b, c\}, X\},$$

is not a topology, since $\{a, b\} \cap \{b, c\}$ is not the element of κ_2 .

Definition 2.1.4. Let (X, τ) be a topology. Then the members of τ are called **open sets**.

Therefore,

- X and \emptyset are open sets,
- The union of any finite or infinite number of open sets are open sets,
- The intersection of any finite number of open sets is an open set.

Definition 2.1.5. Let (X, τ) be a topological space. A set $S \subseteq X$ is said to be **closed**, if $X \setminus S$ is open, where \setminus is the set difference operator.

- \emptyset and X are closed sets,
- The intersection of any finite or infinite number of closed sets is a closed set,
- The union of any finite number of closed set is a closed set.

Some subsets of X , may be both closed and open. In a discrete space, every set is both open and closed, while in an indiscrete space all subsets of X are neither open nor closed, except X and \emptyset . For instance, suppose we take E as the set of points of \mathbb{R}^n with integer coordinates. Let τ be the collection of all subsets of E . Each point is simultaneously open and close [97].

Definition 2.1.6. Let (X, τ) be a topological space. If $x \in X$, then any open set which contains x is said to be a **neighborhood** of x .

Some texts [97] use the term neighborhood differently. They say that A is a neighborhood of x if A merely contains an open set containing x . We shall not follow this definition [75].

Definition 2.1.7. Suppose that (X, τ) is a topological space. A subset \mathcal{B} of τ (i.e., a collection of open sets) is said to be a basis for the topology τ if each member of τ is the union of members of \mathcal{B} .

In algebra, every vector is a linear combination of the basis. Similarly, in a topology τ , every open set can be obtained by a union of members of the basis.

Example 2.1.8. Let $X = \{a, b, c, d, e\}$ and (X, τ) is a discrete topological space. Then $\mathcal{B} = \{\{a\}, \{b\}, \{c\}, \{d\}, \{e\}\}$ is a basis for the topology. Generally, the collection of all one-point subsets of a set X is a basis for the discrete topology on X .

Definition 2.1.9. Each partition τ_P of any finite, non-empty set X into disjoint subsets, together with the empty set \emptyset , is a basis for a topology on X , known as a **partition topology** [104].

In partition topology every open set is also closed. Therefore a partition topology on the set X is a discrete topology.

Example 2.1.10. Let $X = \{a, b, c, d, e, f\}$ and $\tau_p = \{\{a\}, \{b, c, f\}, \{d, e\}\}$ be a partition of X ; then $\{\tau_p\} \cup \{\emptyset\}$ is a basis for a topology on X .

Example 2.1.11. Let $Z \subseteq E^n$ be a bounded subset of n -dimensional Euclidean space. Let $\{P_1, P_2, \dots, P_n\}$ be a partition of Z , where P_i is the partition of the i -th axis E_i into intervals of the form $[j, j + 1)$ (j is an integer). For $n = 2$, the space are partitioned into squares. The open sets of the partition topology associated to this topology are squares of the form $[j, j + 1) \times [i, i + 1)$ (i and j are integers). This example inspired by an example in [89]

Definition 2.1.12. Let (X, τ) be a topology on X . Let S be a non-empty subset of X . The collection $\tau_S = \{T \cap S : T \in \tau\}$ of subsets of S is called the **subspace topology**. The topological space (S, τ_S) is said to be a subspace of (X, τ) .

Example 2.1.13. Let $X = \{a, b, c, d, e\}$ and (X, τ) is a topology on X , where $\tau = \{X, \emptyset, \{a\}, \{a, b\}, \{a, c, d\}, \{a, b, c, d\}, \{a, b, e\}\}$. Let $S = \{a, c, d\}$, then $\tau_S = \{S, \emptyset, \{a\}\}$ is a subspace topology on S .

In topology, the notion of interior of a set is defined for a subset of a topological space. It is defined based on all the open sets that are contained in the set.

Definition 2.1.14. Let (X, τ) be any topological space and A be any subset of X . The largest open set contained in A is called the **interior** of A (denoted by $\overset{\circ}{A}$) and defined by

$$\overset{\circ}{A} = \cup\{B \in \tau : B \subseteq A\}. \quad (2.1)$$

Equivalently, let x be a point in a subset A of the space X . The point x is an interior point of A , if and only if, A is a neighborhood of x . The set of all interior points of A is the interior of A .

Example 2.1.15. Let $X = \{a, b, c, d, e\}$ and (X, τ) is a topology on X , where $\tau = \{X, \emptyset, \{a\}, \{a, b\}, \{a, c, d\}, \{a, b, c, d\}, \{a, b, e\}\}$. Let $A = \{a, c\}$ and $B = \{c, d\}$, then $\overset{\circ}{A} = \{a\}$ and $\overset{\circ}{B} = \{\emptyset\}$.

Closure in topology is the dual operator of the interior. Formally it is defined as follows:

Definition 2.1.16. Let A be a subset of a topological space (X, τ) . **Closure** of A (denoted by \overline{A}), is the intersection of all closed sets that contain A and is defined by:

$$\overline{A} = \cap\{B \in \tau' : A \subseteq B\}. \quad (2.2)$$

where τ' is the set of all closed sets in the topology (X, τ) .

Example 2.1.17. Let $X = \{a, b, c, d, e\}$ and (X, τ) is a topology on X , where $\tau = \{X, \emptyset, \{a\}, \{a, b\}, \{a, c, d\}, \{a, b, c, d\}, \{a, b, e\}\}$. The set of all the closed set is $\tau' = \{\emptyset, X, \{b, c, d, e\}, \{c, d, e\}, \{b, e\}, \{e\}, \{c, d\}\}$. Let $A = \{a, c\}$ and $B = \{c, d\}$, then $\overline{A} = \{X\}$ and $\overline{B} = \{c, d\}$.

Definition 2.1.18. The **boundary** ∂A of a subset A of X is defined by $\partial A = \overline{A} \setminus \overset{\circ}{A}$, where \setminus is the set difference.

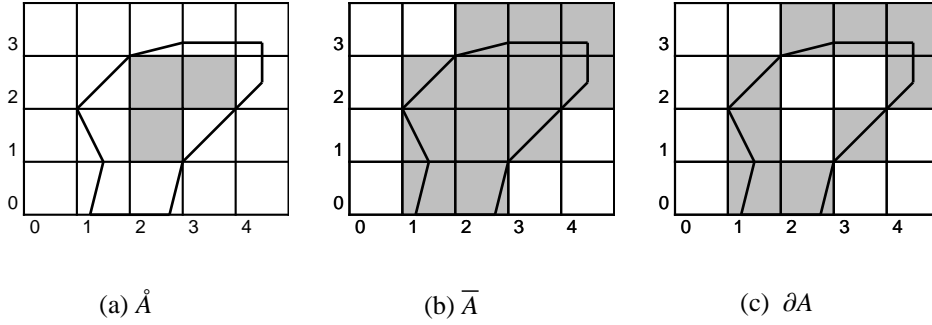


Figure 2.1: A set A in the partitioned space of the form $[j, j + 1)^2$; (a) interior of A , (b) closure of A , (c) boundary of A .

Example 2.1.19. In figure 2.1, we reconsider the partition topology defined in example 2.1.11. The set A is shown with solid lines. Interior, closure and Boundary of A are shaded in gray.

Definition 2.1.20. An operator $\alpha : \mathcal{P}(X) \rightarrow \mathcal{P}(X)$ is called a **closure operator** if, and only if

cCO.1 $\alpha(\emptyset) = \emptyset$,

cCO.2 α is increasing, i.e., $A \subseteq \alpha(A)$,

cCO.3 α is idempotent, i.e., $\alpha(\alpha(A)) = A$,

cCO.4 $\alpha(A \cup B) = \alpha(A) \cup \alpha(B)$.

And for the interior operator (β), four equivalent properties can be deduced by using the duality relation, $\beta(A)^c = \alpha(A^c)$, where c denotes the complement and α is the closure operator. Duality relation may also written by:

$$\beta(A) = X \setminus \alpha(X \setminus A), \tag{2.3}$$

and

$$\alpha(A) = X \setminus \beta(X \setminus A). \tag{2.4}$$

where X is a topological space containing A and \setminus refers to set difference.

Definition 2.1.21. An operator $\beta : \mathcal{P}(X) \rightarrow \mathcal{P}(X)$ is a interior operator if, and only if

cIO.1 $\beta(X) = X$,

cIO.2 β is decreasing, i.e. $\beta(A) \subseteq A$,

cIO.3 idempotent, i.e. $\beta(\beta(A)) = \beta(A)$,

cIO.4 $\beta(A \cap B) = \beta(A) \cap \beta(B)$.

In this section, we covered the basics of what is known as a crisp topology. The next section describes the extension of general (crisp) topology into fuzzy topological space. For more on crisp topology, see [76, 85].

2.2 Fuzzy Topological Space

In 1968, C.L. Chang was the first one who introduced the concept of fuzzy topology [13]. His work followed by others who introduced alternative definitions of fuzzy topology. For instance, J.A. Goguen defined a fuzzy topological space on L-fuzzy sets [33]. R. Lowen altered one of the axioms of Chang's definition [65]. A.P. Šostak began the study of fuzzy structures of the topological type, introducing the degree of openness for fuzzy sets [103]. R.N. Harza et al. [44] define the degree of openness with weaker axioms. Openness degree was studied by many authors, including [39, 47, 74]. We only consider the Chang's definition in this section and other definitions are discussed in appendix A for further information. We start this section with a brief definition of fuzzy sets and then continue to C.L. Chang's definition of fuzzy topology.

2.2.1 Fuzzy Sets

Fuzzy sets was first introduced by L.A. Zadeh in 1965 as an extension of the classical notation of a set [119]. A fuzzy set A in universe X (universe of discourse) is characterized by a membership function $\mu_A(x) : X \rightarrow [0, 1]$ which assigns a real normal number to each point in X . In classical set theory, elements of the universe, belongs to a set (membership value equals to 1) or not (membership value equals to 0), however in fuzzy set theory

elements of a set belongs to a set with some degree. Fuzzy set A is characterized by the set of pairs

$$A = \{(x, \mu_A(x)), x \in X\}$$

or when X is a finite set $\{x_1, \dots, x_n\}$, a fuzzy set on X is expressed as

$$A = \frac{\mu_A(x_1)}{x_1} + \dots + \frac{\mu_A(x_n)}{x_n} = \sum_{i=1}^n \frac{\mu_A(x_i)}{x_i}$$

and when X is not finite, it is characterized as:

$$A = \int \frac{\mu_A(x)}{x}$$

Example 2.2.1. Let $X = \{a, b, c, d, e\}$ be the universe of discourse. Consider the following membership functions for set A and \bar{A} :

$$\mu_A(a) = 0, \mu_A(b) = 1, \mu_{\bar{A}}(a) = 1, \mu_{\bar{A}}(b) = 0, \mu_{\bar{A}}(c) = 1, \mu_{\bar{A}}(d) = 0, \mu_{\bar{A}}(e) = 0$$

, and

$$\mu_A(a) = 0, \mu_A(b) = 0.8, \mu_A(c) = 1, \mu_A(d) = 0.7, \mu_A(e) = 0.$$

The sets A is completely characterized by:

$$A = \{(x, \mu_A(x)), x \in X\} = \{(a, 0), (b, 1), (c, 1), (d, 0), (e, 0)\}, \text{ or}$$

$$A = \frac{0}{a} + \frac{1}{b} + \frac{1}{c} + \frac{0}{d} + \frac{0}{e},$$

The binary membership function of the set A makes it a crisp set. The set \bar{A} is a fuzzy set and characterized by following notations:

$$\bar{A} = \{(x, \mu_{\bar{A}}(x)), x \in X\} = \{(a, 0), (b, 0.8), (c, 0.7), (d, 0.2), (e, 0)\}, \text{ or}$$

$$A = \frac{0}{a} + \frac{0.8}{b} + \frac{1}{c} + \frac{0.7}{c} + \frac{0.2}{d} + \frac{0}{e}.$$

2.2.1.1 Fuzzy Set Operations

L.A. Zadeh proposed the following formulas for fuzzy union (\vee), fuzzy intersection (\wedge) of fuzzy sets and complement of a fuzzy set(c) [119]:

$$\forall x \in X, \mu_{A \vee B}(x) = \max(\mu_A(x), \mu_B(x)), \quad (2.5)$$

$$\forall x \in X, \mu_{A \wedge B}(x) = \min(\mu_A(x), \mu_B(x)), \quad (2.6)$$

$$\forall x \in X, \mu_{A^c}(x) = 1 - \mu_A(x), \quad (2.7)$$

$\mu_{A \vee B}$ and $\mu_{A \wedge B}$ are respectively the membership functions of $A \vee B$ and $A \wedge B$. μ_{A^c} is the membership function of the complement of the fuzzy set A (A^c). Let A and B be two fuzzy sets in universe X , Zadeh [119] defined fuzzy subsethood as follows:

$$A \leq B \Leftrightarrow (\forall x \in X)(A(x) \leq B(x)). \quad (2.8)$$

The above definitions (2.5, 2.6, 2.7) are not the only interpretations of fuzzy union, intersection and fuzzy complement. There are 3 axiomatic systems for each of the fuzzy operators.

Fuzzy Union (s-norm) Axioms

Let $s : [0, 1] \times [0, 1] \rightarrow [0, 1]$ be a mapping that maps the membership functions μ_A and μ_B to $\mu_{A \vee B}$:

$$s[\mu_A, \mu_B] = \mu_{A \vee B},$$

s is a fuzzy union operator, iff it satisfies the following four axioms (fuzzy s-norm axioms):

fsn.1 $s(0, a) = s(a, 0) = a$, $s(1, 1) = 1$ (Boundary condition),

fsn.2 $s(a, b) = s(b, a)$ (Commutativity),

fsn.3 if $a \leq a'$ and $b \leq b'$ then $s(a, b) \leq s(a', b')$ (Monotonicity),

fsn.4 $s(s(a, b), c) = s(a, s(b, c))$ (Associativity).

Any function s that satisfies the fsn axioms is called s -norm [115]. The following s -norms as well as \max (equation 2.5) satisfy the fsn-axioms:

- **Dombi class:** $s_\lambda(a, b) = \frac{1}{1 + [(\frac{1}{a}-1)^{-\lambda} + (\frac{1}{b}-1)^{-\lambda}]^{-\frac{1}{\lambda}}}$, $\lambda \in (0, \infty)$ [21],
- **Dubois-Prade class:** $s_\alpha(a, b) = \frac{a+b-ab-\min(a,b,1-\alpha)}{\max(1-a, 1-b, \alpha)}$ [115],
- **Yager class:** $s_w(a, b) = \min[1, (a^w + b^w)^{\frac{1}{w}}]$ [116],
- **Drastic sum:** $s_{ds}(a, b) = \begin{cases} a, & b = 0, \\ b, & a = 0, \\ 1, & \text{otherwise.} \end{cases}$ [115],
- **Einstein sum:** $s_{es}(a, b) = \frac{a+b}{a+ab}$ [115],
- **Algebraic sum:** $s_{as}(a, b) = a + b - ab$ [115].

Fuzzy Intersection (t-norm) Axioms

Let $t : [0, 1] \times [0, 1] \rightarrow [0, 1]$ be a mapping that maps the membership functions μ_A and μ_B to $\mu_{A \wedge B}$:

$$t[\mu_A, \mu_B] = \mu_{A \wedge B},$$

t is a fuzzy intersection operator, iff it satisfies the following four axioms (fuzzy t-norm axioms):

- ftn.1** $t(0, 0) = 0$, $t(a, 1) = t(1, a) = 1$ (Boundary condition),
- ftn.2** $t(a, b) = t(b, a)$ (Commutativity),
- ftn.3** if $a \leq a'$ and $b \leq b'$ then $t(a, b) \leq t(a', b')$ (Monotonicity),
- ftn.4** $t(t(a, b), c) = t(a, t(b, c))$ (Associativity).

Any function t that satisfies the ftn axioms is called t -norm [115]. The following t -norms as well as \min (equation 2.6) satisfy the ftn-axioms:

- **Dombi class:** $t_\lambda(a, b) = \frac{1}{1 + [(\frac{1}{a}-1)^\lambda + (\frac{1}{b}-1)^\lambda]^{\frac{1}{\lambda}}}$, $\lambda \in (0, \infty)$ [21],
- **Dubois-Prade class:** $t_\alpha(a, b) = \frac{ab}{\max(a, b, \alpha)}$, $\alpha \in [0, 1]$ [115]

- **Yager class:** $t_w(a, b) = 1 - \min[1, ((1 - a)^w + (1 - b)^w)^{\frac{1}{w}}]$ [116] ,

- **Drastic multiplication:** $t_{dt}(a, b) = \begin{cases} a, & b = 1, \\ b, & a = 1, \\ 0, & \text{otherwise.} \end{cases}$ [115],

- **Einstein multiplication:** $t_{et}(a, b) = \frac{ab}{2-(a+b+ab)}$ [115],

- **Algebraic multiplication:** $t_{at}(a, b) = ab$ [115].

Example 2.2.2. Let A and B be two fuzzy sets defined by following membership functions:

$$\mu_A(x) = x ,$$

$$\mu_B(x) = 1 - x.$$

The membership functions have been shown in figure 2.2-(a). Figure 2.2-(b and c) shows $\mu_{A \vee B}$ and $\mu_{A \wedge B}$ for different t -norms and s -norms. Generally for any s -norm (s) and any t -norm(t) the following equalities are satisfied:

$$s_{\max} \leq s \leq s_{ds} \text{ and } t_{dt} \leq t \leq t_{\min}$$

where s_{\max} is max operator (eq. 2.5), s_{ds} is drastic sum. t_{dt} is drastic multiplication and t_{\min} is minimum operator (eq. 2.6) [115].

Fuzzy Complement Axioms

Let $c : [0, 1] \rightarrow [0, 1]$ be a mapping that maps fuzzy set A into its complement (A^c):

$$c[\mu_A(x)] = \mu_{A^c}(x) ,$$

c is a fuzzy complement operator iff it satisfies the following two axioms:

fc.1 $c(1) = 0, c(0) = 1$, (Boundary condition) ,

fc.2 $\forall a, b \in [0, 1]$ if $a < b$ then $c(a) \geq c(b)$ (Monotonicity) .

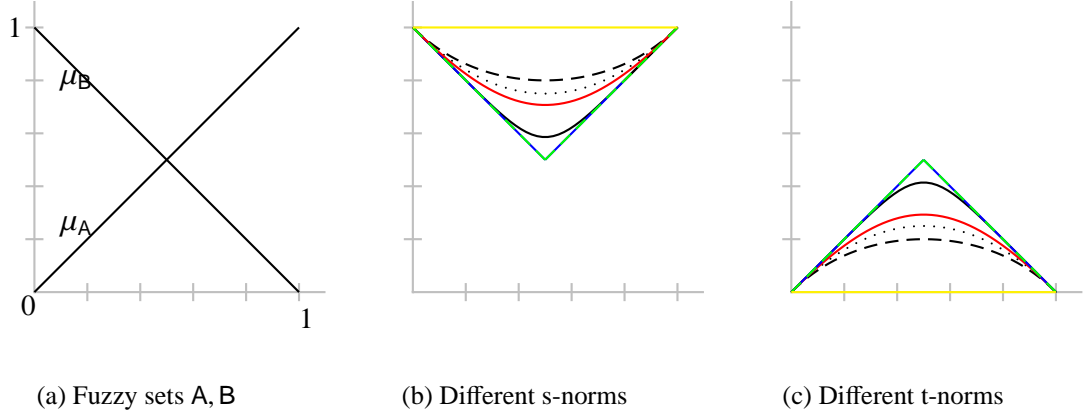


Figure 2.2: Fuzzy s-norms and t-norms (a) Memembreship function of fuzzy sets A and B are shown. (b) $\mu_{A \vee B}$ for different definitions of s-norms have been shown: Drastic sum (yellow), Einstein sum (dashed black), Algebraic sum (dotted black), Yager class $w = 2$ (red), Dombi class $\lambda = 2$ (solid black), Max operator (dashed green) and Dubois-Prade class $\alpha = 0.2$ (blue). (c) $\mu_{A \wedge B}$ for different definitions of t-norms have been shown: Drastic multiplication (yellow), Einstein multiplication (dashed black), Algebraic multiplication (dotted black), Yager class $w = 2$ (red), Dombi class $\lambda = 2$ (solid black), Min operator (dashed green) and Dubois-Prade class $\alpha = 0.2$ (blue).

Any function c that satisfies the fc-axioms is called a fuzzy complement. The following functions as well as equation 2.7 satisfy the fc-axioms:

- **Sugeno class:** $c_\lambda(a) = \frac{1-a}{1+\lambda a}$, $\lambda \in (-1, \infty)$ [106],
- **Yager class:** $c_w(a) = (1 - a^w)^{\frac{1}{w}}$, $w \in (0, \infty)$ [116].

Figure 2.3 shows Sugeno class and Yager class of fuzzy complement with different parameter values. Sugeno class is the same as fuzzy complemet in equation 2.7 for $\lambda = 0$. The same is true for Yager class with $w = 1$.

Example 2.2.3. Let A be a fuzzy set with membership function μ_A :

$$\mu_A = \begin{cases} 2x, & 0 \leq x \leq 0.5, \\ 2 - 2x, & 0.5 < x \leq 1. \end{cases}$$

Figure 2.4 shows μ_A and μ_{A^c} . Three different definitions have been considered for fuzzy complement: equation 2.7, Sugeno class ($\lambda = 2$) and Yager complement ($w = 2$).

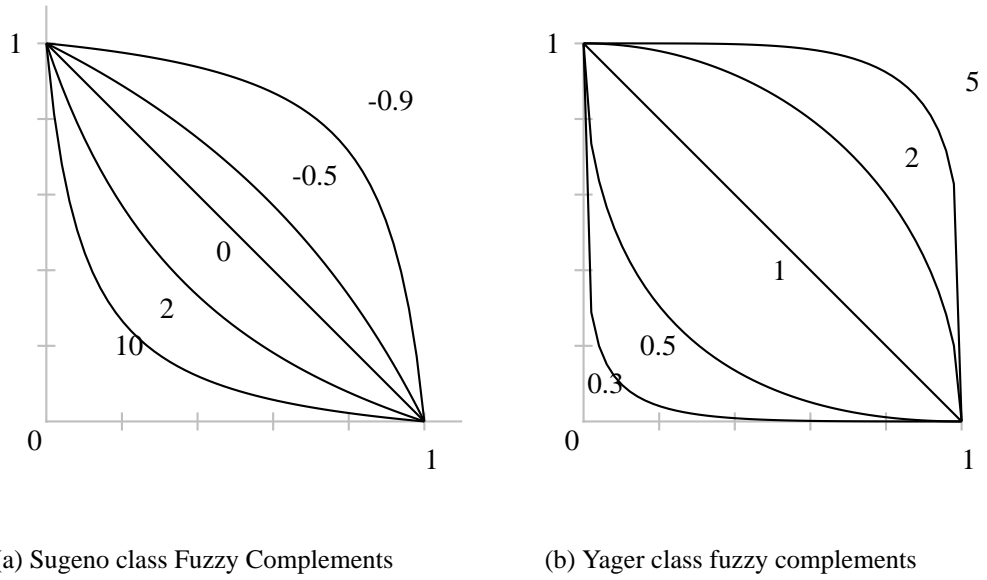


Figure 2.3: Fuzzy Complements (a) Sugeno class of fuzzy complements are shown with different values of w (b) Yager class of fuzzy complements are shown with different values of λ .

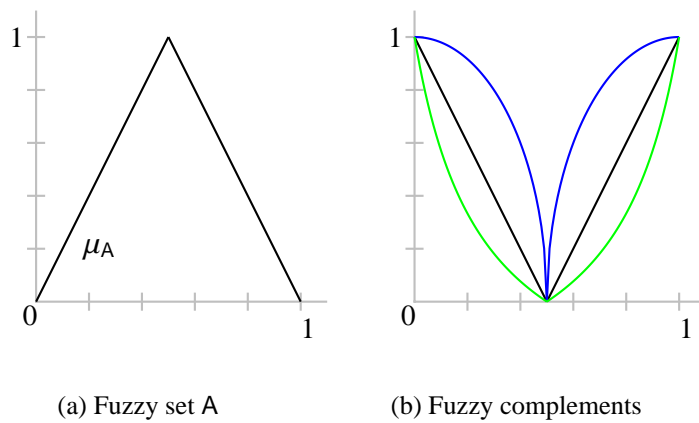


Figure 2.4: Fuzzy Complement. (a) Membership function of a fuzzy set A. (b) Membership functions of fuzzy complement of A, Yager class fuzzy complement with $w = 2$ is plotted in blue. Black lines are fuzzy complement of equation 2.7. Sugeno class complement is shown in green curves.

After a brief overview of fuzzy set theory, next section considers the fuzzy topological space.

2.2.2 Fuzzy Topology: Chang's Approach

The following definition of a fuzzy topological space (fts) is based on C.L. Chang's seminal paper [13].

Definition 2.2.4. A Fuzzy topology is a family $(\delta \subset \mathcal{F}(X))$ of fuzzy sets in X that satisfies the following conditions:

chfTop.1 $\mathbf{0}, \mathbf{1} \in \delta$,

chfTop.2 if $A, B \in \delta$, then $A \wedge B \in \delta$,

chfTop.3 If $A_i \in \delta$ for each $i \in I$, then $\bigvee_I A_i \in \delta$.

δ is called a fuzzy topology for X , and the pair (X, δ) is a fuzzy topological space, or fts for short.

I is an index set and $\mathcal{F}(X)$ represents set of all the fuzzy sets on X . The notation $\mathbf{0}$ is defined by $\forall x \in X, \mathbf{0}(x) = 0$ and $\mathbf{1}$ is defined by $\mathbf{1}(x) = 1$. \bigvee and \wedge are fuzzy union (s-norm) and fuzzy intersection (t-norm), respectively. The elements of δ are called **δ -open fuzzy sets** (or open fuzzy set). The set of complements of open fuzzy sets in topology (X, δ) is denoted by δ' [13]. Elements of δ' are called **δ -closed fuzzy sets** (or closed fuzzy set).

Example 2.2.5. Let $X = \{a, b\}$. Let A be a fuzzy set on X defined by a membership function μ_A :

$$\mu_A(a) = 0.5, \text{ and } \mu_A(b) = 0.4 .$$

$\delta = \{\mathbf{0}, A, \mathbf{1}\}$ is a fuzzy topology for X and (X, δ) is a fuzzy topological space.

Example 2.2.6. Let B_1, B_2 be fuzzy subsets of $X = [0, 1]$ defined as follows:

$$B_1(x) = \begin{cases} 0, & \text{if } 0 \leq x < \frac{1}{3}, \\ \frac{3}{2}x - \frac{1}{2}, & \text{if } \frac{1}{3} \leq x \leq 1. \end{cases}$$

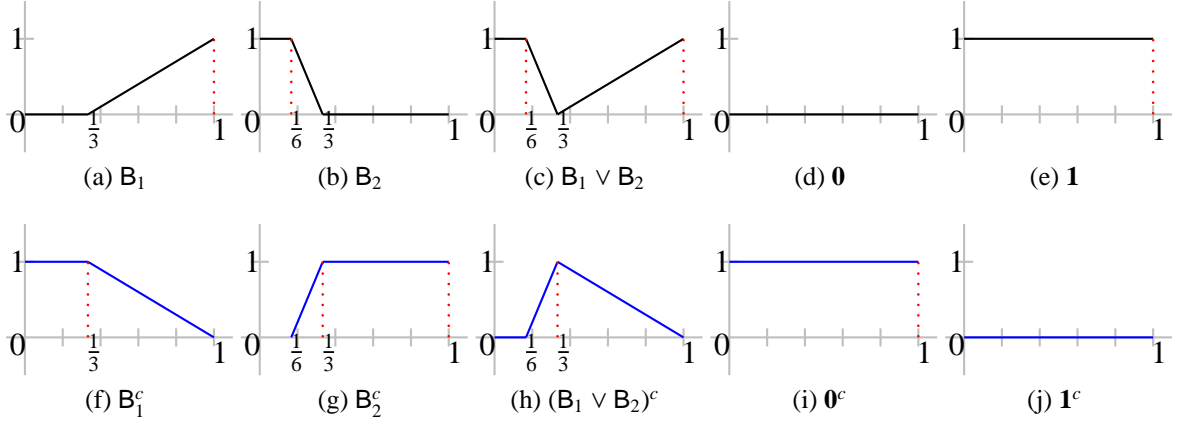


Figure 2.5: Open and closed fuzzy sets of a topology in example 2.2.6 are shown. The fuzzy topology is (X, δ) , where $X = [0, 1]$ and $\delta = \{B_1, B_2, B_1 \vee B_2, \mathbf{1}, \mathbf{0}\}$. Open (Closed) fuzzy sets are shown in first (second) row.

$$B_2(x) = \begin{cases} 1, & \text{if } 0 \leq x < \frac{1}{6}, \\ -6x + 2, & \text{if } \frac{1}{6} \leq x \leq \frac{1}{3}, \\ 0, & \text{if } \frac{1}{3} < x \leq 1. \end{cases}$$

Then $\delta = \{\mathbf{0}, B_1, B_2, B_1 \vee B_2, \mathbf{1}\}$ is a fuzzy topology on X . This example is inspired by [80].

Open and closed fuzzy sets of this topology are shown in figure 2.5.

Definition 2.2.7. A fuzzy set U in a fts (X, δ) is a **neighborhood**, or *nbd* for short, of a fuzzy set A if and only if there exists an open fuzzy set O such that $A \leq O \leq U$, where \leq is fuzzy subsethood (equation 2.8) [13].

It is important to mention that in ordinary topology we talked about the neighborhood of a point (definition 2.1.6) and not the neighborhood of a set. As seen in definition 2.2.7, Chang defined a neighborhood of a fuzzy set. However, like crisp topology, neighborhood of a point was also defined for a fuzzy topology [63]. Let (X, δ) be a fuzzy topology in X , For every $x \in X$, an open supset U of X is called a neighborhood of x , if $x \in U$. Based on two definitions of neighborhood in fuzzy topology, there are two different neighborhood system as well. Chang's defined the neighborhood system of a fuzzy set as the family of all neighborhoods of the fuzzy set A shown by $\mathcal{N}_\delta(A)$ [13]. Liu defined the neighborhood system for a point $x \in X$ as family of all the neighborhoods of x noted by $\mathcal{N}_\delta(x)$ [63].

Definition 2.2.8. Let A and B be fuzzy sets in a fts (X, δ) and let $A \geq B$. Then B is called an **interior fuzzy set** of A iff A is a nbd of B . The union of all interior fuzzy sets of A is called the **interior** of A and is denoted by \mathring{A} [13].

Theorem 2.2.9. Let A be a fuzzy set in a fts (X, δ) . Then \mathring{A} is open and is the largest open fuzzy set contained in A . The fuzzy set A is open iff $A = \mathring{A}$ [13].

Definition 2.2.10. Let (X, δ) be a fuzzy topology on X . The smallest closed fuzzy set \bar{A} containing a fuzzy set A is called the **closure** of A [63].

Closure and interior of a fuzzy set A in a topological space (X, δ) are defined by:

$$\mathring{A} = \vee\{U \mid U \in \delta, U \leq A\}, \quad (2.9)$$

$$\bar{A} = \wedge\{U \mid U^c \in \delta, A \leq U\}, \quad (2.10)$$

where \vee , \wedge and \leq are fuzzy s-norm, fuzzy t-norms and fuzzy subsethood, respectively [63].

Example 2.2.11. Consider the fuzzy topology defined in example 2.2.6. Then $\bar{B}_1 = B_2^c$, $\bar{B}_2 = B_1^c$, $\overline{(B_1 \vee B_2)} = \mathbf{1}$, $(B_1^c)^\circ = B_2$, $(B_2^c)^\circ = B_1$.

As seen in crisp topological space closure operator and interior operator are also defined for fuzzy topology [81].

Definition 2.2.12. An operator $\varphi : \mathcal{F}(X) \rightarrow \mathcal{F}(X)$ is a **fuzzy closure operator** if the following conditions are satisfied:

- $\varphi(\mathbf{0}) = \mathbf{0}$,
- $A \leq \varphi(A)$, $\forall A \in \mathcal{F}(X)$,
- $\varphi(A \vee B) = \varphi(A) \vee \varphi(B)$, $\forall A, B \in \mathcal{F}(X)$,
- $\varphi(\varphi(A)) = \varphi(A)$, $\forall A \in \mathcal{F}(X)$.

Definition 2.2.13. An operator $\theta : \mathcal{F}(X) \rightarrow \mathcal{F}(X)$ is a **fuzzy interior operator** if the following conditions are satisfied:

- $\theta(\mathbf{1}) = \mathbf{1}$,
- $\theta(A) \leq A$, $\forall A, B \in \mathcal{F}(X)$,
- $\theta(A \wedge B) = \theta(A) \wedge \theta(B)$, $\forall A, B \in \mathcal{F}(X)$,
- $\theta(\theta(A)) = \theta(A)$, $\forall A \in \mathcal{F}(X)$.

It is easy to prove that \bar{A} (equation 2.9) and \mathring{A} (equation 2.10) satisfy the above properties for the closure and interior operators. Let us consider the following operators as two examples of fuzzy interior and closure. For a fixed $\alpha \in [0, 1]$, Pascali and Ajmal defined two operations A^α and A_α on $\mathcal{F}(X)$, as follows [81]:

$$A \rightarrow A^\alpha \in \mathcal{F}(X), \quad (2.11)$$

$$A \rightarrow A_\alpha \in \mathcal{F}(X), \quad (2.12)$$

where the fuzzy sets A^α and A_α in X are defined by

$$A^\alpha(x) = \begin{cases} 1, & \text{if } A(x) > \alpha, \\ A(x), & \text{if } A(x) \leq \alpha. \end{cases}$$

and

$$A_\alpha(x) = \begin{cases} A(x), & \text{if } A(x) \geq \alpha, \\ 0, & \text{if } A(x) < \alpha. \end{cases}$$

Proposition 1. *Let $\alpha \in [0, 1]$ be a fixed real number. Then the map $\varphi^\alpha : \mathcal{F}(X) \rightarrow \mathcal{F}(X)$, defined by*

$$A \rightarrow \varphi^\alpha(A) = A^\alpha$$

is a fuzzy closure operator [81].

Proof. Please refer to [81].

□

Proposition 2. *Let $\alpha \in [0, 1]$ be a fixed real number. Then the map $\theta_\alpha : \mathcal{F}(X) \rightarrow \mathcal{F}(X)$,*

defined by

$$A \rightarrow \theta_\alpha(A) = A_\alpha$$

is a fuzzy interior operator [81].

Proof. Please refer to [81] .

□

In addition to Chang's definition of fuzzy topology; there are other ways of defining fuzzy topological spaces. However, since the main focus of this thesis is based on Chang's definition, other interpretations of fuzzy topology (Lowen's, Šostak's and Goguen's approaches) are discussed in appendix A .

2.3 Summary

This chapter contained background information on crisp and fuzzy topologies. The main points of this chapter include:

- Crisp topological space was explained.
- Fuzzy sets were discussed in detail.
- Fuzzy topological space was explained theoretically and accompanied by several examples to clarify the idea.
- In the next chapter new forms of crisp and fuzzy topological operators are proposed and the properties are discussed.

Chapter 3

New Topological Operators

This chapter presents new topological operators namely, crisp (fuzzy) interior and closure with inclusion degree [29]. The newly defined operators are well suited for engineering purposes, when uncertainties and imperfections are inevitable. Inclusion degree has been incorporated into the definitions of the crisp (fuzzy) interior and closure operators, which is the method to deal with uncertainties. In certain situations, one may wish to relax the inclusion constraint and talk about to what extent one set is included in another set. This chapter starts with the definition of inclusion degree in section 3.1. Then inclusion degree is added to the definition of topological operators in section 3.2. In this section, mathematical properties of the operators are also discussed. We also proposed a method to build a fuzzy topology on a collection of fuzzy sets which is discussed in section 3.3. The applications of these operators will be discussed in the next two chapters.

3.1 Inclusion Measure

Although the subsethood relation (\subseteq or \leq (from (2.8))) is considered to be a crisp relation between crisp sets and even between fuzzy sets (based on Zadeh' definition [119]), it is proper to talk about the degree of inclusion. The following definition is the inclusion measure for the crisp sets:

Definition 3.1.1. *Inclusion Measure for Crisp Sets*

Let A and B be members of $\mathcal{P}(X)$ of a set X . An inclusion measure of A in B is defined by (3.1).

$$Inc(A, B) = \begin{cases} \frac{|A \cap B|}{|A|}, & A \neq \emptyset, \\ 0, & A = \emptyset. \end{cases} \quad (3.1)$$

where $|A|$ is the cardinality of the set A . $Inc(A, B)$ is 1, when $A \subseteq B$, it is zero when A and B are disjoint or $A = \emptyset$ and it is $0 \leq Inc(A, B) \leq 1$ for overlapped sets.

Example 3.1.2. *Let*

$$A = \{x_1, x_2, x_3, x_4\},$$

$$B = \{x_1, x_4, x_8, x_9, x_{10}\},$$

$$C = \{x_1, x_2, x_3, x_4, x_5, x_6, x_7, x_8, x_9\},$$

$$D = \{x_{10}, x_{11}\}.$$

From (3.1), observe

$$Inc(A, B) = 0.5, \quad Inc(A, C) = 1, \quad Inc(C, A) = 0.44, \quad Inc(A, D) = 0.$$

This idea is extendable to fuzzy sets. However, when Zadeh defined the subsethood relation for two fuzzy sets, the relation was crisp as written in equation 2.8. There are other interpretations of fuzzy subsethood that are not as rigid as Zadeh's original definition [24, 34, 54, 118].

Motivation to relax the original view of a subset stems from the fact that we may want to talk about inclusion degree or how much one fuzzy set is a subset of another fuzzy set. For $A, B \in \mathcal{F}(X)$, the idea is to define a function $Inc(A, B) \rightarrow [0, 1]$ instead of $Inc(A, B) \rightarrow \{0, 1\}$. There are two well established axiomatic systems for subsethood measures, namely, D. Sinha and E.R. Dougherty [101] and V.R. Young's axioms [118]. The main difference between these axiomatic systems is how they treat containment for crisp sets. D. Sinha and

E.R. Dougherty require that $Inc(A, B) \in \{0, 1\}$ for crisp sets $A, B \in \mathcal{P}(X)$.

There are many interpretations for a fuzzy subethood measure. For instance, B. Kosko [54] defined a measure of subethood of fuzzy sets $A, B \in \mathcal{F}(X)$. If $A(x) \leq B(x)$ holds for all but just a few $x \in X$, A is considered to be a subset of B to some degree.

Definition 3.1.3. Inclusion Measure for Fuzzy Sets: Kosko's Method

Let A and B be two fuzzy sets on X . Kosko's method to measure the amount of inclusion of set A in B defined by

$$Inc_{\{K\}}(A, B) = \frac{\Sigma Count(A \wedge B)}{\Sigma Count(A)}, \quad (3.2)$$

where $\Sigma Count(A \wedge B) = \Sigma Count(A) - \sum_i \max(0, \mu_A(x_i) - \mu_B(x_i))$ and $\Sigma Count(A) = \sum_i \mu_A(x_i)$. μ_A is the fuzzy membership function of the fuzzy set A . $Inc_{\{K\}}(A, B) = 1$ when $A = \mathbf{0}$ [54].

Definition 3.1.4. Inclusion Measure for Fuzzy Sets: Goguen's Method

Let A and B be two fuzzy sets on X . Goguen's inclusion measure of A in B is defined by [34, 118]:

$$Inc_{\{G\}}(A, B) = \frac{1}{n} \sum_x \min(1, 1 - \mu_A(x) + \mu_B(x)), \quad |X| = n. \quad (3.3)$$

Definition 3.1.5. Inclusion Measure for Fuzzy Sets: Inclusion from Implication

Let A and B be two fuzzy sets on X . Inclusion from implication is defined by [118]:

$$Inc_{\{\rightarrow\}}(A, B) = \frac{1}{n} \sum_x (1 - \mu_A(x) + \mu_A(x)\mu_B(x)), \quad |X| = n. \quad (3.4)$$

Example 3.1.6. Let $A = \{(x_1, 0.3), (x_2, 0.35), (x_3, 0.4), (x_4, 0.5), (x_5, 0.3), (x_6, 0.2), (x_7, 0.7)\}$ and $B = \{(x_1, 0.4), (x_2, 0.4), (x_3, 0.45), (x_4, 0.6), (x_5, 0.2), (x_6, 0.1), (x_7, 0.1)\}$ be two fuzzy subsets of the set $X = \{x_1, x_2, \dots, x_7\}$.

According to Kosko's inclusion measure (equation 3.2) :

$$Inc_{\{K\}}(A, B) = 0.7091 ,$$

Also, Gogouen's inclusion measure (equation 3.3) is :

$$Inc_{\{G\}}(A, B) = 0.88 ,$$

Inclusion grade from implication (equation 3.4) is :

$$Inc_{\{\rightarrow\}}(A, B) = 0.73 .$$

In the next section, we incorporate inclusion degree into the crisp and fuzzy interior and closure operators. We call the proposed operators interior (fuzzy interior) with inclusion degree and closure (fuzzy closure) with inclusion degree.

3.2 Interior and Closure with Inclusion Degree

In this section, new forms of crisp and fuzzy interior and closure operators in a solid topological framework are proposed [29]. Inclusion degree enables us to control the relation between boundary and the interior and closure of a set and deal with uncertainties in the definition of topology. First, we consider a crisp topology:

Definition 3.2.1. *Interior Operator with Inclusion Degree for a Crisp Topology*

Given a topology (X, τ) and a set $A \in \mathcal{P}(X)$, the interior of A with inclusion degree $0 \leq \gamma \leq 1$ (denoted by \mathring{A}_γ) is defined to be

$$\mathring{A}_\gamma = \cup\{B \in \tau : Inc(B, A) \geq \gamma\}. \quad (3.5)$$

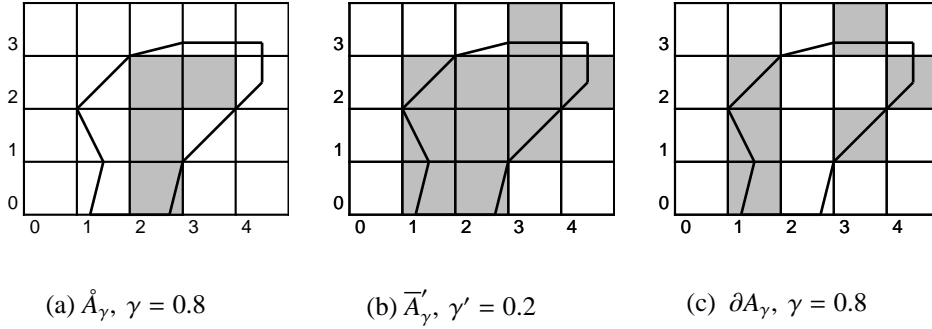


Figure 3.1: A set A in the partitioned space of the form $[j, j + 1)^2$; (a) interior of A , (b) closure of A , (c) boundary of A .

A set $A \in \mathcal{P}(X)$ is called open with respect to inclusion degree γ in the topological space (X, τ) if, and only if, $\mathring{A}_\gamma = A$.

Definition 3.2.2. Closure Operator with Inclusion Degree for Crisp Topology

Given a topology (X, τ) and a set $A \in \mathcal{P}(X)$, the closure of A with inclusion degree $0 \leq \sigma \leq 1$ (denoted by \bar{A}_σ) is defined by

$$\bar{A}_\sigma = \cap \{B \in \tau' : Inc(A, B) \geq \sigma\}. \quad (3.6)$$

where τ' is the set of closed sets. A set $A \in \mathcal{P}(X)$ is called closed with respect to inclusion degree σ and the topological space (X, τ) , if, and only if, $\bar{A}_\sigma = A$.

Example 3.2.3. Consider the example 2.1.19. The space is partitioned into $[j, j + 1)^2$ squares and partition topology (X, τ) is built on it. Set A is shown with solid lines. Figure 3.1 shows interior (\mathring{A}_γ), closure (\bar{A}_γ) and boundary of (∂A_γ) A with the inclusion degree ($\gamma = 0.8$).

For fuzzy operators with inclusion degree, C.L. Chang's definition of fuzzy topology has been considered and inclusion degree has been added to the definition of inclusion used in the interior and closure operators. Fuzzy interior (\mathring{A}) and closure (\bar{A}) defined by definitions 2.9 and 2.10 are based on Zadeh's subsethood in equation 2.8. The following

definitions define the proposed fuzzy closure and fuzzy interior operators with inclusion degree.

Definition 3.2.4. Fuzzy Interior Operator with Inclusion Degree

Given a fuzzy topology (X, δ) and set $A \in \mathcal{F}(X)$, the interior of A with inclusion degree $0 \leq \gamma \leq 1$ (denoted by \mathring{A}_γ) is defined to be

$$\mathring{A}_\gamma = \vee \{B \in \delta : Inc(B, A) \geq \gamma\} . \tag{3.7}$$

A set $A \in \mathcal{F}(X)$ is called open with respect to inclusion degree γ in the fuzzy topological space (X, δ) if and only if $\mathring{A}_\gamma = A$.

In other words, a fuzzy interior with inclusion degree contains some parts of the boundary region (definition 2.1.18) that is more likely (with respect to the user defined inclusion degree) to be in the interior part rather than in the boundary region.

Example 3.2.5. Consider the fuzzy topology (X, δ) defined in example 2.2.6. Figure 3.2 shows the fuzzy open sets B_1 and B_2 in dashed lines. Fuzzy set A is defined by:

$$A(x) = \begin{cases} 1, & \text{if } 0 \leq x < \frac{1}{8}, \\ -8x + 2, & \text{if } \frac{1}{8} \leq x \leq \frac{1}{4}, \\ 0, & \text{if } \frac{1}{4} < x \leq 1. \end{cases}$$

Fuzzy set A is shown with solid line in figure 3.2. Based on Kosko's measure of inclusion (equation 3.2) and with respect to topology (X, δ) , inclusion degrees of the fuzzy open sets in fuzzy set A are:

$$Inc_{\{K\}}(B_1, A) = 0.75 , Inc_{\{K\}}(B_2, A) = 0 , Inc_{\{K\}}(\mathbf{1}, A) = 0.187 ,$$

$$Inc_{\{K\}}(B_1 \vee B_2 , A) = 0.321 , Inc_{\{K\}}(\mathbf{0}, A) = 1 .$$

Based on definition 3.2.6, The interior of A with inclusion degree $\gamma = 0.6$ is $\mathring{A}_{(\gamma=0.6)} = B_1$.

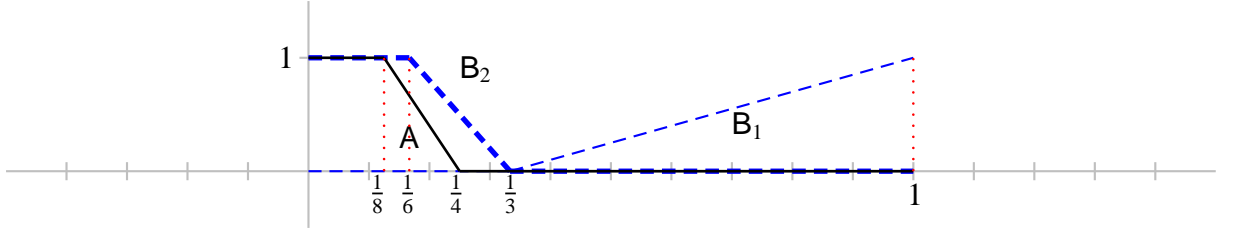


Figure 3.2: Illustration of fuzzy interior operator with inclusion degree. Fuzzy Open sets B_1 and B_2 are shown with dashed lines. B_2 is shown with a thicker dashed line. Fuzzy set A is shown with solid line. The fuzzy topology is (X, δ) , where $\delta = \{B_1, B_2, B_1 \vee B_2, \mathbf{1}, \mathbf{0}\}$. Refer to example 3.2.5 for more details.

By changing γ we may have different results, for instance for $\gamma = 0.8$, $\mathring{A}_{(\gamma=0.8)} = \mathbf{0}$, and fuzzy interior of A , without inclusion degree based on equation 2.10 is $\mathring{A} = \mathbf{0}$.

Definition 3.2.6. Fuzzy Closure Operator with Inclusion Degree

Given a fuzzy topology (X, δ) and a set $A \in \mathcal{F}(X)$, the closure of A with degree $0 \leq \sigma \leq 1$ (denoted by \overline{A}_σ) is defined to be

$$\overline{A}_\sigma = \wedge \{B \in \delta' : \text{Inc}(A, B) \geq \sigma\}, \quad (3.8)$$

where δ' is the set of closed sets. A set $A \in \mathcal{F}(X)$ is called closed with respect to the inclusion degree σ in the fuzzy topological space (X, δ) if and only $\overline{A}_\sigma = A$.

Example 3.2.7. Let us consider example 2.2.6 once again. Let δ' be the set of fuzzy closed sets in the topology (X, δ) . Therefore $\delta' = \{\mathbf{1}, B'_1, B'_2, (B_1 \vee B_2)', \mathbf{0}\}$, where B' is a fuzzy complement of B :

$$B'_1(x) = \mathbf{1} - B_1(x) = \begin{cases} 1, & \text{if } 0 \leq x < \frac{1}{3}, \\ \frac{3}{2} - \frac{3}{2}x, & \text{if } \frac{1}{3} \leq x \leq 1. \end{cases}$$

$$B'_2(x) = \mathbf{1} - B_2(x) = \begin{cases} 0, & \text{if } 0 \leq x < \frac{1}{6}, \\ 6x - 1, & \text{if } \frac{1}{6} \leq x \leq \frac{1}{3}, \\ 1, & \text{if } \frac{1}{3} < x \leq 1. \end{cases}$$

and

$$(\mathbf{B}_1 \vee \mathbf{B}_2)' = \mathbf{B}'_1 \wedge \mathbf{B}'_2 = \begin{cases} 0 & \text{if } 0 \leq x < \frac{1}{6}, \\ 6x - 1, & \text{if } \frac{1}{6} \leq x \leq \frac{1}{3}, \\ \frac{3}{2} - \frac{3}{2}x, & \text{if } \frac{1}{3} < x \leq 1, \end{cases}$$

Let a fuzzy set A be:

$$A(x) = \begin{cases} 0, & \text{if } 0 \leq x < \frac{3}{14}, \\ 28x - 6, & \text{if } \frac{3}{14} \leq x \leq \frac{1}{4}, \\ 1, & \text{if } \frac{1}{4} < x \leq \frac{2}{5}, \\ -10x + 5, & \text{if } \frac{2}{5} < x \leq \frac{1}{2}, \\ 0, & \text{if } \frac{1}{2} < x \leq 1. \end{cases}$$

Based on equation 3.2, we have the following inclusion measures:

$$Inc_{\{K\}}(A, \mathbf{B}'_1) = 0.98, \quad Inc_{\{K\}}(A, \mathbf{B}'_2) = 0.87, \quad Inc_{\{K\}}(A, \mathbf{B}'_1 \wedge \mathbf{B}'_2) = 0.86,$$

$$Inc_{\{K\}}(A, \mathbf{1}) = 1, \quad Inc_{\{K\}}(A, \mathbf{0}) = 0.$$

Therefore, based on equation 3.2.6, fuzzy closure of A with inclusion degree σ , \bar{A}_σ , is:

$$\bar{A}_{(\sigma=0.9)} = \wedge\{\mathbf{B}'_1, \mathbf{1}\} = \mathbf{B}'_1.$$

$$\bar{A}_{(\sigma=0.8)} = \wedge\{\mathbf{B}'_1, \mathbf{B}'_2, \mathbf{B}'_1 \wedge \mathbf{B}'_2, \mathbf{1}\} = \mathbf{B}'_1 \wedge \mathbf{B}'_2.$$

Fuzzy closure of A without inclusion degree, based on equation 2.9 is $\bar{A} = \mathbf{1}$.

Based on these simple examples 3.2.5 and 3.2.7, it is obvious that fuzzy closure and interior operators with inclusion degree, allow for a controlled degree of freedom in form of uncertainty, misclassification or error in the system.

It is expected that the proposed closure and interior operators with the inclusion degree do not satisfy the same properties as the usual fuzzy closure and fuzzy interior operators

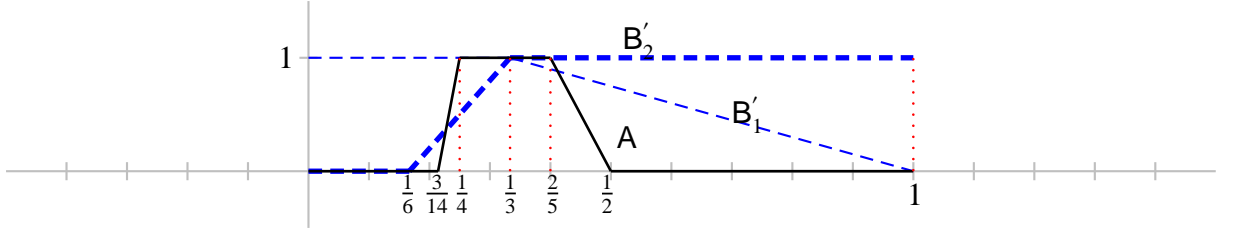


Figure 3.3: Illustration of fuzzy closure operator with inclusion degree. Fuzzy closed sets B'_1 and B'_2 are shown with dashed lines. B'_2 is shown with a thicker dashed line. Fuzzy set A is shown with solid line. The fuzzy topology is (X, δ) , where $\delta = \{B_1, B_2, B_1 \vee B_2, \mathbf{1}, \mathbf{0}\}$. Refer to example 3.2.7 for more details.

mentioned in definitions 2.2.12 and 2.2.13. The following two propositions enunciate the properties of the proposed closure and interior operators for fuzzy topologies. The crisp operators have similar properties.

Proposition 3. Let (X, δ) be a fuzzy topology on set X and let $A \in \mathcal{F}(X)$ be a fuzzy set. \bar{A}_σ represents fuzzy closure with inclusion degree σ . The following properties hold:

$$fC\sigma.1 \quad \bar{\mathbf{0}}_\sigma = \mathbf{0},$$

$$fC\sigma.2 \quad \sigma \leq \text{Inc}(A, \bar{A}_\sigma) \leq 1,$$

$$fC\sigma.3 \quad \overline{(A_1 \vee A_2)_\sigma} \leq \bar{A}_{1\sigma} \vee \bar{A}_{2\sigma},$$

$$fC\sigma.4 \quad \overline{(\bar{A}_\sigma)_\sigma} = \bar{A}_\sigma,$$

$$fC\sigma.5 \quad \text{Inc}(\bar{A}_\sigma, \bar{A}) = 1, \text{ where } \bar{A} \text{ is Chang's fuzzy closure (definition 2.9).}$$

$$\text{Proof. } fC\sigma.1 \quad \bar{\mathbf{0}}_\sigma = \wedge \{B \in \delta' : \text{Inc}(\mathbf{0}, B) \geq \sigma\} = \mathbf{0} \wedge \{B \in \delta' - \{\mathbf{0}\} : \text{Inc}(\mathbf{0}, B) \geq \sigma\} = \mathbf{0}.$$

Since $\mathbf{0}$ is a closed set in the topology (X, δ) , then we have $\bar{\mathbf{0}}_\sigma = \mathbf{0}$.

$$fC\sigma.2 \quad \text{Let } \bar{A}_\sigma = \wedge \{B \in \delta' : \sigma \leq \text{Inc}(A, B) \leq 1\} = \wedge_{i \in J} B_i, \text{ where } J \text{ is the index set. } \text{Inc}(A, \bar{A}_\sigma) = \text{Inc}(A, \wedge_{i \in J} B_i) = \wedge \{\text{Inc}(A, B_i) : i \in J\} = \sigma_1 \geq \sigma. \text{ So } \sigma \leq \text{Inc}(A, \bar{A}_\sigma) \leq 1.$$

$$fC\sigma.3 \quad \bar{A}_{1\sigma} \subseteq \overline{(A_1 \vee A_2)_\sigma} \text{ and } \bar{A}_{2\sigma} \subseteq \overline{(A_1 \vee A_2)_\sigma} \text{ therefore } \bar{A}_{1\sigma} \vee \bar{A}_{2\sigma} \subseteq \overline{(A_1 \vee A_2)_\sigma}. \text{ Unlike the classic form of closure (i.e., closure operator without inclusion degree), } \overline{(A_1 \vee A_2)_\sigma} \subseteq \bar{A}_{1\sigma} \vee \bar{A}_{2\sigma}, \text{ does not hold generally.}$$

fC σ .4 Since $\overline{A_\sigma}$ is a closed set, we have $\overline{(\overline{A_\sigma})_\sigma} = \overline{A_\sigma}$.

fC σ .5 $\overline{A_\sigma} = \wedge\{\mathbf{B} \in \delta' : Inc(\mathbf{B}, A) \geq \sigma\} \leq \wedge\{\mathbf{B} \in \delta' : Inc(\mathbf{B}, A) \geq 1\} = \overline{A}$.

□

Proposition 4. *Let (X, δ) be a fuzzy topology on set X and let $A \in \mathcal{F}(X)$ be a fuzzy set. \mathring{A}_γ represents the interior of set A with inclusion degree γ . The following properties hold:*

fI γ .1 $\mathring{1}_\gamma = \mathbf{1}$,

fI γ .2 $\gamma \leq Inc(\mathring{A}_\gamma, A) \leq 1$,

fI γ .3 $(A_1 \wedge A_2)_\gamma^\circ \leq \mathring{A}_{1\gamma} \wedge \mathring{A}_{2\gamma}$,

fI γ .4 $(\mathring{A}_\gamma)_\gamma^\circ = \mathring{A}_\gamma$,

fI γ .5 $Inc(\mathring{A}, \mathring{A}_\gamma) = 1$.

Proof. *fI γ .1* By definition, we have $\mathring{1}_\alpha = \cup\{\mathbf{B} \in \delta : Inc(\mathbf{B}, \mathbf{1}) \geq \alpha\} = \mathbf{1}$.

fI γ .2 Let $\mathring{A}_\gamma = \vee\{\mathbf{B} \in \delta : Inc(\mathbf{B}, A) \geq \gamma\} = \vee_{i \in J}\{\mathbf{B}_i\}$, where J is an index set. $Inc(\mathring{A}_\gamma, A) = Inc(\vee_{i \in J} \mathbf{B}_i, A) = \vee\{Inc(\mathbf{B}_i, A) : i \in J\} = \gamma_1 \geq \gamma$. Therefore $\gamma \leq Inc(\mathring{A}_\gamma, A) \leq 1$.

fI γ .3 $A_1 \wedge A_2 \leq A_1$ and $A_1 \wedge A_2 \leq A_2$ and both forms of intersection are also true when applied with the interior operation with inclusion degree γ , i.e., $(A_1 \wedge A_2)_\gamma^\circ \leq \mathring{A}_{1\gamma}$ and $(A_1 \wedge A_2)_\gamma^\circ \leq \mathring{A}_{2\gamma}$; Therefore, $(A_1 \wedge A_2)_\gamma^\circ \leq \mathring{A}_{1\gamma} \wedge \mathring{A}_{2\gamma}$. Unlike the classical form of interior, $(A_1 \wedge A_2)_\alpha^\circ \leq \mathring{A}_{1\gamma} \wedge \mathring{A}_{2\gamma}$ does not always hold.

fI γ .4 \mathring{A}_α is an open set with respect to inclusion degree α ; therefore $(\mathring{A}_\alpha)_\alpha^\circ = \mathring{A}_\alpha$.

fI γ .5 $\mathring{A} = \vee\{\mathbf{B} \in \delta : Inc(\mathbf{B}, A) = 1\} \leq \vee\{\mathbf{B} \in \delta : Inc(\mathbf{B}, A) \geq \gamma\}$.

□

In the following two propositions, we demonstrate the relation between fuzzy interior (closure) of a set A and fuzzy interior (closure) of a set A with different inclusion degrees.

Proposition 5. *Let $\{\gamma_1, \dots, \gamma_i, \dots, \gamma_n\}$ be a set of real numbers where $0 \leq \gamma_1 \leq \gamma_2 \dots \leq \gamma_n < 1$. Let (X, δ) be a fuzzy topology and $A \in \mathcal{F}(X)$, then we have $\mathring{A} \leq \mathring{A}_{\gamma_n} \leq \dots \leq \mathring{A}_{\gamma_1}$.*

Proof. Let $0 < \gamma_i \leq \gamma_j \leq 1$ and (X, δ) be a fuzzy topology. The interior of a set A with the inclusion degree γ_j is defined by $\mathring{A}_{\gamma_j} = \vee\{\mathbf{B} \in \delta : Inc(\mathbf{B}, A) \geq \gamma_j\} \leq \vee\{\mathbf{B} \in \delta : Inc(\mathbf{B}, A) \geq \gamma_i\} = \mathring{A}_{\gamma_i}$. Also, $\mathring{A} = \vee\{\mathbf{B} \in \delta : Inc(\mathbf{B}, A) = 1\} \leq \vee\{\mathbf{B} \in \delta : Inc(\mathbf{B}, A) \geq \gamma_j \leq 1\}$.

□

Proposition 6. *Let $\{\sigma_1, \dots, \sigma_i, \dots, \sigma_n\}$ be a set of real numbers where $0 \leq \sigma_1 \leq \sigma_2 \dots \leq \sigma_n < 1$. Let (X, δ) be a fuzzy topology and $A \in \mathcal{F}(X)$, then we have $\bar{A}_{\sigma_1} \leq \dots \leq \bar{A}_{\sigma_n} \leq \bar{A}$.*

Proof. The proof is similar to the proof of proposition 5 .

□

The following section defines the process of building a crisp (fuzzy) topology based on crisp (fuzzy) collection of a set. It may be seen irrelevant to this chapter at this point, but we will use this concept in chapter 4.

3.3 Fuzzy Topology for a Collection of Fuzzy Sets

We start this section with the following propositions (7,8) from M.C Gemignani's book [32, p. 43-44]). Then we extend the idea to fuzzy topological space.

Proposition 7. *Let X be any set. Assume \mathcal{B} to be a family of subsets of X such that*

- (i) X is the union members of \mathcal{B}
- (ii) the intersection of any two members of \mathcal{B} is the union of members of \mathcal{B} .

Define $\tau = \{U \subset X \mid U \text{ is the union of members of } \mathcal{B}\}$. Then τ is a topology on X and \mathcal{B} is a basis for τ .

Proof. For proof, please refer to [32, p. 44]).

□

Proposition 8. Let X be any set and suppose \mathcal{S} to be a collection of subsets of X . Set

$$\mathcal{B} = \{B \mid B \text{ is the intersection of finitely many sets in } \mathcal{S} \text{ or } B = X\}.$$

Then \mathcal{B} is the basis for a topology τ on X defined by

$$\tau = \{U \mid U \text{ is the union of members of } \mathcal{B}\}. \quad (3.9)$$

Proof. For proof, please refer to [32, p. 45]).

□

Example 3.3.1. Let \mathcal{S} be a partition of X , and $\mathcal{B} = \{B \mid B \in \mathcal{S}\}$, based on proposition 8, \mathcal{B} is a basis for topology τ on X defined by equation 3.9. Based on definition 2.1.9, τ is a partition topology on X .

Example 3.3.2. Let \mathcal{S} be a covering on a set X , then based on proposition 8, it is possible to define a topology on X based on \mathcal{S} .

We extend this idea to fuzzy topology and collection of fuzzy subsets of a set X .

Proposition 9. Let X be any set. Assume \mathfrak{B} to be a family of fuzzy subsets of X such that

- (i) $\mathbf{1}$ is the union members of \mathfrak{B} ,
- (ii) the fuzzy intersection of any two members of \mathfrak{B} is the union of members of \mathfrak{B} .

Define $\delta = \{U \in \mathcal{F}(X) \mid U \text{ is the union of members of } \mathfrak{B}\}$. Then δ is a fuzzy topology on X and \mathfrak{B} is a basis for δ . $\mathcal{F}(X)$ is the collection of fuzzy sets on X .

Proof. We must verify that δ satisfies Definition 2.2.4.

- By hypothesis $\mathbf{1}$ is the union members of \mathfrak{B} , and by (ii) $\mathbf{0}$ is the union of the empty subfamily of \mathfrak{B} . Therefore $\mathbf{0}$ and $\mathbf{1}$ are members of δ .
- Suppose U and V are in δ . We have to show that $U \wedge V \in \delta$. By hypothesis $U = \bigvee_I B_i$ and $V = \bigvee_J B_j$, where I and J are appropriate index sets and where B_i and B_j are members of \mathfrak{B} for each $i \in I$ and $j \in J$. Then

$$U \wedge V = \bigvee_{I,J} (B_i \wedge B_j) .$$

Since each $B_i \wedge B_j$ is the union members of \mathfrak{B} by (ii), $U \wedge V$ is the union of members of \mathfrak{B} , and hence is in δ . The intersection of any two members of δ is again a member of *delta*.

- If $\{U_k\}$, $k \in K$, is any family of members of δ , then U_k s the union of members of \mathfrak{B} for each $k \in K$. Therefor $\bigvee_K U_k$ is the union of members of \mathfrak{B} , and hence is in δ . That is, the union of any family of members of δ is again a member of δ . Therefore δ satisfies the definition of fuzzy topology on X .

□

Proposition 10. *Let X be any set and suppose \mathfrak{S} to be a collection of fuzzy subsets of X .*

Set

$$\mathfrak{B} = \{B \mid B \text{ is the fuzzy intersection of finitely many sets in } \mathfrak{S} \text{ or } B = \mathbf{1}\} .$$

Then \mathfrak{B} is the basis for a fuzzy topology δ on X defined by

$$\delta = \{U \mid U \text{ is the union of members of } \mathfrak{B}\} . \quad (3.10)$$

Proof. We must verify that \mathfrak{B} satisfies conditions (i) and (ii) of proposition 9.

- By hypothesis, $\mathbf{1} \in \mathfrak{B}$. Therefore, $\mathbf{1}$ is the union of members of \mathfrak{B} .

- If B_1 and B_2 are both members of \mathfrak{B} , Then both are intersection of finitely many members of \mathfrak{B} . Therefore $B_1 \wedge B_2$ is itself intersection of finitely many numbers of \mathfrak{B} and hence are in \mathfrak{B} . The intersection of any two members of \mathfrak{B} is thus again a member of \mathfrak{B} . Therefore, by proposition 9, \mathfrak{B} is the basis for the fuzzy topology δ as defined above. Clearly $\mathfrak{B} \subset \delta$.

□

Example 3.3.3. Let U, V be fuzzy subsets of $X = [0, 1]$ defined as follows:

$$U(x) = \begin{cases} 1, & \text{if } 0 \leq x < \frac{1}{3}, \\ -6x + 3, & \text{if } \frac{1}{3} \leq x \leq \frac{1}{2} \\ 0, & \text{if } \frac{1}{2} < x \leq 1. \end{cases}$$

$$V(x) = \begin{cases} 0, & \text{if } 0 \leq x < \frac{1}{3}, \\ 6x - 2, & \text{if } \frac{1}{3} \leq x \leq \frac{1}{2}, \\ 1, & \text{if } \frac{1}{2} < x \leq 1. \end{cases}$$

Let $\mathfrak{C} = \{U, V\}$ be a collection of fuzzy subsets on $X = [0, 1]$. Let

$$\begin{aligned} \mathfrak{B} &= \{B \mid B \text{ is the fuzzy intersection of finitely many sets in } \mathfrak{C} \text{ or } B = \mathbf{1}\} \\ &= \{\mathbf{1}, \mathbf{0}, U, V, U \wedge V\}. \end{aligned}$$

Based on proposition 10, \mathfrak{B} is the basis for a topology δ on X defined by

$$\begin{aligned} \delta &= \{W \mid W \text{ is the union of members of } \mathfrak{B}\} \\ &= \{\mathbf{1}, \mathbf{0}, U, V, U \vee V, U \wedge V\}. \end{aligned}$$

Figure 3.4 shows the fuzzy subsets of U and V . The open sets of the basis of the topology δ are shown in figure 3.5.

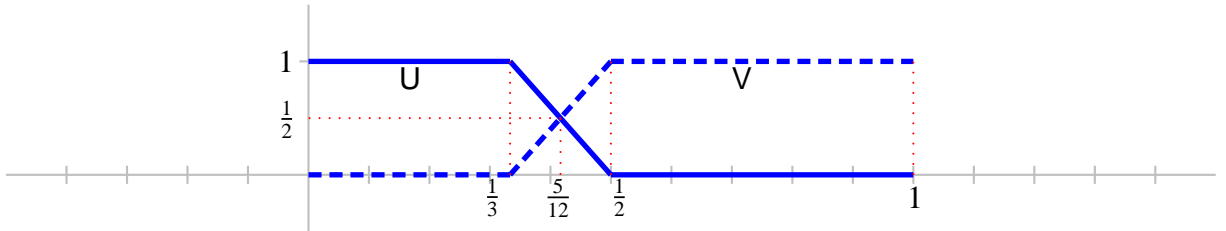


Figure 3.4: Fuzzy subsets U (solid line) and V (dashed line) of example 3.3.3 are shown.

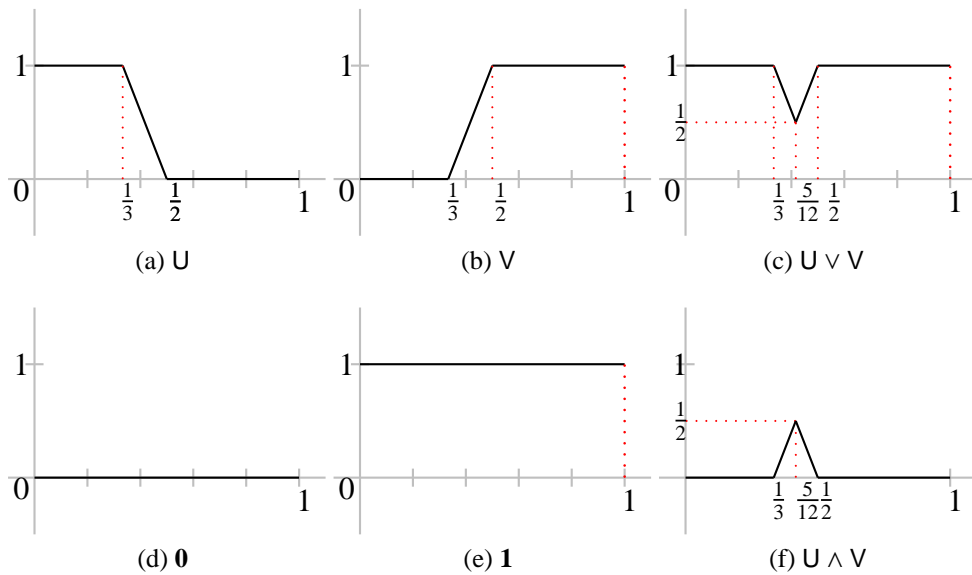


Figure 3.5: Open fuzzy sets of the fuzzy topology (X, δ) defined in example 3.3.3 are shown .

3.4 Summary

The main points of this chapter include:

- Fuzzification of subsethood for both crisp and fuzzy sets was explained. Different inclusion measure were considered.
- The main contribution of this chapter is the introduction of inclusion degree into the definition of interior and closure operator for both crisp and fuzzy topologies. The idea was explained in detail and the properties of new operators were discussed. Different examples were designed to explain the concept clearly.
- We also proved two new propositions 9 and 10 for fuzzy topologies. Building the fuzzy topology (X, δ) from a collection of fuzzy subsets on X have been proposed in these propositions.
- Next chapters utilizes the new crisp/fuzzy interior and closure operators with inclusion degree in three different areas namely, mathematical morphology and image database classification.

Part II

Applications

This part describes the applications of the proposed topological operators: closure and interior operator with inclusion degree. Three areas are considered for applying the proposed operators. Their Topological properties make them suitable for the proposed operators. Mathematical morphology have similar operators as topological closure and interior. Moreover, we proposed to apply the new operators on image database classification and on shape classification. This part is organized in two chapters as shown in figure 3.6. Each chapter describes the application of the proposed operators in one of the above mentioned areas.

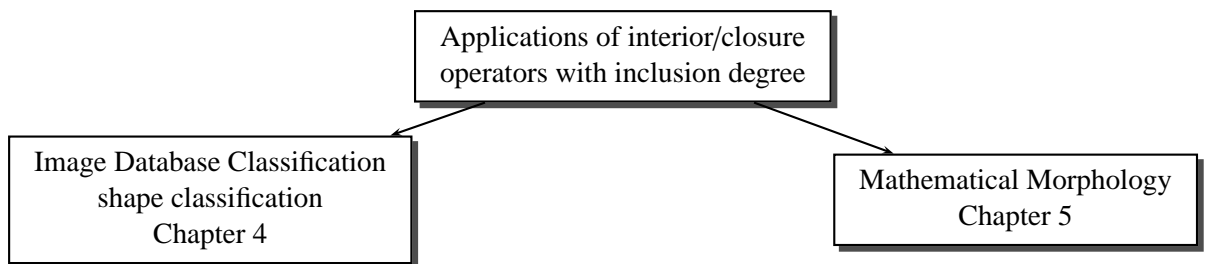


Figure 3.6: Our proposed topological operators (fuzzy interior/closure operators with inclusion degree) have been applied in two different areas, namely: image/shape database classification and mathematical morphology .

Chapter 4

Interior Operator with Inclusion Degree Applied to Image Database Classification

We considered the problem of image/shape database classification in this chapter. These applications demonstrate the effectiveness and applicability of our proposed interior and closure operators with inclusion degree. An image in large image databases may belong to one or more categories. An image category (image concept) is represented by a set of images with visual and semantic similarities. We propose a topological framework to model each image concept and also classify images. Here, we briefly mention the problem statement:

Problem Statement: Crisp Case

Let $\mathcal{X}_i \subset \mathcal{P}(X)$ be a collection of subsets of the set X , where $i \in \{0, 1, \dots, n\}$. Each \mathcal{X}_i have similar elements and represents a ‘concept i ’. By ‘concept’, we mean the elements with semantic or visual similarities. Let us build a topology (X, τ_i) based on the collection \mathcal{X}_i (refer to proposition 8 for more information). Let $\mathcal{Y} \subset \mathcal{P}(X)$ and $\mathring{\mathcal{Y}}_{\tau_i, \gamma}$ be the interior of \mathcal{Y}

with inclusion degree γ with respect to topology τ_i . Define y_i as follows:

$$y_i = \mathcal{Y} \setminus \mathring{\mathcal{Y}}_{\tau_i, \gamma},$$

where \setminus is the set difference. We argue that if open sets in the topology (X, τ_i) are more similar to elements of \mathcal{Y} , then y_i is almost equal to \emptyset . In other words, \mathcal{Y} could be rebuilt with open sets in topology τ_i . We conclude that \mathcal{Y} more likely belongs to the concept depicted by \mathcal{X}_i . We considered the interior operator with inclusion degree to deal with small error and imperfections. We extended the idea to fuzzy topologies and adapted the idea for shape classification and image database classification and showed the validity of the argument. We explained the idea in more detail in section 4.1.4.

This chapter is organized as follows: Section 4.1 addressed the related works in image database classification, shape classification and topological approaches toward image processing problems. Section 4.1.4 explain the proposed topological classification method for image databases. Feature extraction is explained in section 4.2 . Different shape features and color features have been explained in this section. Shape classification is addressed in section 4.3. Color image database classifications considered in section 4.4. Finally, this chapter is summerized in section 4.5 .

4.1 Related Works

This section addressed the related works to image database classification, shape classification and topological approaches toward image processing. Image database classification is the task of identifying semantically coherent categories for image databases. This term, image database classification, has been used mainly for color image databases. In case of binary images, the term shape classification has been used in the literature. Finally, we addressed the research related to application of topological spaces in image processing .

4.1.1 Image Database Classification

An image category is represented by a set of images with visual and semantic similarities [121]. Classification methods capable of handling uncertainties associated with image content are needed because the number, size and complexity of image databases are rapidly increasing. Improved digital technology in capturing images/videos and the growth of the internet have contributed to the growth of image database. The main motivation underlying image database classification is the need for semantic organization to facilitate image searches and image database browsing.

Image database classification, semantic image annotation and content based image retrieval (CBIR) systems are main areas of research concerning image databases. Commonly, CBIR systems find images similar to a user-specified query image. The goal of semantic image annotation is to extract the semantic labels or captions that best describes a query image [10]. Image database classification may be considered as a main step in image annotation that facilitates semantically adaptive searching methods for CBIR systems in narrowing down the search range in an image database [114].

Generally speaking, classification techniques consist of three parts, namely, representation (feature extraction), classifier design (training) and test (system usage). For image database classification, feature extraction is applied either to a whole image like global histogram based techniques [14, 22, 111], or to regions or blocks of an image [91, 114, 121]. For instance, in [14], three dimensional image color histograms are considered as an image representation in a 16^3 bins histogram. In [91], an image is divided into 5 blocks and for each block, the mean and standard deviation in the color space and the average energy in each high-frequency sub band on the luminance component of the image are calculated. Feature extraction from the image regions is represented in [114]. In this work, an image is segmented in to the regions. Color, texture and shape features are extracted from each segment. Averages of color components in LUV space and square roots of the second order moment of wavelet coefficients in the HL band, LH and HH bands are calculated. Shape is represented by normalized inertia of order 1 to 3. For more information on various

techniques for feature extraction for visual objects refer to [77].

There are many choices for the classifiers. However, the high dimensional feature vectors make image database classification challenging. Both instance based learning and eager learning classifiers have been used in classifying images. These types of classifier have been explained in subsection 4.1.4. Examples of eager (parametric) classifiers used in image database classification are support vector machines (SVM) [14, 35, 91] and the 2D hidden Markov model [58]. An example of an instance based classifier used for image database classification is Nearest Neighbor (NN) classifier (see, *e.g.*, [5]). The nature of categories differs in various systems. For instance, only four semantic categories (textured-non textured, graph and photograph) are considered in [114], whereas other systems use the narrower categorizations [14, 35]. The image database classification method reflects recent work on solving the image correspondence problem using fuzzy, near and rough set methods [6, 27, 30, 42, 79, 84, 86, 87, 93],(see, also, [76, 85]).

4.1.2 Shape Classification

Shape classification is the fundamental step in object recognition task. It requires presenting the object in feature space, such that similar shapes would be near each other. The task is a challenging one, since rotation, translation or angle of view make one object completely different. Shape classification task has two steps: shape feature extraction and classifying shape features. Shape features should have some essential properties:

- **identifiability:** shapes which are found perceptually similar by human perception,
- **translation, rotation and scale invariance,**
- **noise resistance:** features must be resistance to the noise and small imperfections in shape contour and etc.
- **occlusion invariance:** if some parts of the object occluded by other objects or missing, the feature of the remaining part be unchanged with respect the original shape features.

There is a wide variety of shape features that could be used in the shape classification problem. The shape features could be broadly classified to: polygonal approximation [57], moments [60] [61] [59] [31], scale space methods [73], shape transform domains like Fourier domain and wavelet domain, spatial features and one dimensional functions [71]. Y. Mingqiang presented a comprehensive survey on shape feature extraction techniques [71]. There are several works presented for shape classification. However the main difference is in the feature extraction part and most of the techniques used Bayesian classifier for the classification part. For instance, B. Wang introduced a method to define shape tree from object skeleton and then classify the feature vectors by a Bayesian classifier [113]. X. Bai introduced a new technique which could be implemented on top of any available shape classification or shape clustering technique and could improve the result of the available methods. The new similarity is learned iteratively so that the neighbors of a given shape influence its final similarity to the query. X. Yang proposed the use of pruned skeleton and a Bayesian Classifier [117]. A three level statistical framework proposed by K. Sun [107]. He implemented three distinct models for database, class and part. The idea extends the advantage of example based approach by allowing shapes of a class to contribute to the classification of an input shape of that class.

4.1.3 Topological Approaches in Image Processing

Basic topological concepts have been applied to the field of image processing previously. For instance, Kovalevsky's published a paper on finite topology and image analysis [55]. The paper dealt with the idea of encoding images as cellular complexes and image segmentation is considered as splitting a cellular complex into blocks of cells. He utilized a theory indicating that *'any finite topological space with the separation property [T0-property] is isomorphic to an abstract cellular complex'*. In [51] a fuzzy set U_x is defined as the neighborhood of point $x \in X$, where X is the entire space. Since X represents all the finite pixel sets, the fuzzy topology formed on the neighbors is called a finite fuzzy topology. The topological concepts of interior, closure and boundary is defined by using the neighbor-

hood as open sets. Polkowski also uses the idea of neighborhood to define the topology on image space. He splits the image plane into non-overlapping squares and use them as open sets [89]. In more recent works, fuzzy topology is used for object extraction from images. An object on the image considered as a fuzzy object having interior, boundary region and background [62, 99, 100]. Tang utilized fuzzy sets and fuzzy topology to define fuzzy spatial objects and the topological relations (*e.g.*, disjoint, contain, inside, equal, meet, covers, covered by, overlap) between them in geographic information systems (GIS) [109].

Another important usage of topology is in the definition of mathematical morphology (MM). It was first introduced by G. Matheron and J. Serra [67, 97]. MM is a theory for shape analysis and processing geometrical forms inside an image. Basic mathematical morphological operators resemble the basic topological operators. For instance, topological closure and interior are comparable with closing (dilation) and opening (erosion) operators in MM [2, 89, 97, 105].

4.1.4 Our proposed Classification Method

We have proposed a classification technique particularly for image databases based on interior operator with inclusion degree [28]. Generally speaking, classification techniques have two broad categories, namely, lazy also known as instance based learner and eager learners [72]. Instance based learners simply store the training examples and postpone the learning process to the time of encountering a query (test) sample. Each time a new query instance enters the system, its relationship to the previously stored examples (training set) is examined and the target function value (appropriate class in case of classification) is assigned to the test sample. In contrast to lazy learners, eager learning methods generalize the training data before receiving queries. Eager learners do not keep the training samples. Examples of instance based learning are k-nearest neighbor [82], locally weighted regression [18] and case based reasoning [53]. Artificial neural networks [43, 110], naive Bayes [17, 25, 72], radial basis functions [8, 90] are examples of eager learners.

Our proposed method of classification mostly falls into the instance based learning

methods. For each class of samples, a training set is selected that contains a few samples of that class. If applicable, each training sample is partitioned into its building blocks. For instance, in case of image database classification, each image is being segmented using a segmentation method (We used a Gaussian mixture model and expectation maximization technique to partition each image. This will be discussed in subsection 4.4.1). We call each of these parts, a training instance. Then appropriate features are extracted from each training instance. The goal is to utilize these extracted features as open fuzzy sets. Therefore, the features are in the form of one dimensional or two dimensional feature vectors that can be considered as 1D or 2D open fuzzy sets.

Each training instance in the feature space acts as an open fuzzy set in the language of topology. For each category, a fuzzy topology is constructed from the open sets in that category (refer to chapter 3 proposition 9 and 10). Hence, for each class there is a corresponding topological space (subspace to be exact). The procedure of the training phase of the classification method is shown in figure 4.1. The goal is to find the interior of the test image with respect to the corresponding topology of each class. The difference between the query and its interior is our measure for classification. The low value for this measure for a specific class means that the query image may belong to that class. Training instances in each category act as building blocks of that category. So the goal is to use them to reconstruct the test sample. If the reconstructed test sample is similar to itself then the test sample may belong to that category. To reconstruct the test sample, its interior with inclusion degree with respect to different topological spaces is utilized.

We formulated the problem for a crisp topology in the introduction section of chapter 4. However, we used a fuzzy version of that statement for image database classification. The problem is formulated as follows:

Problem Formulation:

Let $C_i \subset DB$ be a set of images used as a training set for concept i , where $i = 1, \dots, n$ and DB is an image database. Let $C_i = \{I_{ji}\}$ be a set of training images for concept i , where $j = 1, \dots, m$, (for instance, five images from the concept ‘*Beach*’ are selected). Each image

is segmented by the EM segmentation technique (Discussed in section 4.4.1). Therefore, concept i 's training set could be shown by a set of m training images:

$$C_i = \{I_{i1}, I_{i2}, \dots, I_{im}\}$$

which converted to a set of n image segments (connected components):

$$S_i = \{s_{i1}, s_{i2}, \dots, s_{in}\}$$

From each image segment in training set of concept i , we extract k different feature vectors in the form of fuzzy sets:

$$F_{i1} = \{f_{i11}, f_{i12}, \dots, f_{i1n}\}$$

...

$$F_{ik} = \{f_{ik1}, f_{ik2}, \dots, f_{ikn}\}$$

and then we build fuzzy topologies with respect to feature vectors extracted from concept i :

$$(F_j, \delta_{ij})$$

where $j = 1, \dots, k$ and F_j is the feature space corresponding to the feature j and δ_{ij} is the fuzzy topology for concept i and feature space j . Please refer to proposition 3.3 for building a fuzzy topology from a collection of fuzzy sets. So each concept is modeled with a set of fuzzy topologies built based on feature vectors extracted from the training set.

To test the system, a query (test) image is chosen by a user. Image segmentation is applied on the query and feature vectors in the form of fuzzy sets are extracted from it. Then interior of the test image is calculated with respect to different topologies in the system (one set of topologies for each concept). The difference between the interior of the query and the query is our measure to determine the category of the query image. The query belongs to

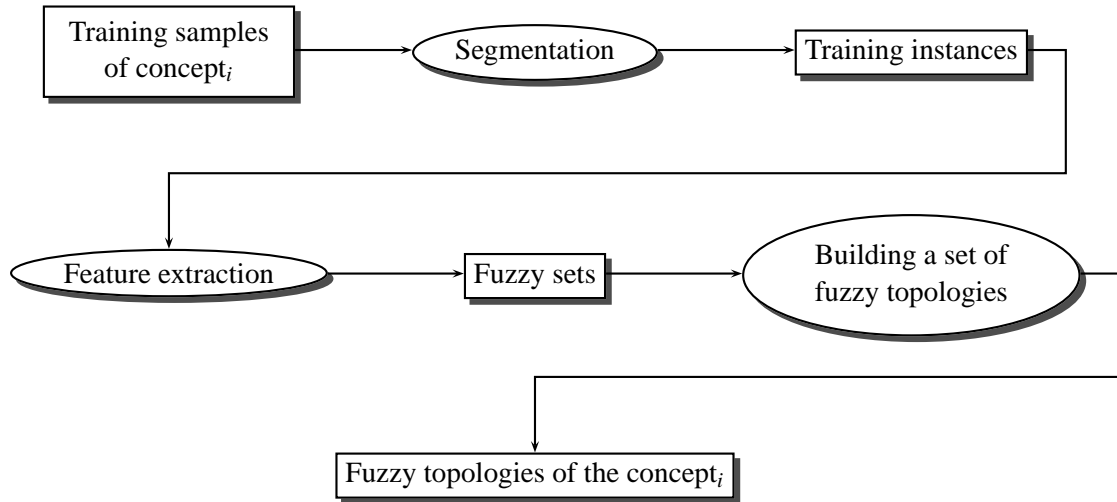


Figure 4.1: Training phase of our proposed classification method for concept_{*i*} .

the category that has the lowest difference. It means that the corresponding topology of that concept was able to build (reconstruct) the query image better. That implicitly implies that the open sets in the topology are resembling the elements of the query image. The method originally proposed for color image data base classification. However to test the effectiveness of the proposed classification method, we also test it for shape classification which is discussed in section 4.3 . Image database classification results are explained in section 4.4.

4.2 Feature Extraction

This section discussed the types of the features extracted from an image segment. The process of obtaining an image segment has been discussed later in subsection 4.4.1. Different types of feature histograms [30] are extracted from each image segment. Feature histograms are normalized and considered as fuzzy sets.

4.2.1 Shape Features

In this section, we considered several shape features used later in the classification part. As mentioned before, we are restricted to the type of features that could be used in the form of one dimensional or two dimensional fuzzy sets to be used in fuzzy topologies. For this reason, we chose shape features in the form of feature histograms, including: distance histogram, angle histogram and chord distributions. The following subsections discussed them in details.

4.2.1.1 Distance Histogram

Distance histogram is the spatial distribution of the Euclidean distance of the points inside each image segment and the center of mass (c) of the image segment. An image segment is considered as a binary image I_B :

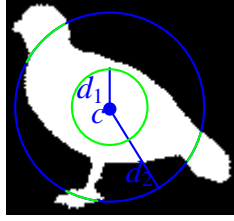
$$I_B(x, y) = \begin{cases} = 1, & \text{for points on the image segments,} \\ = 0, & \text{for background points.} \end{cases}$$

Center of mass, $c = (x_c, y_c)$, is the second moment of the object and is calculated as follows:

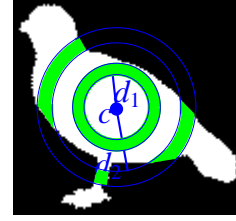
$$x_c = \frac{\sum \sum x I_B(x, y)}{\sum \sum I_B(x, y)} \quad (4.1)$$

$$y_c = \frac{\sum \sum y I_B(x, y)}{\sum \sum I_B(x, y)} \quad (4.2)$$

The distance between the point p and c is normalized with respect to the maximum distance among the pixels. The normalized distances are used to form a 51-bin histogram [95]. The histogram is also normalized with respect to the maximum value of the histogram. We have shown the process of obtaining the distance histogram in figure 4.2 . Distance histogram is rotation and translation invariant and it is also scale invariant by using the normalization process. Figures 4.3 and 4.4 show some images and their corresponding histograms. Rotation and scale invariance properties are clear in images on rows one to



(a) $n(n \rightarrow \infty)$ bin distance histogram



(b) $n(n < \infty)$ -bin distance histogram

Figure 4.2: Distance histogram. (a) The process of obtaining a $n(n \rightarrow \infty)$ -bin distance histogram is shown. For each distance $d > 0$, a circle ($C(c, d)$) centering at the center of mass(c) of the object is considered. The value of the distance histogram at the corresponding bin to d is the number of pixels of the object that lie on $C(c, d)$. These pixels are shown with green colors on two depicted circle $C(c, d_1)$ and $C(c, d_2)$. (b) For coarser distance histogram, each bin represents a range of distances from center of mass shown in circular bands, the number of green colored pixels in each band is the value for the histogram's bin. Bird image is from Kimia image database [96]

three in figure 4.3. Slight difference are due to the nature of digital images.

4.2.1.2 Angle Histogram

This histogram stores the counter-clockwise angle between pixel vectors and the unit vector on the x -axis (e_x) [95]. A pixel vector is the vector connecting the center of mass ($c = (x_c, y_c)$) to a point $p = (x_p, y_p)$. The coordinates of the center of mass are calculated by equations 4.1 and 4.2. The angle between the unit vector ($c\vec{x}$) and the pixel vector ($c\vec{p}$) is calculated by:

$$\theta(c\vec{x}, p\vec{x}) = \begin{cases} \arctan(\frac{y}{x}) & p \text{ is located in quadrant I,} \\ \arctan(\frac{y}{x}) + \pi & p \text{ is located in quadrant II,} \\ \arctan(\frac{y}{x}) - \pi & p \text{ is located in quadrant III,} \\ \arctan(\frac{y}{x}) & p \text{ is located in quadrant IV.} \end{cases} \quad (4.3)$$

The result will vary from $-\pi$ to π . $x = x_p - x_c$ and $y = y_p - y_c$. Four quadrant are shown in figure 4.5-(b) . We built a 36-bin histogram and normalized it with respect to the maximum

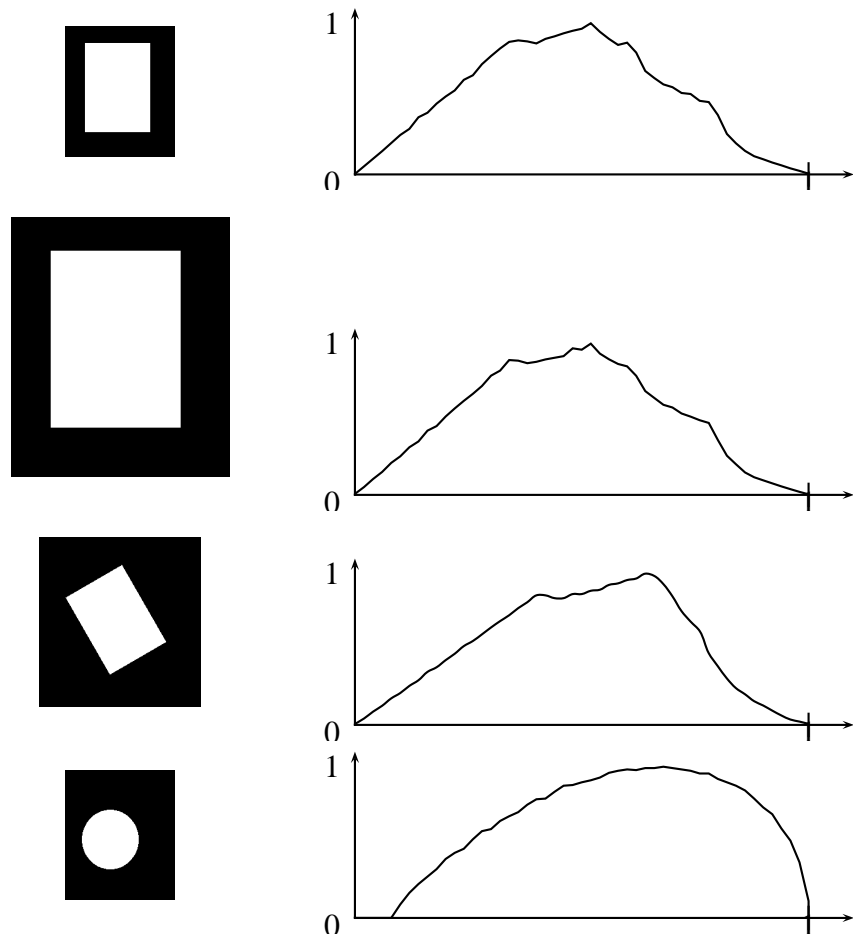


Figure 4.3: Normalized distance histograms - on each row an object (shown in white color on black background) and its normalized distance histogram are shown.

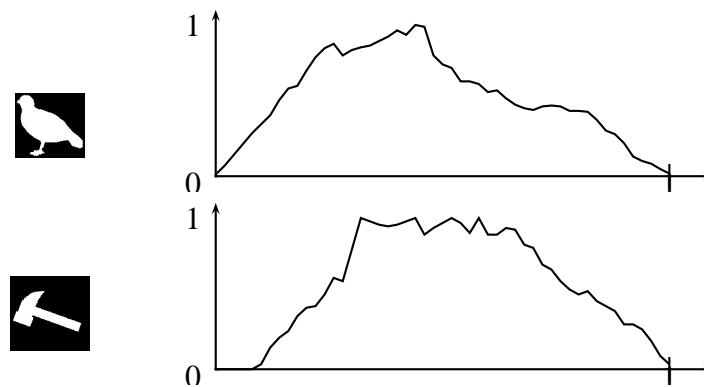


Figure 4.4: Normalized distance histograms- Images (from Kimia shape database [96]) and their corresponding normalized distance histograms.

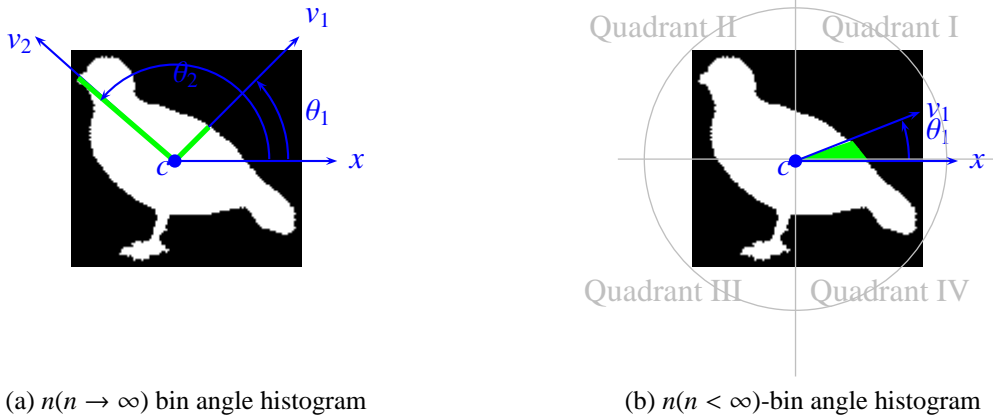


Figure 4.5: Angle histogram. (a) The process of obtaining a $n(n \rightarrow \infty)$ -bin histogram is shown. For each angle $-\pi \leq \theta \leq \pi$, a vector ($c\vec{v}$) is considered, and the value of the histogram at the corresponding bin to θ is the number of pixels of the object that lie on $c\vec{v}$. These pixels are shown with green color. (b) For coarser angle histogram, each bin represents a range of angles, the number of green colored pixels are the value for the histogram's bin representing $0 \leq \theta \leq \theta_1$. Bird image is from Kimia image dataset [96]

value of the histogram. Therefore, each bin represents a 10 degrees range. To clarify the idea, consider a $n(n \rightarrow \infty)$ -bin histogram. In this case, the bin that represents the angle $-\pi \leq \theta \leq \pi$ counts the number of pixels in the object that lies on a vector $c\vec{v}_\theta$, where $c\vec{v}_\theta$ is a vector originating from center of mass and the angle between the unit vector on x -axis and the vector $c\vec{v}$ is θ . For coarser angle histogram, each bin represents a range of angles, the number of green colored pixels are the value for the histogram's bin representing $0 \leq \theta \leq \theta_1$. Figure 4.5 shows the process. Figures 4.6 and 4.7 show different images and their normalized angle histograms. Normalization is also done on the angle values and $[-\pi, \pi]$ mapped to $[0, 1]$. Normalized angle histogram is scale invariant and translation invariant, but it is obviously not rotation invariant.

4.2.1.3 Chord Distribution

Chord distribution finds the distribution of lengths and angles of all the points on the boundary of the object. Two histograms based on distances and orientations of the points on the boundary are formed, namely chord length distribution and chord angle distribution. Chord length distribution is invariant to rotation and scale linearly with the size of the object. Chord angle distribution is invariant to object size and translations. Figure 4.8 demon-

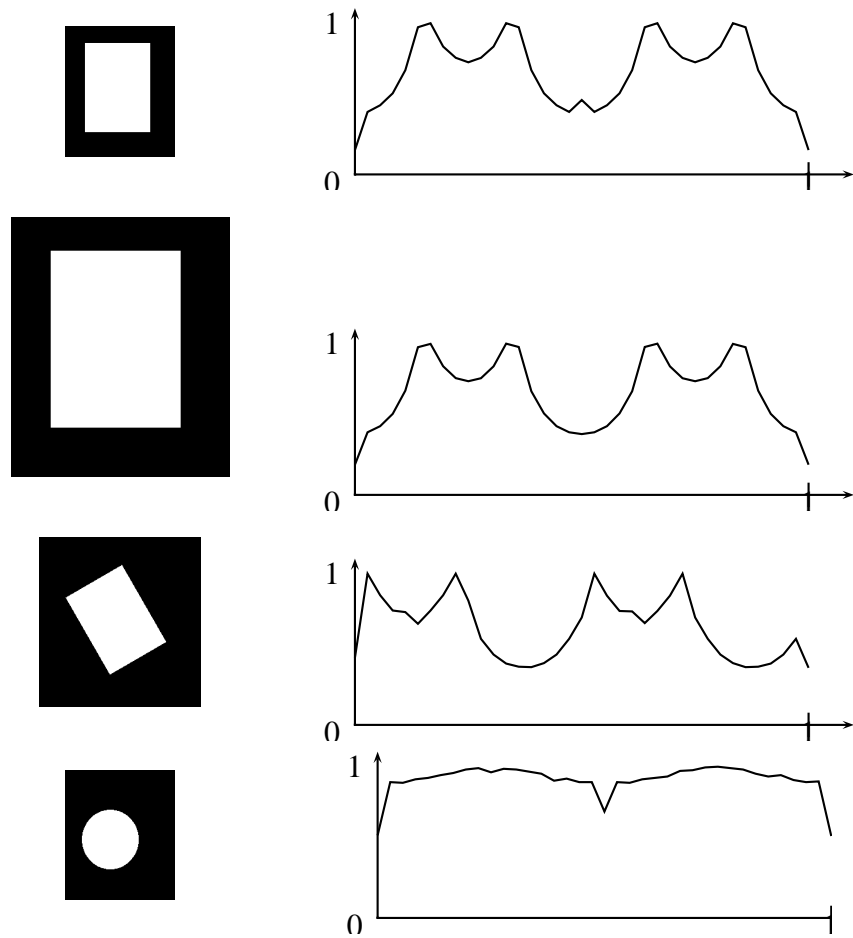


Figure 4.6: Normalized angle histograms - on each row an object (shown in white color on black background) and its normalized angle histogram are shown.

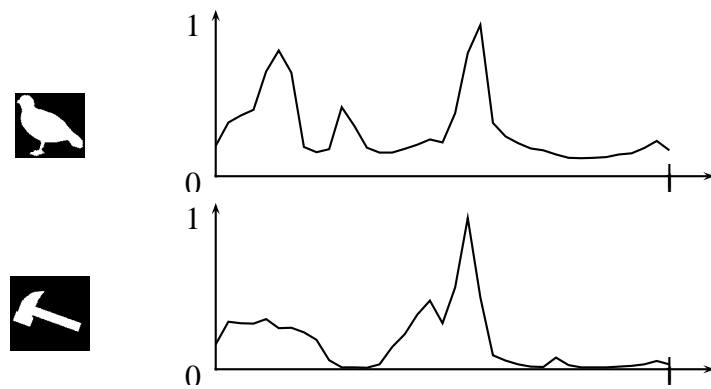


Figure 4.7: Normalized angle histograms- Images (from Kimia shape database [96]) and their corresponding normalized angle histograms.

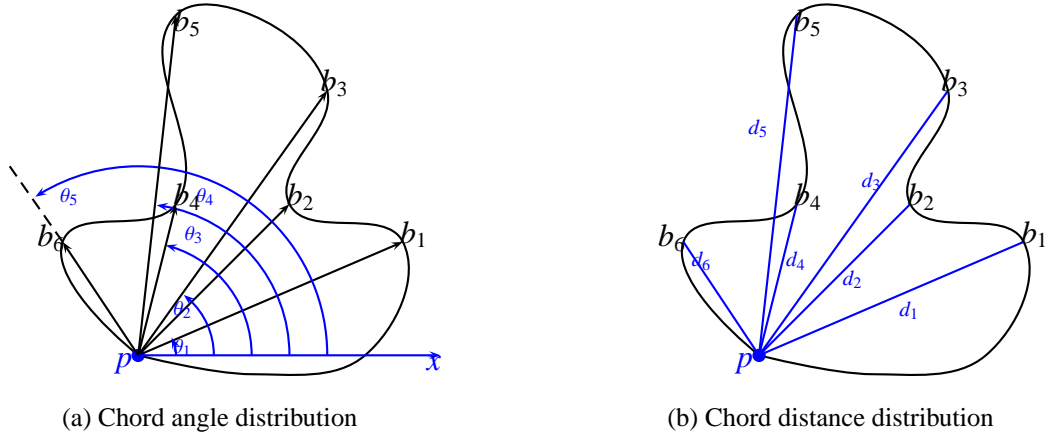


Figure 4.8: Chord Distribution- Point p on the boundary of the object is shown. Six other points ($b_i, i = 1, \dots, 6$) on the boundary are shown (a) Chord angle distribution- The angle between the $p\vec{x}$ and $p\vec{b}_i$'s are depicted. Angles are calculated for between all the points on the boundary of the object and an a histogram is obtained based on all the calculated angles. (b) Chord distance histogram- Distances between a point p on the boundary of the object and six other points on the boundary are shown (d_1, \dots, d_6). A histogram is obtained between all the points on the boundary of the object .

strates the process of calculating chord length histogram and chord angle histogram. Point p is shown on a boundary of the object. Distances and angels are calculated for point p and all the other points on the boundary. The process repeats itself for all the other points on the boundary. The angels and distances then form two chord histograms. Angels are calculated by equation 4.3. Figure 4.9 shows chord distribution for some rectangles in different sizes and orientation and also a circular shape. As seen in this figure, chord length distribution is invariant to rotation and scale linearly with the size of the object. Chord angle distribution is invariant to object size and translations. Figure 4.10 shows chord distributions for two images from Kimia image database [96].

4.2.2 Color Features

Color histograms represent a compact description of the color content inside an image segment. In this work, the RGB color space (Red, Green, Blue) is considered. Three one dimensional color histograms $h_{il}^R, h_{il}^G, h_{il}^B$ are extracted from each segment. The color histograms are normalized with respect to the size of each image. Figure 4.11 shows two

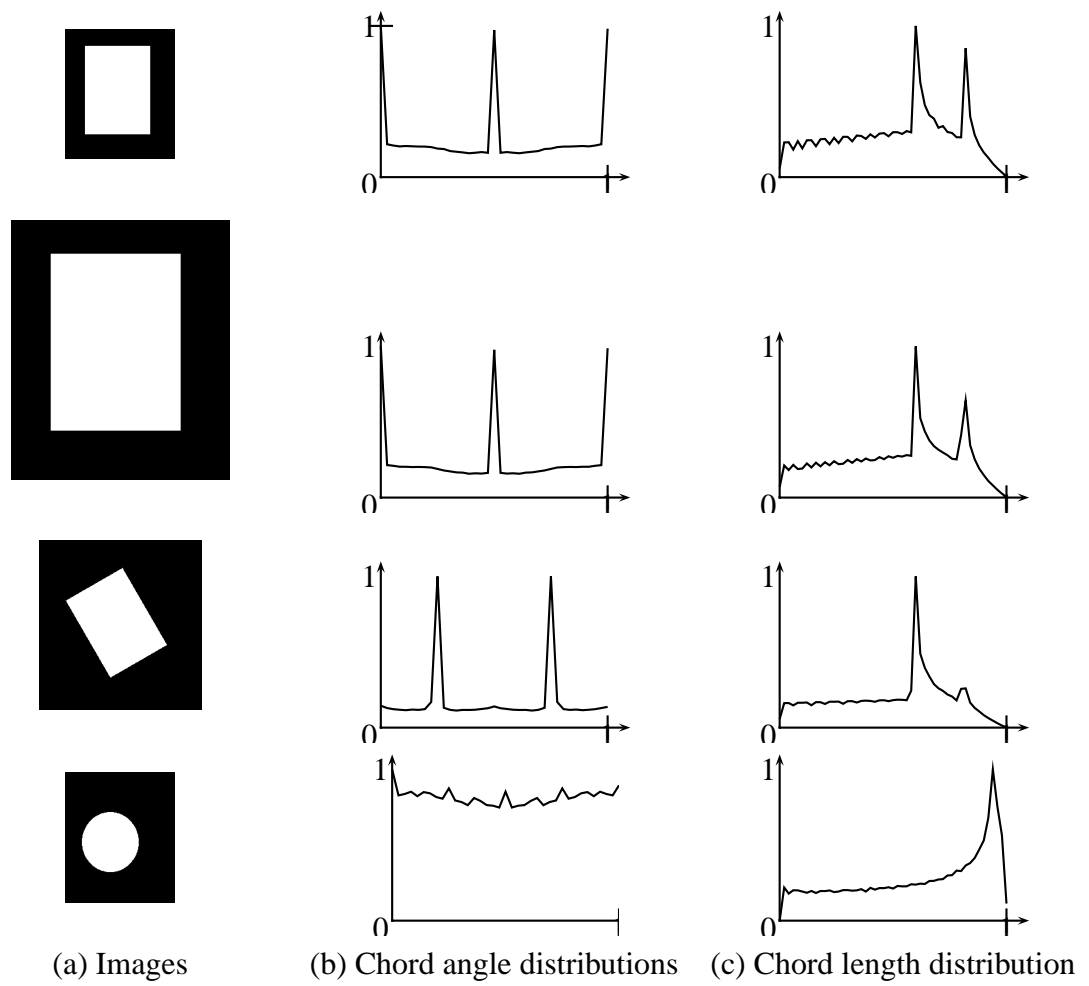


Figure 4.9: Normalized Chord Distributions

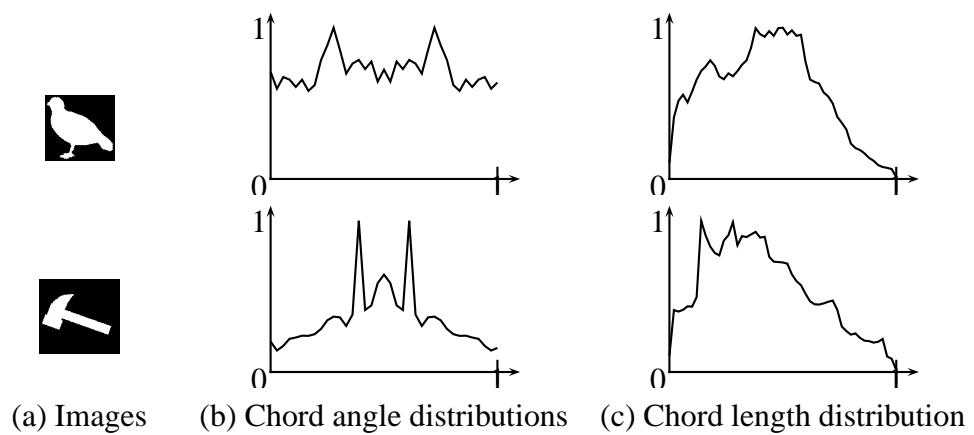


Figure 4.10: Normalized chord distributions- Images (from Kimia shape database [96]) and their corresponding normalized angle histograms.

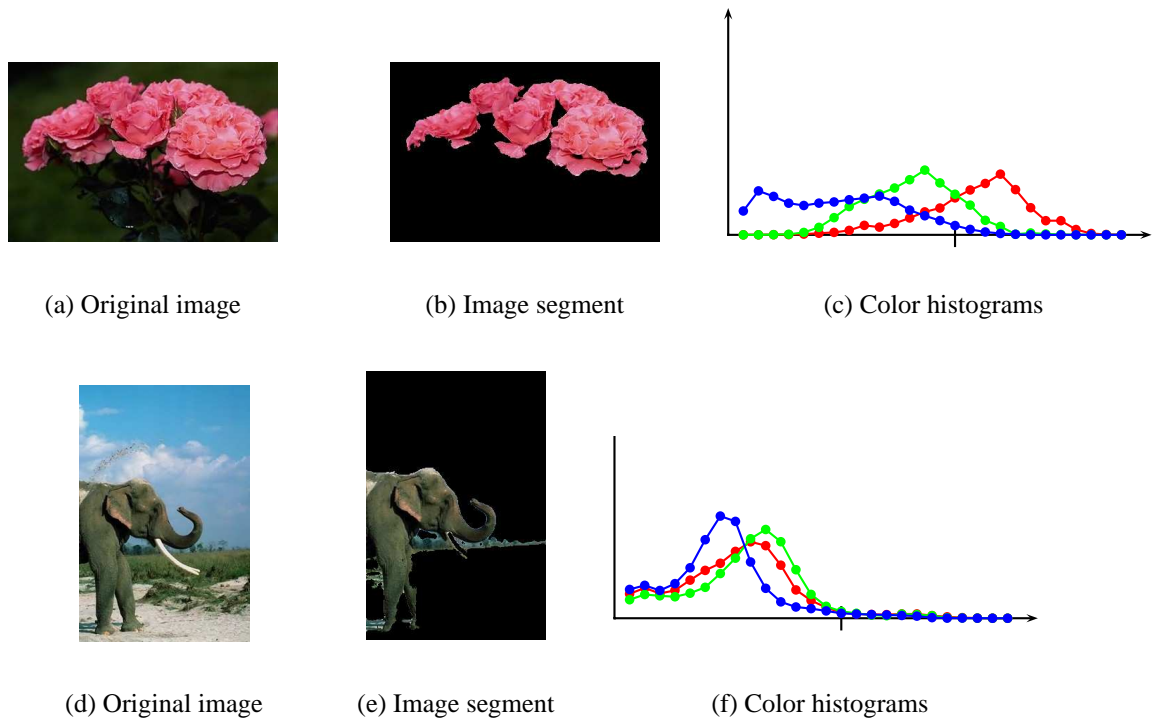


Figure 4.11: Image segments and red, green and blue color histograms. Images are from SIMPLiCity database [58, 114].

image segments and their corresponding color histograms. Color range is between 0 and 255 in each of the color bands and we consider a 10 shades wide bins. Therefore the color histograms are 25-bins histograms.

4.3 Shape Classification

As mentioned in subsection 4.1.2, shape classification is an important and challenging task in image analysis and object recognition. To evaluate our topology based classification method, we have chosen shape classification. Using binary shape databases simplifies the evaluation process of classification, since we are not concern about image segmentation and the possible errors and imperfections. There are some test databases in this area which contain black and white images demonstrating only one object in each image. We reported the results on Shapes216 also known as Kimia database [96]. This database contains 216 binary images. There 18 categories (bird, bone, brick, camel, car, children, classic,

elephant, face, fork, fountain, glass, hammer, heart, key, misk, ray and turtle), each category contains 12 images. The database is shown in figure 4.12. Each category has different examples of the concept. Since Shapes216 database is a binary dataset, we only use shape information. We conducted several tests and we report on the two most successful ones:

- Combination of distance histogram and angle histogram ,
- Combination of chord angle histogram and chord distance histogram .

To run the test, a number of images in each category are considered as training samples and the rest are used as the test samples. An image is successfully classified, if the output of classification and the category of the test image are the same. The accuracy of the classification are calculated based on percentage of correct classifications on test dataset. For the classification part, inclusion degree is set to $\gamma = 0.7$ which is based on trial and error. Figure 4.13 shows different runs of the method with different number of training samples, $n = 1, 5, 6, 7, 8, 11$. Since training samples are selected randomly, we run the system three times and the results are shown for combination of angle and distance histogram and chord distribution. As seen in the result, using angle and distance histograms showed better performance. Figure 4.14 shows the result of classification. Seven samples in each category are considered for training. The accuracy of the results is 83. It takes about 0.4 second to classify an object with seven training sample in each category. This time could become lower significantly by loading all the training files in advance and also by converting the MATLAB program to C. Misclassified samples are marked in red color. As seen in the results, some of the misclassifications are the result of the between classes similarities. For instance, consider the bird image shown in figure 4.14-query(b and d) is rotated in such a way that it looks like a turtle, and it is classified as a turtle. Therefore, considering the accuracy of the system by just one number does not demonstrate the capability of the system. Although the accuracy of our classification on shapes 216 dataset, is not as high as the ones in literature ([1, 107, 113, 117]) that reported accuracies of 94.4%, 97.7, 94.1 and 97.2, respectively, we highlight the following facts about this method:

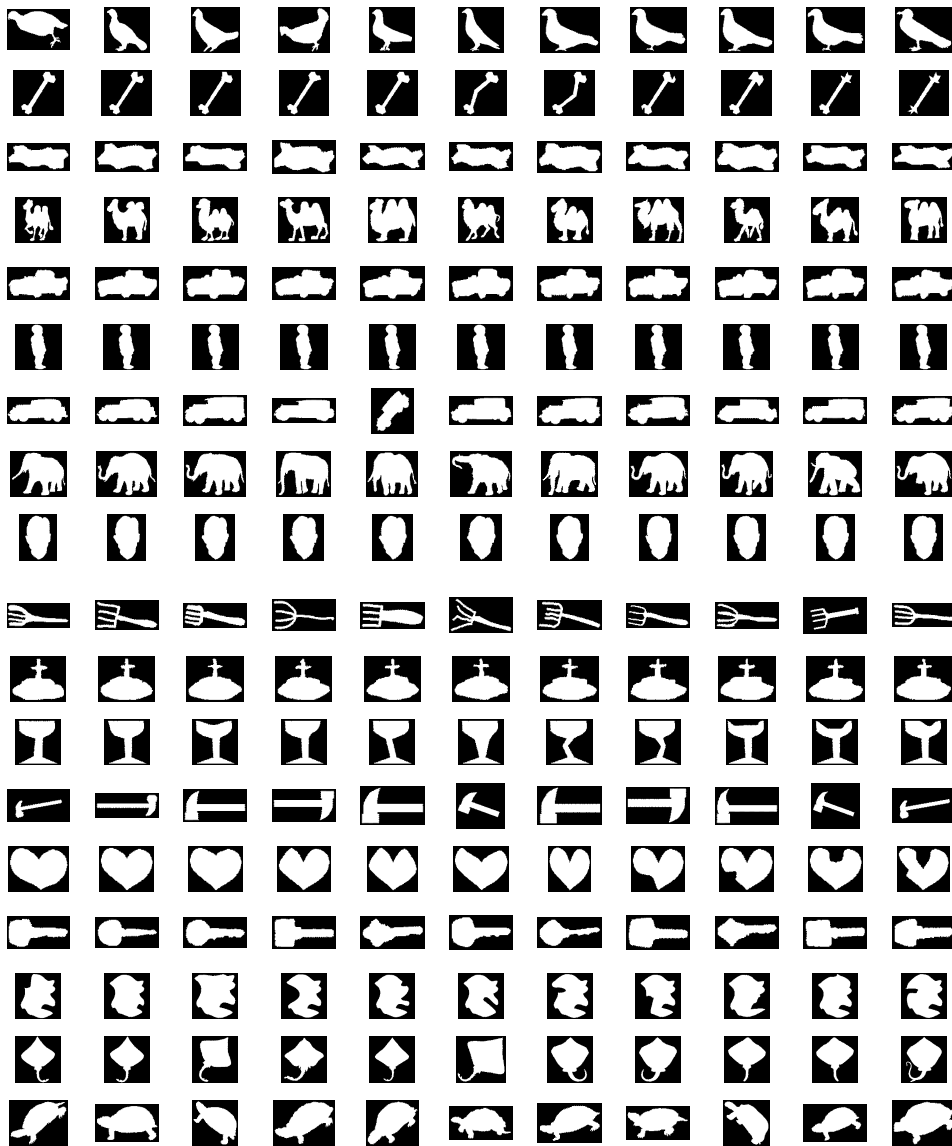
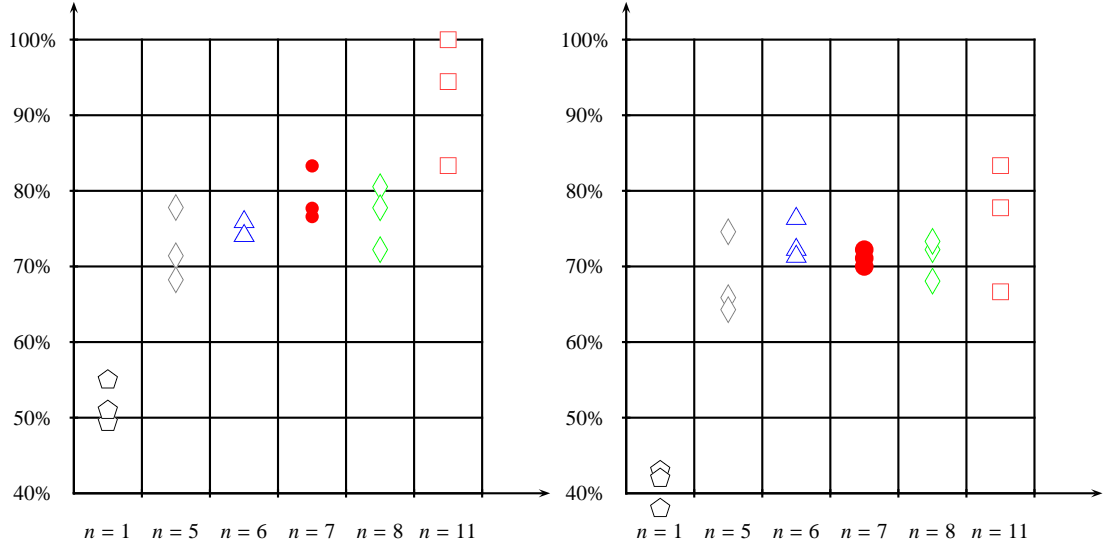


Figure 4.12: Shapes 216 or Kimia database [96]: 12 images in 18 different categories namely: bird, bone, brick, camel, car, children, classic, elephant, face, fork, fountain, glass, hammer, heart, key, misk, ray and turtle .



(a) Distance and angle histograms are used as extracted features. (b) Chord angle and distance distributions are used as the extracted features.

Figure 4.13: Accuracy of the proposed shape classification method (inclusion measure is set to $\gamma = 0.7$) is shown for different number of training samples ($n = 1, 5, 6, 7, 8, 11$). The data set is Shapes 216 ([96]) and the training samples are selected randomly from each category. Results are shown on three random runs.

- We have considered only a portion of the database as a training set (126 sample in total or 7 for each category), while the results reported in the literature [1, 107, 113] used leave one out validation method (215 sample in each run). This shows the generalization quality of our method.
- The two low dimensional feature vectors (distance histogram and angle histogram) are considered, in comparison to other high computational forms of shapes features .
- We applied our topological framework with inclusion degree to shape classification to demonstrate the efficiency of the method in this types of tasks.

4.4 Color Image Database Classification

This section presents the steps for image database classification process. This part has been published in [28]. It contains two steps: Learning and Testing. Learning phase is


































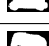














































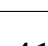


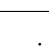
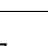
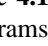
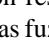
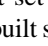
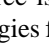
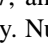
Query(a)	Result	Query(b)	Result	Query(c)	Result	Query(d)	Result	Query(e)	Result
	bird		turtle		bird		turtle		bird
	bone		bone		bone		bone		bone
	brick		brick		brick		brick		brick
	camel		camel		camel		turtle		camel
	car		car		car		car		car
	child		child		child		child		child
	classic		classic		car		classic		bone
	elephant		elephant		elephant		camel		elephant
	face		face		face		face		face
	fork		fork		fork		fork		key
	fountain		fountain		fountain		fountain		fountain
	glass		glass		glass		glass		glass
	hammer		hammer		hammer		hammer		hammer
	heart		heart		heart		ray		hammer
	key		key		hammer		key		fork
	misk		ray		camel		misk		misk
	ray		ray		camel		ray		ray
	turtle		turtle		bird		turtle		turtle

Figure 4.14: Classification results on the test set- Inclusion degree is set to $\gamma = 0.7$, angle and distance histograms are considered as fuzzy features to built subspace topologies for each category. Number of training sample in each category is set to 7. Accuracy of the results is 83% . Images are from Kimia iamge dataset [96]

the building of fuzzy topologies for each image concept. Testing phase is finding the fuzzy interior of the query with respect to different concepts' topologies. This section is organized as follows: In subsection 4.4.1 image segmentation process is explained. Cluster validation and initialization techniques are explained in subsection 4.4.2. Results are reported in subsection 4.4.3.

4.4.1 Image Segmentation

Image segmentation is the first step in building the fuzzy topologies for each concept. Training samples in each concept as well as the query image is segmented and then necessary features are extracted from each segment. Image segmentation partitions an image into multiple regions so that the pixels in each region have similar features, *e.g.* color, texture, etc. The goal is to partition an image into meaningful objects. There are many different techniques for image segmentation such as clustering methods (*e.g.*, k-means [66] and expectation maximization [20]), region growing methods [94], histogram thresholding [78], Watershed [40, 70], and graph partitioning [98] We used the expectation maximization (EM) method to determine the image regions. In general, EM is a statistical method used to find the maximum likelihood estimates of parameters as a means of simplifying difficult maximum likelihood problems. EM was first developed in [20]. In this work, a Gaussian mixture model (GMM) is considered for each image. The goal is to find the unknown parameters of the GMM, including mixing parameters (π_i , $i = 1, \dots, k$) and Gaussian parameters (θ_i , $i = 1, \dots, k$) based on observed data (y_i , $i = 1, \dots, n$). Consider the function f defined by

$$f(y_i; \psi) = \sum_{i=1}^k \pi_i f_i(y_i; \theta_i),$$

where $\psi = (\pi_1, \dots, \pi_k, \theta_1, \dots, \theta_k)$ and k is the optimal number of clusters in an image. We have used several clustering validation techniques to calculate k (this is explained subsec-

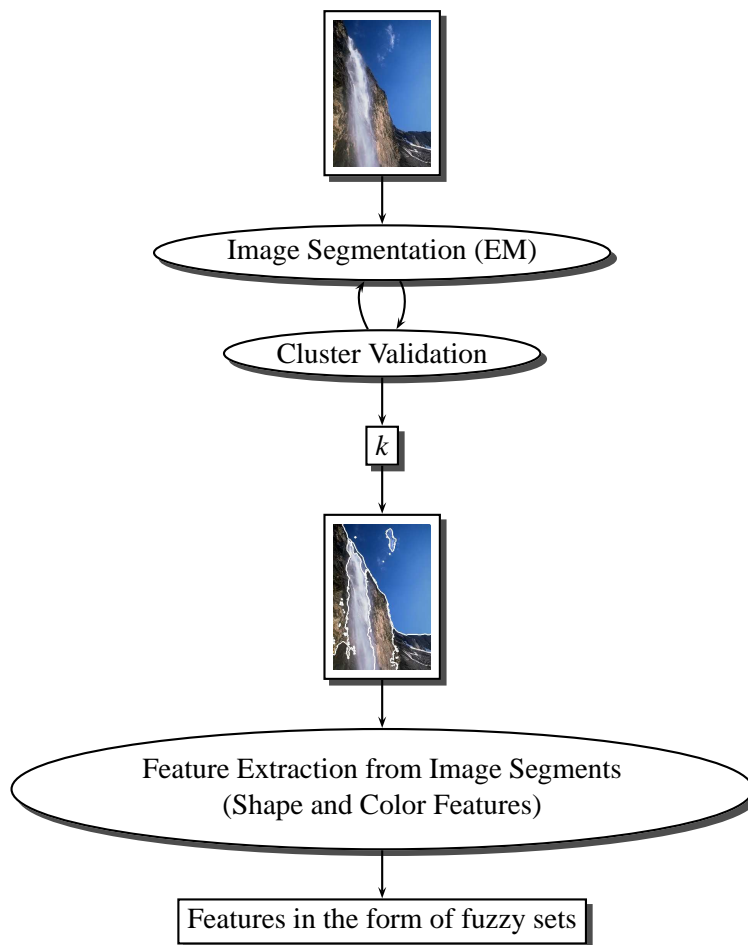


Figure 4.15: Feature extraction process. Optimum number of cluster is obtained $k = 5$ for this particular image. RGB colors and position information have been considered for segmentation process. Each process is explained in detail in subsections 4.4.1, 4.4.2, 4.2 .

tion 4.4.2). The log likelihood for ψ is based on observed data:

$$\log L(\psi) = \sum_{j=1}^n \log f(y_j; \psi) = \sum_{j=1}^n \log \sum_{i=1}^k \pi_i f_i(y_j; \theta_i).$$

To compute the maximum likelihood estimation (MLE) of ψ , the following equation is solved iteratively using the EM algorithm:

$$\partial \log L(\psi) / \partial \psi = 0.$$

For a complete introduction to the EM algorithm, see [68, 69]. Application of image segmentation on an image results in the rough estimation of the objects in the image. By way of illustration of the proposed feature extraction method, only color and position information has been utilized. In this illustration, texture information did not change the results significantly and, hence, has been ignored. Figure 4.19 shows some samples of the image segmentation applied to SIMPLiCity image categories (for more info about the database refer to [58, 114]). Contours of the segmentation is shown with white color on each image. The initialization method and the choice of the number of clusters are briefly explained, next.

4.4.2 Cluster Validation and Initialization

Data clustering methods provide a straightforward approach to image segmentation and computer vision. The majority of clustering methods requires a known number of clusters as an input. The basic approach in what is known as k-means clustering (introduced by J. MacQueen in 1967 [66]) is to partition n observations into k clusters so that each observation belongs to a cluster with the closest mean. An optimal number of clusters $k \in [1, n]$, where $k = 1$ (having all the data in one cluster) and $k = n$ (n is the total number of observed data and every element is a cluster). Increasing the number of clusters (above $k = 1$) decreases the error. In the extreme case, where $k = n$ (each data point is a cluster),

the error reaches zero. However, in this case of overfitting to the data, the possibility of generalization is lost.

There are several methods to determine the optimal number of clusters. Most of the cluster validation methods are using different value for k from 1 to a maximum number (e.g. 10), a validation method applies to the result of the clustering using k as a number of clusters. Finding the optimum number of clusters depends on the selection of a validation technique. However, since validation techniques have different criteria for obtaining the optimal number of clusters, not all of them give the same results. For this reason, we have chosen 5 different indexes. The optimum number of cluster is based on the majority of votes. We have used Davis-Bouldin [19], Calinski-Harabasz [9], Dunn [26], Krzanowski-Lai [56] and Hartigan [41] indices:

Davies Bouldin Index: $DB(k) = \frac{1}{n} \sum_{i=1}^k \max_{i \neq j} \left\{ \frac{S_n(Q_i) + S_n(Q_j)}{S(Q_i, Q_j)} \right\}$, where k is the number of clusters, S_n average distance of all objects inside the cluster to the center of the cluster, $S(Q_i, Q_j)$ distance between cluster centers i and j . The optimum number of clusters minimizes the DB index.

Dunn Index: $D(k) = \min_{1 \leq i \leq k} \left\{ \min_{\substack{1 \leq j \leq k \\ i \neq j}} \left\{ \frac{D(c_i, c_j)}{\max_{1 \leq h \leq k} D'(c_h)} \right\} \right\}$, where k is the number of clusters, $d(c_i, c_j) = \min_{u \in c_i, w \in c_j} d(u, w)$ and d is the Euclidean distance between u and w . $D'(c) = \max_{u, w \in c} d(u, w)$ is the diameter of the cluster c . The optimal value of k maximizes the Dunn's index.

Calinski-Harabasz Index: $CH(k) = \frac{[traceB]/(k-1)}{[traceW]/(n-k)}$, n is the number of points and k is the number of clusters. B and W are the between and within cluster scatter matrices. $traceB = \sum_{i=1}^k n_i \|z_i - z\|^2$, where n_i is the number of points in cluster i and z is the centroid of the entire data set. Optimal number of k maximizes CH index. $traceW = \sum_{i=1}^k \sum_{j=1}^{n_i} \|x_j - z_i\|^2$.

Krzanowski-Lai Index: $KL(k) = \left| \frac{DIFF(k)}{DIFF(k+1)} \right|$, where $DIFF(k) = (k-1)^{2/p} W(k-1) - k^{2/p} W(k)$. W denotes the within cluster sums of squares of the partitions. k is the number of clusters and optimal k maximizes KL.

Hartigan Index: $H(k) = \gamma(k) \frac{W(k) - W(k+1)}{W(k+1)}$, k is the number of clusters, $W(k)$ is the intra cluster dispersion, defined as the total sum of square distances of the objects to their cluster centroids. The parameter γ is added in order to avoid an increasing monotony with increasing k . The optimum number of clusters minimizes the Hartigan index.

For initialization part, we tried two techniques and then choose the latter, based on the performance and speed. We first tried random initialization. k points were selected from the feature space randomly with uniform mixing proportions and a diagonal covariance matrix. The EM algorithm was run for $k = 2, \dots, 10$ and the best case is chosen based on 5 mentioned validation techniques. Secondly, we tried Carson's method explained in [11]. Since an image collection generally follows the conventions of photographic composition, the window arrangements shown in figure 4.16 tends to yield better results than random initialization. The best k is chosen based on the five validation technique. Figure 4.17 shows three images and the values of the cluster validation indices for different number of clusters. Number of clusters are based on Carson's initial windows For instance, as shown in subimage 4.17a, four out of five validation indices are selecting $k = 5$ as the optimum number of clusters. Therefore $k = 5$ is selected.

The results of the segmentation with Carson's initialization techniques are shown in figure 4.19. Before segmentation, we applied a median filter of size 3×3 twice on an image. The median filter has a smoothing effect on an image and makes the segmentation contours smoother. Figure 4.18 shows an original image, the preprocessed one by median filter and the segmented image [58, 114]. In this work, connected component (CC) labeling is used on image segmentations. Small connected components are discarded and a feature extraction method applied to the remaining segments. Image segments or image connected components may be used interchangeably throughout this document.

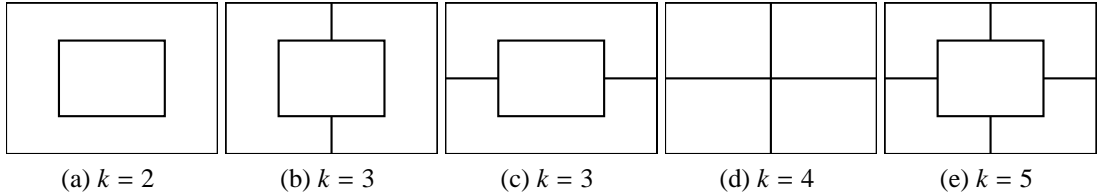
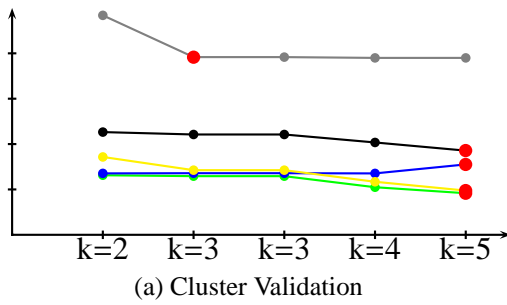
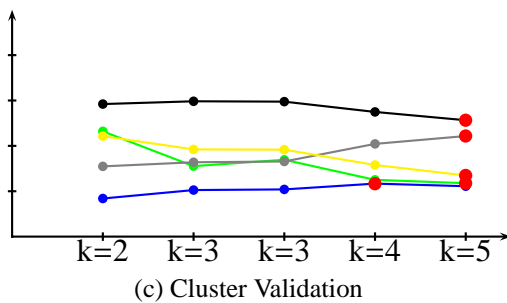


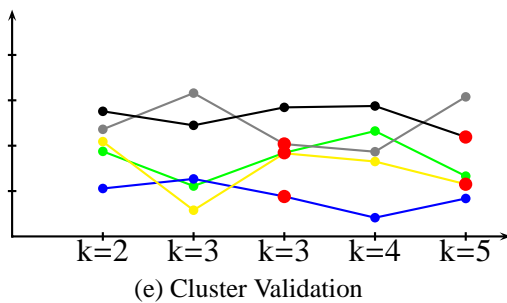
Figure 4.16: Windows [11] for initializing the EM: $k = 2, \dots, 5$. The best k is chosen based on the validation techniques described in subsection 4.4.2



(b) Segmented image with $k=5$



(d) Segmented image with $k=5$



(f) Segmented image with $k=3$

Figure 4.17: Cluster validation indicators: EM segmentation algorithm has been run for 5 times. The cluster initialization are based on initial windows shown in figure 4.16. Davis Bouldin(DB), Calinski-Harabasz(CH), Dunn(D), Krzanowski-Lai(KL) and Hartigan(H) Indices are shown in green, gray, blue, black and yellow colors, respectively. Maximum values of CH and Dunn indexes are shown in red dots. Also, minimum values of KL, Han and DB indices are shown in red dots. Images are from SIMPLiCity image database [58, 114]



Figure 4.18: Application of median filter on an image(from SIMPLIcity image database [58, 114]) and the segmented result.

4.4.3 Results

To provide the numerical results, the proposed image database classification method has been tested on a controlled image database. We used a subset of the COREL database contains 1000 images in 10 categories. The database is called SIMPLIcity image database [58, 114]. The categories are Africa, beach, buildings, buses, dinosaurs, elephants, flowers, horses, mountains and food. Five samples (segmented samples) from each category are shown in figure 4.19. Although this is a controlled and comparatively small database, it is a challenging classification problem. Images in some categories such as horses and dinosaurs are very similar, whereas others such as beach, Africa, food and buildings are difficult to classify because of their diversity. Figure 4.20 shows some samples of the Africa, buildings, food and beach categories demonstrating within class diversity in some categories. Figures 4.21 and 4.22 demonstrate the between classes similarity. For instance the beach and mountain categories have overlaps. There are also some similar images in the elephant and Africa categories.

To evaluate the system, the accuracy of the classification on the test set is considered. We have randomly chosen $n = 33$ images from each category as a training set for each concept and the remaining 67 images in each category are used for testing (total of 670 images). Since we select the training set randomly, each experiment run 4 times and the results shown in table 4.1 are the averages of the four runs. To evaluate the proposed classification method, the accuracy of classification is compared with a 2-dimensional multi resolution hidden Markov model explained in [58]. We chose to compare our results with



Figure 4.19: Results of the EM segmentation shown with white contours on images from the SIMPLiCity image database [58, 114]. Each row represents samples from a different category, namely, Africa, beach, buildings, buses, dinosaurs, elephants, flowers, horses, mountains and food.



(a) Samples of the Africa category



(b) Samples of the building category

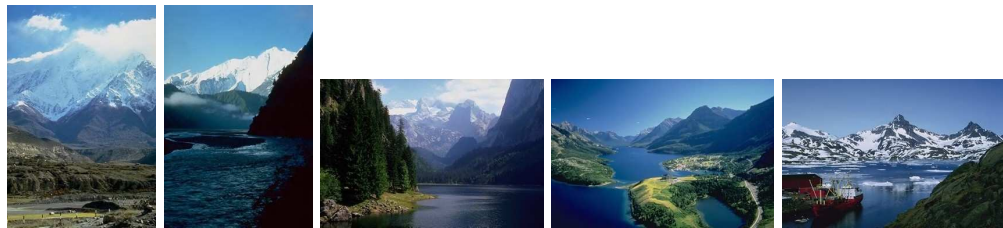


(c) Samples of the food category



(d) Samples of the beach category

Figure 4.20: Within class diversity in some image categories. Images are from SIMPLiCity image database [58, 114] .



(a) Samples of the mountain category



(b) Samples of the beach category

Figure 4.21: Between classes similarity: Some samples from the mountain and beach categories are shown . Images are from SIMPLiCity image database [58, 114] .



(a) Samples of the elephant category



(b) Samples of the Africa category

Figure 4.22: Between classes similarity: Some samples from the elephant and Africa categories are shown . Images are from SIMPLIcity image database [58, 114] .

[58] because the same image database was used. They used 40 images from each category for training; however only 500 (instead of the remaining 600) images used for testing.

Table 4.1 shows our classification results which is the average of 4 runs. The numbers inside the parentheses are the standard deviations. Each row shows the percentage of test images in one category classified to each of ten categories. Numbers on the diagonal, shaded in light gray, show the classification accuracy for each category. The off-diagonal numbers give the classification errors. The last column, shaded in dark gray, added for comparison purposes and shows the classification accuracies for the category on each row reported in [58]. Although we do not have the information about the details of the training set and the test set and how they have been selected in [58], we add the last column for comparison. In Africa, beach, elephants and horses there is higher classification accuracy than in [58] and the remaining results are either similar or lower than those given in [58]. Considering only the classification accuracy may not demonstrate the effectiveness of the classification when there are between classes similarities. Table 4.2 shows the result of the classification on the food category. 33 images are chosen randomly for training set. The images shown in this table are from test images. Classification system classifies images based on the similarity of the interior of the query image to the query image with respect to different topologies. The first three most similar categories are reported in this table. When the first choice is not the food category, a misclassification is occurred. However,

the food category is reported as a second or third choice in most of the samples and marked in green. The same results are reported for the mountain category in table 4.3. As seen in these tables, when misclassification occurred, images are classified to the other categories that have similar images to the target class. We also used a subset of COREL 10,000 image database [58, 114]. We selected 778 images in 8 categories. The list of categories and number of images in each of the is as follows: sunset (100), flowers (98), cars (100), sailing (99), fall (68), forest (93), mountains (87), ocean/wave (130). Figure 4.23 shows some samples of the images used for this experiments. The segmentation algorithm applied to these images. Figure 4.23 shows segmented samples of the categories. Table 4.4 shows the results of classification for the test images. $1/3$ of each category is considered for modeling the subspaces and $2/3$ is used for the testing. The worse results are obtained for mountain and fall categories. Considering the mountain category, 58.91% of the test images are misclassified as ocean. Looking at the ocean images, most of them are combination of ocean and mountains. Also for fall images, 33.68% are misclassified as the forest category, which is highly correlated to fall images.

4.5 Summary

The main points of this chapter include:

- Fuzzy topological spaces have been used effectively for both shape classification and image database classification.
- Interior operator with inclusion degree has successfully utilized for mapping a query image to the target category.
- Feature vectors in the form of fuzzy sets are extracted from image segments.
- Image segmentation is implemented by EM algorithm and the number of clusters are determined by cluster validity indices.

imcat ¹	Off-diagonal % misclassified, on-diagonal % correctly classified										% in [58]
	Africa	beach	buildings	buses	dinosaurs	elephants	flowers	horses	mountains	food	
Africa	66.79(4.93)	1.11(1.49)	10.07(3.31)	2.61(3.31)	0(0)	5.59(2.23)	0(0)	1.86(2.23)	2.61(2.23)	7.83(3.31)	52
beach	10.82(2.54)	34.70(7.14)	17.53(4.93)	10.07(2.54)	1.12(0.74)	10.07(3.31)	0.37(0.74)	1.49(1.21)	11.56(1.87)	2.23(1.92)	32
buildings	27.98(3.31)	7.83(3.31)	43.65(2.54)	3.35(1.43)	0(0)	3.35(3.07)	1.12(0.74)	0.74(0.86)	7.83(2.54)	4.41(1.43)	64
buses	16.41(8.08)	4.47(1.21)	7.09(2.23)	54.10(10.00)	0(0)	2.23(0.86)	2.61(1.43)	1.12(1.43)	4.85(2.23)	7.90(3.06)	46
dinosaurs	0.37(0.74)	0(0)	0(0)	0(0)	98.89(1.42)	0(0)	0(0)	0(0)	0.37(0.74)	0.37(0.74)	100
elephants	15.67(3.55)	4.47(3.22)	10.82(4.93)	1.12(1.43)	0(0)	55.97(3.55)	0.37(0.74)	3.37(1.49)	2.23(0.86)	5.59(3.07)	40
flowers	8.20(0.86)	0.74(0.86)	4.47(2.11)	3.35(2.54)	0(0)	1.12(0.74)	69.77(4.29)	5.22(2.85)	0(0)	7.08(3.92)	90
horses	8.95(2.98)	0(0)	1.12(0.74)	0.74(0.86)	0(0)	2.61(1.42)	1.12(1.43)	83.20(2.82)	0.37(0.74)	1.86(0.74)	60
mountains	21.27(2.54)	13.43(5.31)	8.95(5.31)	7.46(3.22)	0(0)	3.73(1.92)	1.12(0.74)	3.73(0.86)	36.56(4.47)	3.73(2.58)	84
food	25.37(8.08)	0.37(0.76)	8.58(5.63)	1.86(2.23)	0.37(0.74)	2.98(2.11)	1.49(0)	1.12(0.74)	0.74(0.86)	57.09(9.92)	68

Table 4.1: Results of our classification method on SIMPLcity images [58, 114]. The results are averages of 4 different runs. numbers inside the parantheses show the standard deviation. The results are reported in test images (67 images in each category). On-diagonal numbers shows the accuracy of the classification for the category of each row. Off diagonal numbers are the classification errors (¹ image category)

Query	1 st	2 nd	3 rd	Query	1 st	2 nd	3 rd
	Africa	food	elephant		food	flower	bus
	food	bus	Africa		food	N/A	N/A
	Africa	food	elephant		food	horses	Africa
	food	Africa	building		beach	buiding	elephant
	food	Africa	elephant		flower	bus	food
	food	elephant	bus		Africa	food	elephant
	food	Africa	building		food	Africa	elephant
	food	Africa	building		food	Africa	elephant
	food	Africa	elephant		food	elephant	Africa
	food	building	horse		food	Africa	building
	food	bus	building		food	Africa	elephant
	food	bus	building		food	Africa	elephant
	Bus	Africa	food		dinosaur	food	horse
	food	Africa	horse		food	horse	Africa

Table 4.2: Classification results: Query images (taken from the test set) of the food category and three first choices of the system are shown. Inclusion degree is set to $\gamma = 0.6$, training set are 33 images. The accuracy of this run for this category is 71.6 and is calculated only on the first output of the system .

Query	1 st	2 nd	3 rd	Query	1 st	2 nd	3 rd
	building	bus	mountain		bus	Africa	mountain
	mountain	building	bus		beach	mountain	Africa
	mountain	elephant	beach		building	beach	elephant
	mountain	elephant	Africa		mountain	building	elephant
	mountain	beach	building		mountain	beach	bus
	mountain	bus	building		mountain	building	Africa
	mountain	elephant	beach		mountain	elephant	building
	mountain	bus	beach		mountain	beach	elephant
	elephant	mountain	bus		Africa	building	mountain
	mountain	building	beach		elephant	beach	building
	mountain	elephant	food		elephant	mountain	beach
	mountain	building	beach		mountain	elephant	Africa
	horses	Africa	elephant		mountain	beach	bus
	mountain	beach	building		Africa	mountain	building

Table 4.3: Classification results: Query images (taken from the test set) of the mountain category and three first choices of the system are shown. Inclusion degree is set to $\gamma = 0.5$, training set are 33 images. The accuracy of this run for this category is 53.7 and is calculated only on the first output of the system .

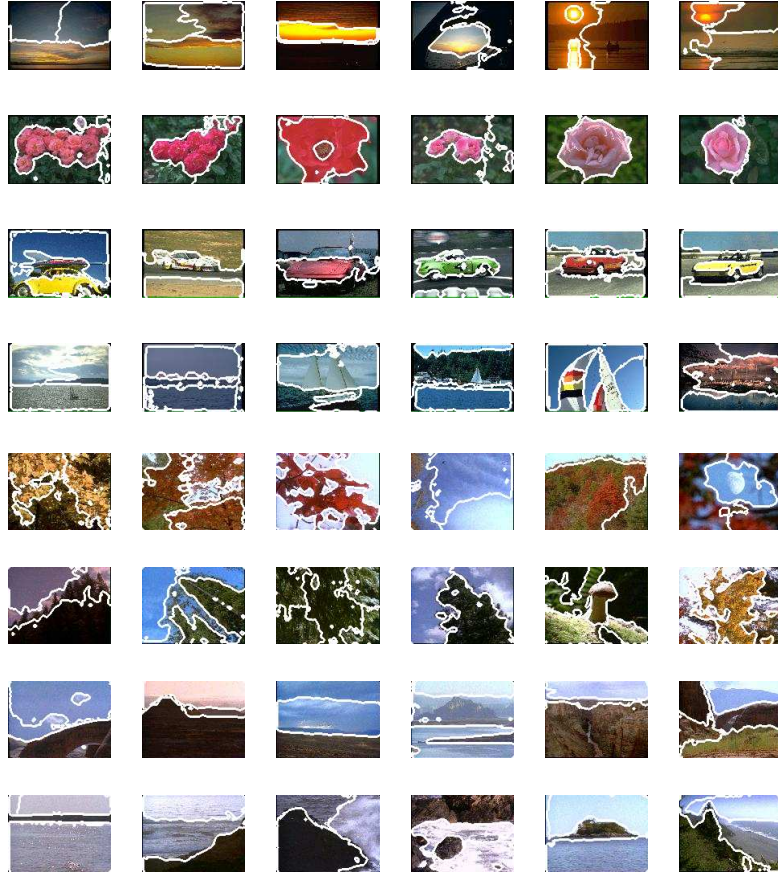


Figure 4.23: Samples of our selected images from COREL database [58, 114]. Images are drawn and segmented from 8 categories, namely: sunset, flowers, cars, sailing, fall, forest, mountains, ocean.

image category	Off-diagonal % missclassified, on-diagonal % cor. class.							
	sunset	flowers	cars	sailing	fall	forest	mountains	ocean
sunset	58.57	2.6	18.78	3.35	9.32	4.48	0	2.98
flower	2.35	64.54	2.35	0	0.37	4.47	0	4.84
cars	4.77	2.20	73.15	10.28	0	4.41	0	5.14
sailing	1.86	1.11	16.78	68.27	0	1.11	0.37	10.44
fall	5.97	1.08	1.08	1.62	40.21	33.68	2.19	14.12
forest	3.17	0.79	3.17	0.39	1.18	74.2	0.79	16.26
mountains	1.26	3.80	2.11	0.42	2.53	4.23	24.32	58.91
ocean	0.28	0.28	1.13	1.7	0.56	8.21	7.09	80.67

Table 4.4: Results of our classification method on a subset of COREL 10K image database. The number of images in each category range between 68 to 130.

- We could classify our learning method as an instance based learning.
- Since each concept is modeled independently with respect to other concepts in the system, adding a new concept is both straightforward and effective.
- We experienced the comparable results which make our novel topological image database/shape database classification technique an interesting one.

Chapter 5

Application of Proposed Operators in Mathematical Morphology

This chapter focuses on the application of the proposed topological operators with inclusion degree in mathematical morphology (MM). Some parts of this chapter will appear in [29]. Topological properties of mathematical morphology make them suitable for our operators. Morphological erosion/closing resembles the topological interior operators. This is also true for morphological dilation/closing and the topological closure operators. The modified topological operators with inclusion degree have been utilized in the definition of morphological operators. The newly defined morphological operators are performing better in noise reduction and edge detection. We should mention that the operators are only developed for binary morphological operators and the extension to gray level morphology are considered as future works.

This chapter is organized as follows: First, a brief description of mathematical morphology operators as well as their topological properties are considered in section 5.1. In section 5.2 new operators with inclusion degree are defined. Section 5.3 explains the applications of the new operators in noise reduction and edge detection. Finally, the chapter concludes in section 5.4.

5.1 Background Information on Mathematical Morphology

Mathematical morphology is a theory designed to extract relevant topological or geometrical structures from images. It was first introduced by George Matheron and Jean Serra in 1964, and later completely discussed in [67] and [97]. MM is based on set theory, lattice theory [38, 45, 46], topology and random functions. More practical applications of mathematical morphology could be found in [36] and [23]. Topological properties of mathematical morphology have been considered in terms of the erosion/opening being related to topological interior and dilation/closing to topological closure [2, 4, 27, 67, 97]. We start this section with the definitions of dilation and erosion operators for binary images.

Dilation and Erosion are two primary MM operators. Let $A, B \subset X \subseteq E^n(Z^n)$, where E^n is the Euclidean space and Z^n is the integer space suitable for digital images. Dilation ($d_B(A)$) of the set (image) A by set (image) B (called a structuring element (SE)) is

$$d_B(A) = \{x \in X : \hat{B}_x \cap A \neq \emptyset\}, \quad (5.1)$$

where \hat{B}_x is obtained by first reflecting B about its origin and then shifting it such that its origin is located at point x . Dilation of A by B , is the set of all the points x such that \hat{B}_x and A have overlapping. Erosion of A by B is defined by:

$$e_B(A) = \{x : B_x \subseteq A\}. \quad (5.2)$$

$e_B(A)$ is the set of all points x such that B_x is contained in A . In figure 5.1 different structuring elements and their reflections about their origins (centers) have been shown. SE can have any shape, size and connectivity. The characteristic of structuring element is application dependent. Figure 5.2 shows a 2×2 square structuring element B at different positions on the image plane. The set A is shaded in gray. By moving the structuring element B on the image A , we gather information about the medium A in terms of B . The simplest rela-

tionships can be obtained by B moving on the medium A , are of the form $B \subset A$ (remember erosion- or opening) and $A \cap B \neq \emptyset$ (dilation or closing). Let us clarify this idea by quoting what G. Matheron wrote in his book in 1975 [67, p. xi](J. Serra also referred to this in his book [97, p. 84]):

‘In general, the structure of an object is defined as the set of relationships existing between elements or parts of the object. In order to experimentally determine this structure, we must try, one after the other, each of the possible relations and examine whether or not it is verified. Of course, image constructed by such a process will depend to the greatest extent on the choice made for the system \mathfrak{R} of relationships considered as possible. Hence this choice plays an à priori (in the Kantian sense) constructive role and determines the relative worth of the concept of structure at which we will arrive at. In the case of a porous medium, let A be a solid component(union of grains), and let A^c be a porous network. In this medium, we shall move a figure B , called the structuring pattern that plays the role of a probe collecting information. This operation is experimentally attainable.’

Figure 5.3 demonstrates the dilation and erosion of the binary image shown in 5.3a with the 3×3 structuring element (subimage 5.3b) with the origin at the center. Subimage 5.3a shows a digital binary image which could also be considered as set A . Shaded squares (pixels) are elements of set A . Foreground color is gray and background color is solid white. Dilation expands the shapes in foreground color contained in the image. In contrast, erosion shrinks the shapes in foreground color or equivalently expands the shapes in background color. Dilated and Eroded images are shown in subimages 5.3c and 5.3d, respectively. Opening ($o_B(A)$) and closing ($c_B(A)$) are two operators obtained by the following compositions.

$$o_B(A) = d_B(e_B(A)) \text{ , } c_B(A) = e_B(d_B(A)) \quad (5.3)$$

Closed and Opened images of the image A (subimage 5.3a) are shown in subimages 5.3e

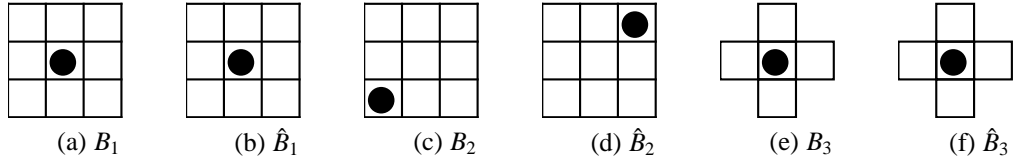


Figure 5.1: Examples of structuring elements (B_1, B_2, B_3) and their reflections ($\hat{B}_1, \hat{B}_2, \hat{B}_3$). The dots denote the centers of SEs.

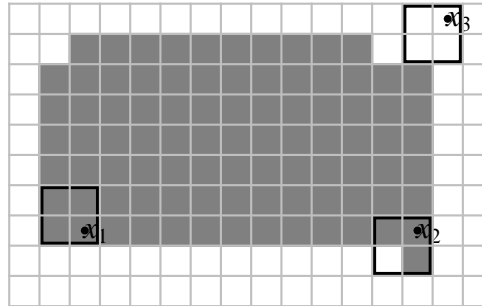


Figure 5.2: Structuring element is the 2×2 square shown in various positions on image plane. The origin of the structuring element is dotted.

and 5.3f, respectively.

Table 5.1 shows the summary of morphological operators .

Definition	Description
$B_x = \{b + x : b \in B\}$	B_x is B translated along vector x .
$\hat{B} = \{-b : b \in B\}$	Reflection of B about the origin .
$e_B(A) = \{x : B_x \subseteq A\}$	Erosion of set A by set B .
$d_B(A) = \{x : \hat{B}_x \cap A \neq \emptyset\}$	Dilation of set A by set B .
$o_B(A) = \cup\{B_x : B_x \subseteq A\}$	Opening of set A by set B .
$c_B(A) = \cap(X \setminus \{\hat{B}_x : \hat{B}_x \cap A \subseteq X \setminus A\})$	Closing of set A by set B .

Table 5.1: Basic morphological operators .

Topological Properties of Mathematical Morphology

Here, we briefly explain the topological properties of the morphological operators (see also,

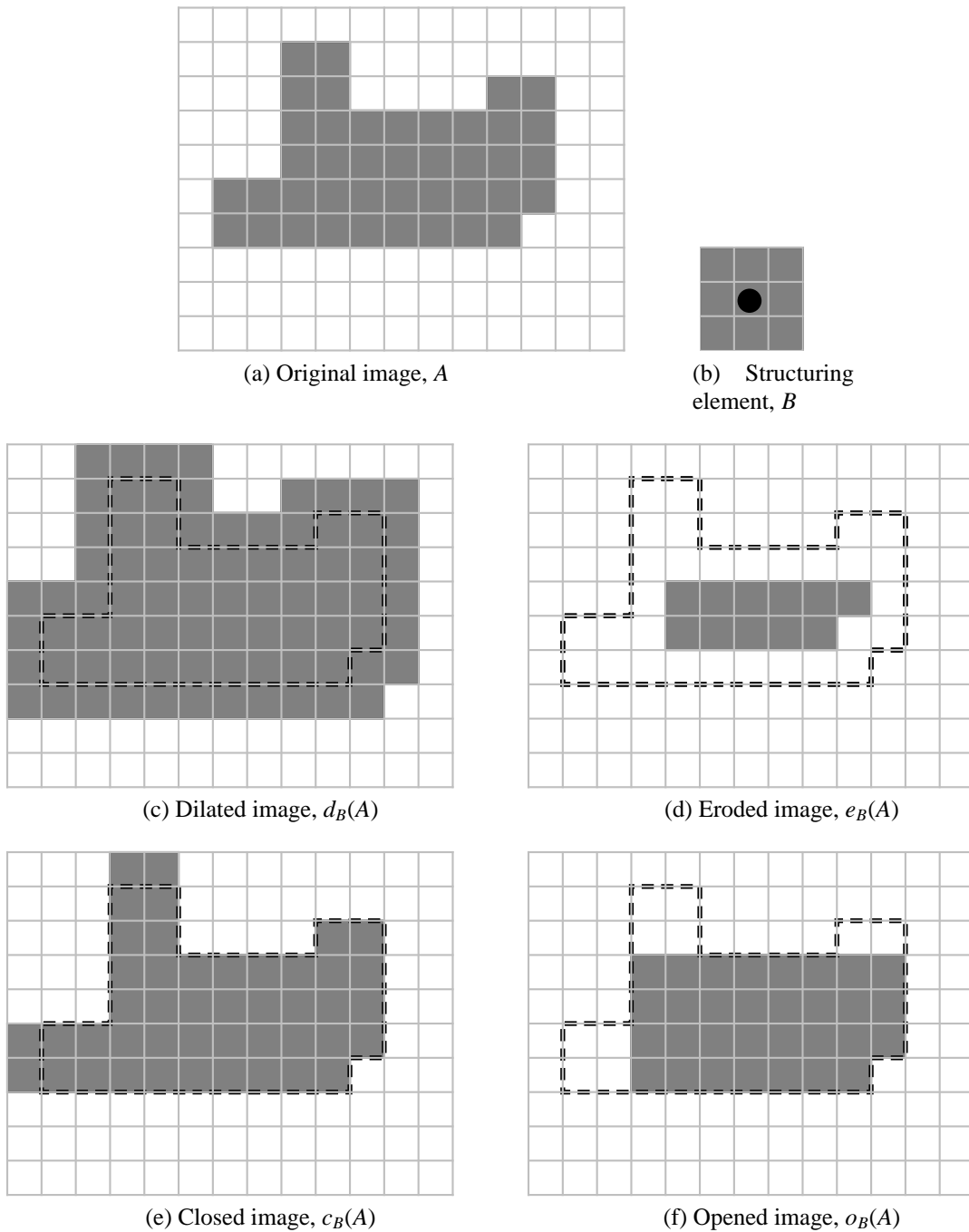


Figure 5.3: Examples of mathematical dilation and erosion. Gray squares are members of the set and considered as the foreground color in these images. The dashed lines in (c),(d),(e) and (f) is the boundary of set A , shown only for reference.

e.g., [27, 67, 97]). Let \mathring{B}_r and \bar{B}_r be an open ball and closed ball of radius r , respectively. Consider the sets of structuring elements $\bar{\mathbf{B}}$ and $\mathring{\mathbf{B}}$ defined as follows:

$$\bar{\mathbf{B}} = \{\bar{B}_r \mid r > 0\}, \quad \mathring{\mathbf{B}} = \{\mathring{B}_r \mid r > 0\}. \quad (5.4)$$

The following equations show the relations between mathematical morphology's opening and closing to topological closing and opening for a set $A \subset X$ in euclidean space, let \mathring{A} and \bar{A} be interior and closure of a set A . Then

$$\mathring{A} = \bigcup_{B \in \mathring{\mathbf{B}}} o_B(A) = \bigcup_{B \in \bar{\mathbf{B}}} o_B(A), \quad (5.5)$$

and

$$\bar{A} = \bigcap_{B \in \mathring{\mathbf{B}}} c_B(A) = \bigcap_{B \in \bar{\mathbf{B}}} c_B(A). \quad (5.6)$$

The following equations also relate the interior and closure to erosion and dilation [97]:

$$\mathring{A} = \bigcup_{B \in \mathring{\mathbf{B}}} e_B(A) = \bigcup_{B \in \bar{\mathbf{B}}} e_B(A), \quad (5.7)$$

and

$$\bar{A} = \bigcap_{B \in \mathring{\mathbf{B}}} d_B(A) = \bigcap_{B \in \bar{\mathbf{B}}} d_B(A). \quad (5.8)$$

In words, the interior of a set A is the union of the opening or erosions of the set A with open or closed balls of different sizes. The closure of a set A is the intersection of the closing or dilations of A with open/closed balls of different sizes. For our application in image processing, we propose to use a finite set of structuring elements instead of infinite sets defined in equation 5.4:

$$\mathbf{B} = \{B_i \mid B_i \text{ is a structuring element and } i \in I\} \quad (5.9)$$

where I is an index set. Considering the finite set of structuring elements, we approximate

the interior and closure of a set A by the following equations:

$$\mathring{A} \approx \bigcup_{B \in \mathbf{B}} o_B(A), \quad (5.10)$$

$$\mathring{A} \approx \bigcup_{B \in \mathbf{B}} e_B(A). \quad (5.11)$$

where $x \approx y$ means x is the approximately equal to y . Similar definitions could be written for closure of A based on dilation and closing operators:

$$\bar{A} \approx \bigcap_{B \in \mathbf{B}} c_B(A), \quad (5.12)$$

$$\bar{A} \approx \bigcap_{B \in \mathbf{B}} d_B(A). \quad (5.13)$$

In the extreme case, there is only one structuring element, B :

$$\mathring{A} \approx o_B(A), \quad (5.14)$$

$$\mathring{A} \approx e_B(A). \quad (5.15)$$

and,

$$\bar{A} \approx c_B(A), \quad (5.16)$$

$$\bar{A} \approx d_B(A). \quad (5.17)$$

5.2 Mathematical Morphology Operators and Interior & Closure Operators with Inclusion Degree

This section provides a topological foundation for incorporating inclusion degree into the definitions of morphological operators. Equations 5.5, 5.6, 5.7 and 5.8 or their approximated versions (equations 5.10, 5.11, 5.12 and 5.13) clarify the topological properties of the morphological operators and reveal how one can use the proposed closure and inte-

rior operators with inclusion degree in MM applications. These equations are comparable with definitions of interior and closure operations in equations 2.1 and 2.2 . But first, let us rewrite the closure definition (equation 2.2) in a way more similar to morphological dilation.

Proposition 11. *Let (X, τ) be a crisp topological space and $A \subset X$. The closure of set A defined by*

$$\bar{A} = \cup\{B \in \tau : B \cap A \neq \emptyset\} . \quad (5.18)$$

Proof. Topological closure operator is defined based on closed sets (elements of τ') in topology, as defined in equation 2.2. For reference we bring the definition again:

$$\bar{A} = \{B \in \tau' : A \subseteq B\} .$$

The goal is to rewrite the above definition based on open sets in τ . Based on duality relation in equation 2.3, we have:

$$\begin{aligned} \bar{A} &= X \setminus \overbrace{(X \setminus A)}^{\circ} \\ &= X \setminus \cup\{B \in \tau : B \subseteq X \setminus A\} \\ &= X \setminus \cup\{B \in \tau : B \cap A = \emptyset\} \\ &= \cup\{B \in \tau : B \cap A \neq \emptyset\} . \end{aligned}$$

□

Proposition 11 shows how to define a closure of a set A in terms of open sets in topology (X, τ) . Equation 5.18 is similar to equation 5.1. Structuring elements at different locations on the image plane, could be perceived as open sets in the topological space. Inclusion degree introduced in the definition of interior and closure operators in chapter 3-section 3.1. We use the same technique to introduce the inclusion degree to the definitions of morphological operators.

Definition 5.2.1. Dilation with inclusion degree σ of set A with structuring element B is defined as follows:

$$d_{B\sigma}(A) = \{x \in X : \text{Inc}(\hat{B}_x, A) \geq \sigma\} \quad (5.19)$$

where \hat{B}_x is the reflected and translated structuring element such that its origin is located at point x . Inc is the inclusion measure (equation 3.1). Dilation with inclusion degree σ of A by B is the set of all the points x such that \hat{B}_x and A overlapped more than a threshold determined by σ .

$d_{B\sigma}(A)$ has the same properties as closure operator with inclusion degree.

Definition 5.2.2. Erosion with inclusion degree γ of set A with structuring element B is defined as follows:

$$e_{B\gamma}(A) = \{x \in X : \text{Inc}(B_x, A) \geq \gamma\} \quad (5.20)$$

where B_x is the translated structuring element such that its origin is located at point x . Erosion with inclusion degree γ of A by B is the set of all the points x such that B_x and A overlapped more than a threshold determined by γ .

$e_{B\gamma}(A)$ has the same properties as interior operator with inclusion degree.

Proposition 12. Dilation operator with inclusion degree σ and erosion operator with inclusion degree γ have duality relation iff $\sigma = 1 - \gamma$. Both operators are using the structuring element B .

Proof. In traditional mathematical morphology, duality relation for erosion and dilation is as follows:

$$d_B(A) = (e_B(A^c))^c .$$

For simplicity, we consider $B = \hat{B}$. We add the inclusion degree to the definition of erosion,

we have:

$$\begin{aligned}
\left(e_{B\gamma}(A^c)\right)^c &= \{x \in X : \text{Inc}(B_x, A^c) \geq \gamma\}^c \\
&= X \setminus \{x \in X : \text{Inc}(B_x, X \setminus A) \geq \gamma\} \\
&= X \setminus \{x \in X : \text{Inc}(B_x, A) < 1 - \gamma\} \\
&= \{x \in X :: \text{Inc}(B_x, A) \geq 1 - \gamma\} \\
&= d_{B(1-\gamma)}(A) .
\end{aligned}$$

Therefore

$$d_{B(1-\gamma)}(A) = \left(e_{B\gamma}(A^c)\right)^c .$$

□

In order to keep the extensivity/anti-extensivity properties of dilation and erosion, $\gamma > \sigma$. In order to preserve the duality property $\sigma < 0.5$ which results in $\gamma = 1 - \sigma > 0.5$.

Figure 5.4 shows structuring element B at various locations on the image plane. Based on the position of the structuring element the inclusion of B in $A(\hat{B} = B)$ varies:

$$\text{Inc}(B_x, A) = 0 , \text{Inc}(B_y, A) = \frac{1}{9} , \text{Inc}(B_w, A) = \frac{6}{9} , \text{Inc}(B_z, A) = 1 .$$

In traditional morphology, only inclusion degree of zero and one are considered. Let us rewrite the definitions of erosion and dilation based on inclusion degree:

$$e_B(A) = \{x : B_x \subseteq A\} = \{x : \text{Inc}(B_x, A) = 1\} .$$

$$d_B(A) = \{x : \hat{B}_x \cap A \neq \emptyset\} = \{x : \text{Inc}(\hat{B}_x, A) > 0\} .$$

The proposed morphological operators introduced two thresholds γ and σ ($\gamma = 1 - \sigma$) to soften the crisp inclusion effects.

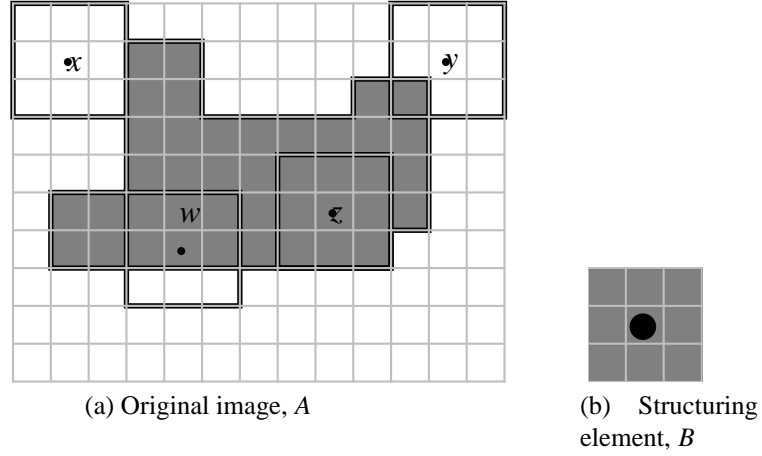


Figure 5.4: Structuring element (B) is shown at various locations on the image plane. Based on location of B_i and $i \in \{w, x, y, z\}$, $Inc(B_i, A)$ varies between zero and one.

Definition 5.2.3. *Opening/closing with inclusion degree σ of a set A by B defined by*

$$o_{B\sigma}(A) = d_{B\sigma}(e_{B(1-\sigma)}(A)) \quad , \quad c_{B\sigma}(A) = e_{B(1-\sigma)}(d_{B\sigma}(A)) \quad .$$

Here is not the first time that inclusion degree introduced for mathematical morphology. In [108], inclusion degree is added to the definitions of dilation/closing and erosion/opening without considering the topology underneath. The operators are called variable precision (VP) morphological operators. Sun [108] showed that the new operators showed a better performance in image noise reduction (salt and pepper noise) comparing the traditional morphological operators. To remove the noise, morphological opening followed by morphological closing ($c_B(o_B(A))$) is applied to an image. The work presented in this thesis are based on topological spaces and the main focus of the thesis is the definition of new topological operators and then using them in different image processing tasks. The difference between this chapter and Z. Sun's paper is the origin of the idea. We introduced the inclusion measure in the topological interior and closure operators which have their applications in mathematical morphology. This provides a foundation for introducing these new operators in application areas such as mathematical morphology. Although, there are some papers using inclusion degree in rough set approximations and mathematical morphology operators, none of them consider the topological properties of these operators.

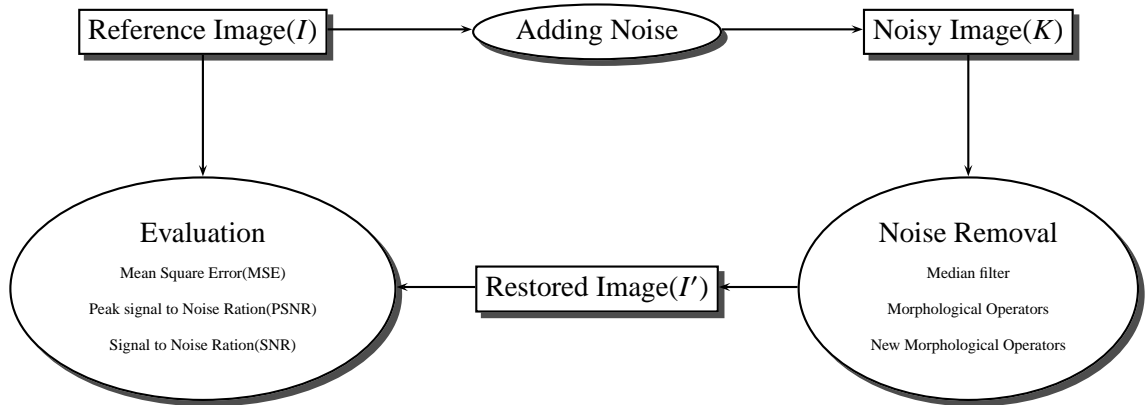


Figure 5.5: Noise Removal Evaluation Process

To demonstrate the effectiveness of the morphological operators with inclusion degree, we demonstrate their effectiveness in noise reduction and edge detection for binary images. Since fuzzy mathematical morphology introduced for gray scale images [3, 4, 15], using the fuzzy interior and fuzzy closure operators with inclusion degree would be interesting. This area is suggested as a future work.

5.3 Applications of Proposed Morphological Operators

In this section, we applied the proposed morphological operators in morphological noise reduction and edge detection in noisy images. We compare the efficiency of the proposed operators to traditional morphological operators. Traditional morphology have been used to remove salt and pepper noise from binary images. Since our goal is to compare the traditional mathematical morphology with the morphology with inclusion degree, we choose the binary images and salt and pepper noise. So, it should be emphasized that the goal is not the development of a general purpose noise removal filter for images.

5.3.1 Noise Reduction

Noise reduction is the process of removing noise from images. Image noise refers to any unwanted variation in values of pixels. We follow the process shown in figure 5.5 to evaluate the efficiency of the new morphological operators in noise reduction. Noise added

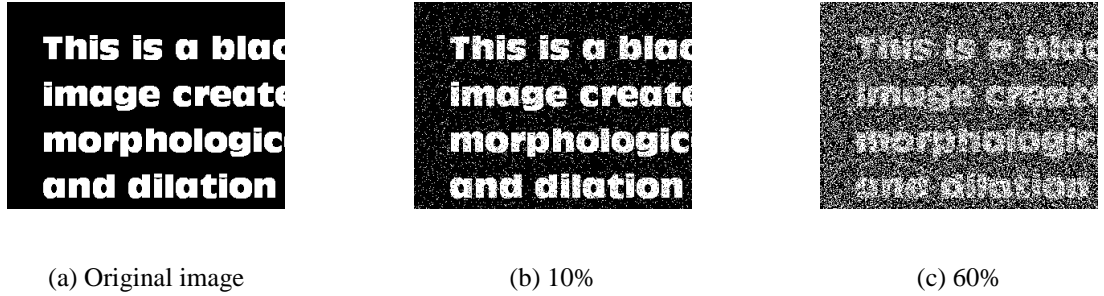


Figure 5.6: Salt and pepper noise. (a) Original image. (b) Noisy image has a 10% probability of being contaminated with noise, (c) Noisy image with 60% probability of contamination .

Noise Removal Indicators	Definition
Mean Square Error (MSE)	$MSE = \frac{1}{MN} \sum_i \sum_j (I(i, j) - I'(i, j))^2$
Peak Signal to Noise Ratio	$PSNR = 10 \times \log_{10} \left(\frac{MAX_I^2}{MSE} \right) = 20 \times \log_{10} \left(\frac{MAX_I}{\sqrt{MSE}} \right)$ $MAX_I =$ Maximum possible pixel value of image I .
Signal to Noise Ratio(SNR) [36]	$SNR = \frac{\sum_i \sum_j I(i, j)^2}{\sum_i \sum_j (I(i, j) - I'(i, j))^2}$

Table 5.2: Some noise removal indicators. I is the reference image with $M \times N$ pixels, I' is the processed image (noise removed) .

to the reference image (I), noise reduction method applies to the noisy image (K) and the restored image (I') is evaluated based on some indicators. There are various indicators to measure the quality of noise reduction techniques, including but not limited to mean square error (MSE), peak signal to noise ration (PSNR) and signal to noise ratio (SNR). Table 5.2 defines these indicators which we used for evaluation process. Larger values for PSNR and SNR and smaller values for MSE mean better performance.

We consider binary images in this section. Binary images only have 2 values, black and white. They are used in shape classification [37, 64, 71], optical character readers (OCR), fax machines, scanners, newspapers, etc. Salt and pepper noise added to an image and the goal is to remove the noise from the image using new morphological operators. Salt and pepper noise is a type of impulse noise caused by malfunctioning pixels in camera sensors, faulty memory locations in hardware, or transmission in noisy channel [7, 12].

Figure 5.6 shows images contaminated with salt and pepper noise with different probabilities of contamination. We are proposing the use of the morphological operators with inclusion degree for noise removal in binary images. To have a comparison with other noise removal methods, the following filters have been used for our evaluation process:

Median Filter

Median filter is one of the most popular methods in removing salt and pepper noise [48, 112]. It has been evolved during the time, like adaptive median filter [49], multi scale median filter [16], multi-stage filters [12]. Median filtering is a nonlinear filtering process which every pixel is replaced with the median of neighboring pixels. It is an effective way in removing impulse noises in images. Median filter is chosen as a reference for comparing the efficiency of our morphological noise reduction method.

Open-Close Sequence (OC)

Morphological operators are also used for noise reduction. One of the well known morphological noise reduction method is open-close sequence [23, 88] :

$$OC(A, B) = o_B(c_B(A)) .$$

Open-close sequence is specially efficient method in removing salt and pepper noise. The opening filter removes the pepper parts of the noise and closing filter reduce the salts.

Open-Close-Close-Open Sequence (OCCO)

OCCO filter was first introduced in [88]. It has the smoothing effect on the image. The process is as follows:

$$OCCO(A, B) = \frac{1}{2}(o_B(c_B(A)) + c_B(o_B(A))) .$$

where A is the image and B is the structuring element. It is the average of open-close sequence and close-open sequence.

Open-Close Sequence with Inclusion Degree (OC_σ)

Open-close sequence with inclusion degree is the process of closing an image with struc-

turing element B and inclusion measure σ followed by opening the result with same SE and inclusion measure σ :

$$OC_{\sigma}(A, B) = o_{B\sigma}(c_{B\sigma}(A)) .$$

This process proposed in [108] by Z. Sun, when the variable precision morphological operators were defined. We also used this method for comparison purposes. We proposed the following morphological sequence for noise removal from binary images:

Open-Close-Close-Open Sequence with Inclusion Degree ($OCCO_{\sigma}$)

$OCCO_{\sigma}$ filter defined as follows:

$$OCCO_{\sigma}(A, B) = \frac{1}{2}(o_{B\sigma}(c_{B\sigma}(A)) + c_{B\sigma}(o_{B\sigma}(A))) .$$

We applied salt and pepper noise to a black and white image shown in figure 5.6-(a). The contamination probability varies between 10% and 70%. Five different noise removal methods as discussed above applied on the noisy image. Three different noise removal indicators have been chosen to calculate the efficiency of the methods, including signal to noise ratio (SNR), mean square error (MSE) and peak signal to noise ratio (PSNR). The results are shown in table 5.3. As mentioned earlier, higher results for SNR and PSNR and lower results for MSE show better performance. These values have been shaded in gray for different methods and different noise contamination. Based on the results, median filter has a better performance in lower noise contamination. But in higher noise contamination probabilities (>30%), OC_{σ} and our proposed $OCCO_{\sigma}$ have better performances. Figures 5.7, 5.8, 5.9, 5.10 show the noisy image with different contamination probabilities and the results of different filters. As suggested by the results, in higher noise contamination, the traditional morphology outperforms the traditional mathematical morphology operators. The reason is the ability of the operators with inclusion degree to ignore errors due to the inclusion degree. In traditional morphology, even a single noisy pixel changes the result of erosion. this ultimately changes the output of opening/closing operators. However, in morphological operators with inclusion degree the noisy pixels can be ignored with

Probability		10%	20%	30%	40%	50%	60%	70%
Median	SNR	30.99	16.5505	9.5507	5.7269	3.4505	2.2441	1.6498
	MSE	0.0077	0.0145	0.0252	0.0433	0.0765	0.1301	0.1998
	PSNR	69.2703	66.5217	64.1204	61.7685	59.2964	56.9872	55.1248
OC	SNR	10.4363	5.2708	1.6099	0.7586	0.3721	0.2069	0.1112
	MSE	0.0214	0.0462	0.0928	0.1376	0.176	0.2007	0.2182
	PSNR	64.8174	61.4856	58.4553	56.7449	55.6746	55.1052	54.7418
OCCO	SNR	8.8565	3.9910	1.5668	0.7478	0.3674	0.2038	0.1099
	MSE	0.0247	0.0486	0.0942	0.1383	0.1765	0.2008	0.2182
	PSNR	64.2066	61.2620	58.3895	56.7240	55.6633	55.1038	54.7415
OC_σ	SNR	14.3942	11.0210	8.7309	6.7632	4.53	2.8849	1.6353
	MSE	0.0162	0.0208	0.0258	0.0324	0.0465	0.0671	0.1047
	PSNR	66.0343	64.9421	64.0169	63.0209	61.435	59.8626	57.9323
$OCCO_\sigma$	SNR	14.3942	10.8871	8.6905	6.7648	4.5205	2.8829	0.3674
	MSE	0.0162	0.0210	0.0258	0.0324	0.0466	0.0671	0.1765
	PSNR	66.0252	64.9048	64.0093	63.0300	61.4467	59.8633	55.6633

Table 5.3: Noise Removal Evaluation- 3×3 median filter, Open-close (OC) and Open-close-close-open (OCCO) sequence of both traditional morphology and morphology with inclusion degree are tested. σ is set to 0.4 as the threshold of the inclusion degree. Best results are shaded in gray. Median filter is more efficient in lower probability noise contamination. For higher noise contamination (>30%) Open-close sequence with inclusion degree and Open-close-close-open sequence with inclusion degree perform better.

respect to the threshold chosen for the inclusion degree.

5.3.2 Edge Detection

Edges are those points in a digital image at which the image brightness changes rapidly.

Morphological edge detection is defined by:

$$E(A, B) = d_B(A) \setminus e_B(A) .$$

where A is the image, B is the structuring element and $d_B(A)$ is the dilation of A with B and $e_B(A)$ is the erosion of A with B and \setminus is set difference operator [23, 36].

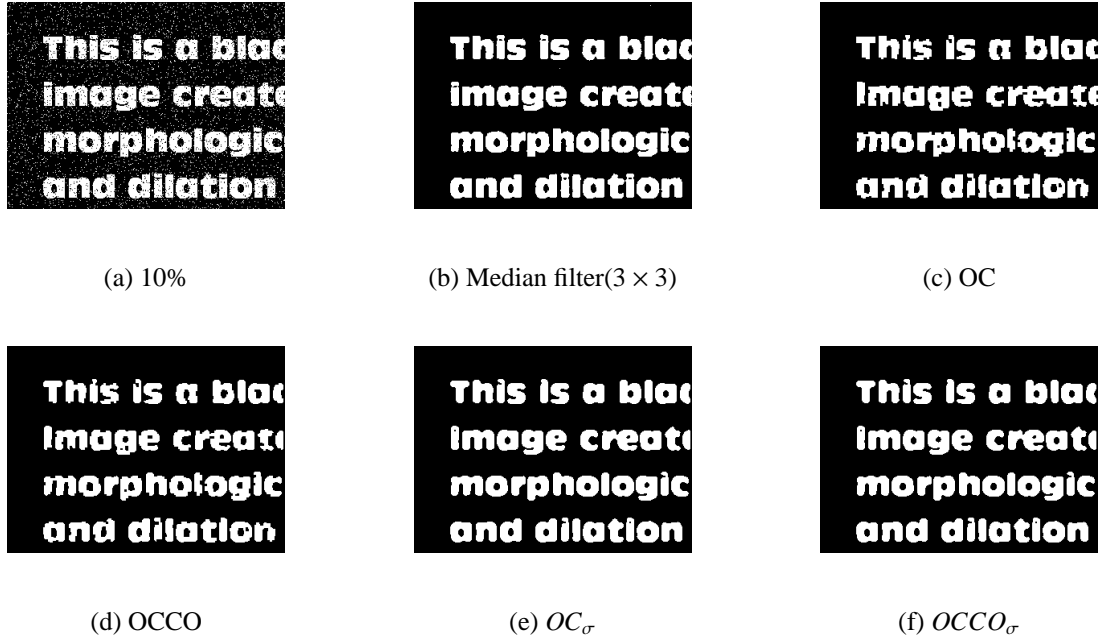


Figure 5.7: Salt and pepper noise removal. (a) Noisy image has a 10% probability of being contaminated with noise, (b) Result of 3×3 Median filter, (c) Open-close sequence, (d) Open-Close-Close-Open sequence (e) Open-close sequence with inclusion degree $\sigma = 0.4$ (f) Open-Close-Close-Open sequence filtering with $\sigma = 0.4$. Structuring element is a 3 square in (c-f).



Figure 5.8: Salt and pepper noise removal. (a) Noisy image has a 40% probability of being contaminated with noise, (b) Result of 3×3 Median filter, (c) Open-close sequence, (d) Open-Close-Close-Open sequence (e) Open-close sequence with inclusion degree $\sigma = 0.4$ (f) Open-Close-Close-Open sequence filtering with $\sigma = 0.4$. Structuring element is a 3 square in (c-f).



Figure 5.9: Salt and pepper noise removal. (a) Noisy image has a 50% probability of being contaminated with noise, (b) Result of 3×3 Median filter, (c) Open-close sequence, (d) Open-Close-Close-Open sequence (e) Open-close sequence with inclusion degree $\sigma = 0.4$ (f) Open-Close-Close-Open sequence filtering with $\sigma = 0.4$. Structuring element is a 3 square in (c-f).



Figure 5.10: Salt and pepper noise removal. (a) Noisy image has a 70% probability of being contaminated with noise, (b) Result of 3×3 Median filter, (c) Open-close sequence, (d) Open-Close-Close-Open sequence (e) Open-close sequence with inclusion degree $\sigma = 0.4$ (f) Open-Close-Close-Open sequence filtering with $\sigma = 0.4$. Structuring element is a 3 square in (c-f).

We propose the use of new morphological operators with inclusion degree for morphological edge detector which have the better performance specially in noisy images. The new edge detection method is defined as follows:

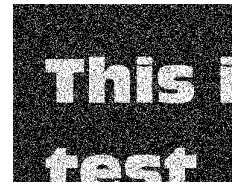
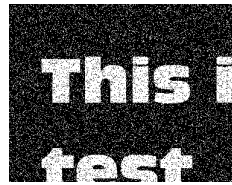
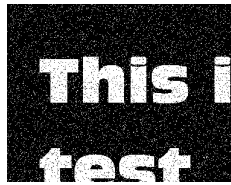
$$E_{\sigma}(A, B) = d_{B\sigma}(A) \setminus e_{B(1-\sigma)}(A) .$$

where $d_{B\sigma}$ is dilation operator with inclusion degree and $e_{B(1-\sigma)}(A)$ is the erosion operator with inclusion degree $(1 - \sigma)$. Figure 5.11 shows the results of morphological edge detection on a noisy image. Traditional morphology and morphology with inclusion degree are applied on the images with different noise contamination. The results show that morphological edge detection with inclusion degree performs better in noisy images. Again, the ability of the operators with inclusion degree to ignore small errors and imperfections due to the inclusion degree is the reason of their better performance.

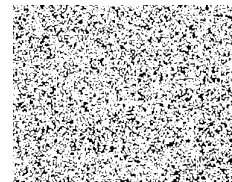
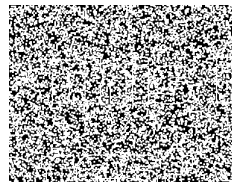
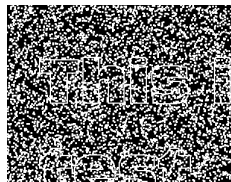
5.4 Summary

This chapter contained background information on crisp and fuzzy topologies. The main points of this chapter include:

- Topological properties of mathematical morphology operators have been discussed.
- Topological properties of mathematical morphology make them an obvious choice in applying the proposed interior/closure operators with inclusion degree in this area.
- Although inclusion degree had been defined for morphological operators before, topological properties were not discussed.
- The morphological operators with inclusion degree shows better performance in noise(salt and pepper) removal in comparison to median filter and traditional morphological filters in higher noise contaminations.



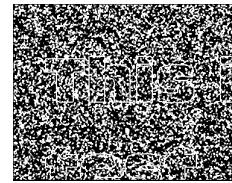
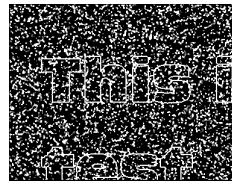
(a) noise contaminated 10% (b) noise contaminated 20% (c) noise contaminated 30%



(d) $(E(A, B))$

(e) $(E(A, B))$

(f) $(E(A, B))$



(g) $(E_{\sigma=0.2}(A, B))$

(h) $(E_{\sigma=0.2}(A, B))$

(i) $(E_{\sigma=0.2}(A, B))$



(j) $(E_{\sigma=0.3}(A, B))$

(k) $(E_{\sigma=0.3}(A, B))$

(l) $(E_{\sigma=0.3}(A, B))$



(m) $(E_{\sigma=0.4}(A, B))$

(n) $(E_{\sigma=0.4}(A, B))$

(o) $(E_{\sigma=0.4}(A, B))$

Figure 5.11: Morphological Edge Detection

- The $OCCO_\sigma$ were proposed as a noise removal filter.
- The morphological operators with inclusion degree shows a better performance in edge detection in noisy images in comparison with traditional morphology edge detectors due to their ability to ignore small errors.

Chapter 6

Conclusion

The focus of this research was on the extension of topological operators with the aim of inclusion degree. Both crisp and fuzzy topological spaces were considered and properties of new operators are discussed in details and compared with traditional operators. We also proposed a method to define a fuzzy topology based on a collection of fuzzy sets which was used in the application part of this thesis. We expected that the extended version of topological operators make them practical for image processing and digital spaces. Ignoring small errors and imperfections were handled effectively by the introduction of inclusion degree and applied in image/shape database classification and mathematical morphology. The proposed method for image database classification used the idea of subspace topologies to model each image category in the database. The interior operator with inclusion degree was utilized to classify the query image into the target category. The interior of the query image was calculated with respect to different topologies (one for each image category). The decision was made on the difference between the query and its interiors. For shape classification, only shape information was used and for the image databases color information was also utilized. The results presented in chapter 4 and chapter 5 demonstrated that the extended topological operators are a powerful tool in the mentioned image processing applications. Moreover, the proposed classification method presented in chapter 4 modeled each image category effectively with topological subspaces and finding the

interior (with inclusion degree) with respect to different categories was the novel approach in this area.

The extended interior and closure operators were also applied in mathematical morphology area and the results are used for noise removal and edge detection. The operators with inclusion measure showed better performance in comparison to the traditional morphology. For classification parts, we are limited to the type of the features that could be considered as fuzzy sets. Also, the inclusion degree is defined by a user. It is also important to note that the method is dependent on the value of the inclusion degree and the type of the extracted features. For the morphological application the method is dependent on the type of the structuring element and the value of inclusion measure. The applications presented in this thesis for the extended topological operators showed the advantage and could be improved overtime.

Considering the results of this thesis the following suggestions are recommended for future works. Other types of fuzzy topology may be considered instead of C.Chang's approach. In the application part, we recommend considering the Rough sets which have similar operators to interior and closure operators. Rough set was first introduced by Z. Pawlak [83] which is a formal approximation of a crisp set. It should be mentioned that variable precision rough sets have been introduced before by [122] however, not much done in terms of exploring topological properties and also applications. Mathematical morphology for gray scale images are related to fuzzy approaches. Considering fuzzy topology with inclusion measure in this area is also recommended.

Appendix A

Fuzzy Topological Space: Alternative Definitions

Fuzzy topological space was first introduced by C.M. Chang in 1968 [13] . His definition was explained in chapter 2 and used throughout this document. Alternative definitions were proposed throughout the years and this appendix describes a few of them. R. Lowen's [65], J. Gougan's [33] and A.P. Sostak's [102, 103] approaches are considered in this appendix.

A.1 Lowen's Approach

R. Lowen suggested an alternative definition to Chang's fuzzy topological space. Let (X, δ) be a C.M Chang's fuzzy topology, R.Lowen changed the condition *chfTop.1* of the definition 2.2.4 to $\forall \alpha$ constant, $\alpha \in \delta$, where $\mu_\alpha(x) = \alpha$ for all $x \in X$ [65].

Definition A.1.1. $\delta_L \subset \mathcal{F}(X)$ is a fuzzy topology on X based on R.Lowen's definition if, and only if

LfTop.1 $\forall \alpha$ constant, $\alpha \in \delta_L$,

LfTop.2 $\forall A, B \in \delta_L \Rightarrow A \wedge B \in \delta_L$,

LfTop.3 $\forall (A_j)_{j \in J} \subset \delta_L \Rightarrow \bigvee_{j \in J} A_j \in \delta_L$.

Lowen called Chang's definition a quasi-fuzzy topology. The interior and closure of

a set A are defined using equations 2.10 and 2.9, respectively. However, the interior and closure operators are defined as follows in Lowen's work:

Definition A.1.2. *An operator $\psi : \mathcal{F}(X) \rightarrow \mathcal{F}(X)$ is a fuzzy closure operator based on R.Lowen's definition [65] if and only if,*

- $\psi(\alpha) = \alpha, \forall \alpha \text{ constant},$
- $\psi(A) \geq A \quad \forall A \in \mathcal{F}(X),$
- $\psi(A) \vee \psi(B) = \psi(A \vee B), \quad \forall A, B \in \mathcal{F}(X),$
- $\psi(\psi(A)) = \psi(A), \quad \forall A \in \mathcal{F}(X).$

Definition A.1.3. *An operator $\phi : \mathcal{F}(X) \rightarrow \mathcal{F}(X)$ is a fuzzy interior operator based on R.Lowen's definition [65] if and only if,*

- $\phi(\alpha) = \alpha, \forall \alpha \text{ constant},$
- $\phi(A) \leq \mu \quad \forall A \in \mathcal{F}(X),$
- $\phi(A) \wedge \phi(B) = \phi(\mu \wedge B), \quad \forall A, B \in \mathcal{F}(X),$
- $\phi(\phi(A)) = \phi(A), \quad \forall A \in \mathcal{F}(X).$

A.2 Šostak's Approach

Šostak argued that in all of the previous definitions of fuzzy topology, the so-called fts is always crisp, *i.e.*, it is a crisp subfamily of some family of fuzzy sets. He began the study of fuzzy structures of topological type [102, 103]. The idea of his work is to allow the fuzzy subsets to be open to some degree, ranging from 1 (completely open) to 0 (completely non-open sets). The fuzzy topology in Šostak's work is a pair (X, δ) , where X is a set and $\delta \in I^{\mathcal{F}(X)}$. He defined a fuzzy topology as a function $\delta : \mathcal{F}(X) \rightarrow I$, which assigns to every fuzzy subset of X the real number, which shows to what extent this set is open, $I = [0, 1]$. $\mathcal{F}(X)$ represents fuzzy sets on X .

Definition A.2.1. Let X be a non-empty set. For a fuzzy topology on X , A.P. Šostak introduced a function $\delta_S : \mathcal{F}(X) \rightarrow I$ satisfying the following three axioms [102]:

SfTop.1 if $A, B \in \mathcal{F}(X)$, then $\delta_S(A \wedge B) \geq \delta_S(A) \wedge \delta_S(B)$,

SfTop.2 if $A_i \in \mathcal{F}(X)$ for all $i \in J$, then $\delta_S(\bigvee_i A_i) \geq \bigwedge_i \delta_S(A_i)$,

SfTop.3 $\delta_S(\mathbf{0}) = \delta_S(\mathbf{1}) = 1$,

where $I = [0, 1]$ and $\mathcal{F}(X)$ is the set of all fuzzy sets on X . (X, δ_S) is a fuzzy topology based on Šostak's definition. δ_S is called 'openness' degree.

Axiom *SfTop.1* states that the intersection of two fuzzy sets is not 'less open' than the minimum of the 'openness' of these sets. Axiom *SfTop.2* requires that the degree of openness of the union of any crisp family of fuzzy sets should be not less than the smallest degree of openness of these sets. The last axiom states that the empty set and the whole space are 'absolutely open'. Let us have an example inspired by [92].

Example A.2.2. Let $X = [0, 1]$, and consider fuzzy sets $\{G_n \in \mathcal{F}(X)\}$ and $G \in \mathcal{F}(X)$, where $n \in \{2, 3, 4, \dots\}$ as follows:

$$G_n(x) = \begin{cases} 0.8, & x = 0, \\ nx, & 0 < x \leq \frac{1}{n}, \\ 1, & \frac{1}{n} < x \leq 1. \end{cases}$$

$$G = \begin{cases} 0.8, & x = 0, \\ 1, & \text{otherwise.} \end{cases}$$

Now, let us consider the following function, δ_S , as the degree of openness:

$$\delta_S(A) = \begin{cases} 1, & \text{if } A \in \{\mathbf{0}, \mathbf{1}\}, \\ \frac{1}{n}, & \text{if } A = G_n, \\ 0.7, & \text{if } A = G, \\ 0, & \text{otherwise.} \end{cases}$$

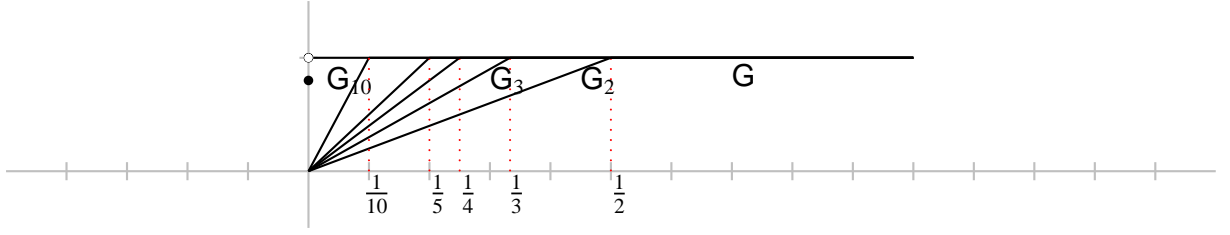


Figure A.1: fuzzy sets G_n for $n \in \{2, 3, 4, 5, 10\}$ and the fuzzy set G of example A.2.2 are shown.

It is clear that the function δ_S is a fuzzy topology based on Šostak's definition A.2.1.

A.3 Goguen's Approach

J. Goguen defined the fuzzy topological space on L-fuzzy sets [33]. Let L be a set. An L-fuzzy set A is associated with a function μ_A from the universe X to L [24], instead of the unit interval in fuzzy sets. In other words, L-fuzzy sets are a generalization of fuzzy sets. If L has a given structure, such as a lattice or group structure, $\mathcal{F}_L(X)$, the set of L -fuzzy sets on X , will have this structure, too. To clarify this idea, consider an example inspired by an example in [50]

Example A.3.1. Suppose that U consists of a group of people. The L-fuzzy set, whose membership function φ is shown in figure A.2, describes how well the people in U can cook. This example inspired an example in [50] Here, an L-fuzzy set φ on U is a mapping $\varphi : U \rightarrow L$, where L is a transitive partially ordered set.

Let L be a completely distributive lattice with the smallest element \perp and the greatest element \top , where $\perp \neq \top$. Let $\underline{\perp}$ and $\underline{\top}$ be the smallest element and greatest element in L^X , respectively. An L-fuzzy topology on X is defined as follows [120]:

Definition A.3.2. An L-fuzzy topology on X is a map $\delta_G : \mathcal{F}_L(X) \rightarrow L$ satisfying the following three axioms:

GfTop.1 $\underline{\perp} = \top$,

GfTop.2 $\delta_G(A \wedge B) \geq \delta_G(A) \wedge \delta_G(B)$, for every $A, B \in \mathcal{F}_L(X)$,

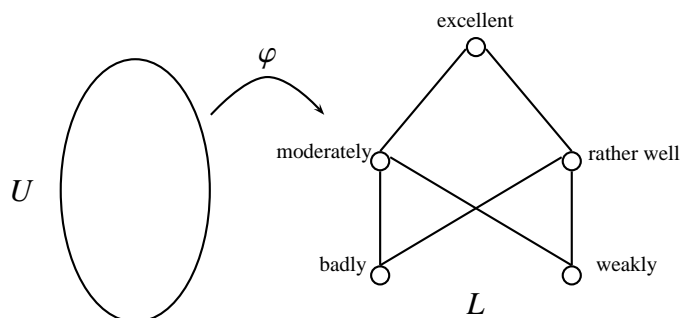


Figure A.2: example of L-fuzzy sets. Figure is used with permission [50].

GfTop.3 $\delta_G(\bigvee_{i \in \Delta} \mathbf{A}_i) \geq \bigvee_{i \in \Delta_G} \delta_G(\mathbf{A}_i)$.

The pair (X, δ_G) is called an L-fuzzy topological space (L-fts). For every $\mathbf{A} \in \mathcal{F}_L(X)$, $\delta_G(\mathbf{A})$ is called the degree of openness of the fuzzy subset \mathbf{A} .

A.4 Summery

This appendix explained different definitions of fuzzy topological space. We have considered, C.L. Chang's definition throughout this thesis. However, introducing the inclusion measure to the definition of other forms of fuzzy topologies including R. Lowen's and G. Gougen's method are recommended for future works.

Appendix B

Gaussian Mixture Model and Expectation Maximization

This appendix describes the basics of mixture models, Gaussian mixture models, Maximum likelihood and EM algorithm. The main reference is McLachlan and Peel 's book on finite mixture models [69].

B.1 Finite Mixture Model

Finite mixture models have provided a mathematical based approach to statistical modeling of a wide variety of random phenomena. Let Y_1, \dots, Y_n denote a random sample of size n , where Y_j is a p -dimensional random vector with probability density function $f(y_j)$ on \mathbb{R}^p . y_j is the realization of a random vector Y_j . Suppose that the density $f(y_j)$ of Y_j can be written:

$$f(y_j) = \sum_{i=1}^k \pi_i f_i(y_j) \quad (\text{B.1})$$

where the $f_i(y_j)$ are densities, k is the number of mixtures and the π are nonnegative quantities that sum to one:

$$0 \leq \pi_i \leq 1 \quad (i = 1, \dots, k)$$

and

$$\sum_{i=1}^k \pi_i = 1$$

The parameters π_1, \dots, π_k are called mixing proportions or weights. Density B.1 is called k -component finite mixture and $f_i(y_j)$ called component density function.

B.2 Parametric Formulation of Mixture Model

In many applications, the component densities, $f_i(y_j)$, belong to some parametric families. In these cases the component densities are specified by $f_i(y_j, \theta_i)$. the mixture densities is written on the following form:

$$f(y_j; \Psi) = \sum_{i=1}^k \pi_i f_i(y_j; \theta_i) \quad (\text{B.2})$$

where

$$\Psi = (\pi_1, \dots, \pi_k - 1, \xi^T)^T$$

the ξ is the vector containing all the parameters $\theta_1, \dots, \theta_k$. In this document, we are using Gaussian density functions as probability densities, therefore the finite mixture model called Gaussian Mixture Model (GMM). Gaussian mixture model is a wighted sum of k component Gaussian densities and is defined as follows:

$$g(y; \Psi) = \sum_{i=1}^k \pi_i g(y; \mu_i, \Sigma_i) \quad (\text{B.3})$$

where y is a D -dimensional countinuis valued data vector and $g(y; \mu_i, \Sigma_i)$ is the i -th component Gaussian density:

$$g(y; \mu_i, \Sigma_i) = \frac{1}{(2\pi)^{D/2} |\Sigma_i|^{1/2}} \exp\left\{-\frac{1}{2}(y - \mu_i)' \Sigma_i^{-1} (y - \mu_i)\right\} \quad (\text{B.4})$$

where μ_i is a mean vector and Σ_i is the covariance matrix of the i -th component.

B.3 Maximum Likelihood Estimation

Maximum likelihood (MLE) estimation for finite mixture model is discussed in this section. Parameter vector Ψ in a postulated density $f(y_j; \Psi)$ for a random vector Y_j is estimated as the $\widehat{\Psi}$. The estimate is provided by an appropriate solution to the following equation:

$$\partial \mathcal{L}(\Psi) / \partial \Psi = 0$$

or equivalently

$$\partial \log \mathcal{L}(\Psi) / \partial \Psi = 0$$

where

$$\mathcal{L}(\Psi) = \prod_{j=1}^n f(y_j; \Psi)$$

The likelihood function for Ψ formed under the assumption of independent data y_1, \dots, y_n .

B.4 Formulation of ML as an Incomplete-Data Problem

Since we use ML for image segmentation the observed data vector

$$y = (y_1^T, \dots, y_n^T)^T$$

is considered as incomplete data, as the associated component label vectors, z_1, \dots, z_n are not available. It is assumed that each y_i arised from one of the components. Let consider z_j as a k -dimensional vector, where k is the number of components. $z_{ij} = 1$ or 0 , according to whether y_j did or did not arise from the i -th component of the mixture. The complete data is shown by

$$y_c = (y^T, z^T)$$

where

$$z = (z_1^T, \dots, z_n^T)^T$$

The random variables corresponding to z_1, \dots, z_n are Z_1, \dots, Z_n . The complete data log likelihood for Ψ , $\log \mathcal{L}_c(\Psi)$ is

$$\log \mathcal{L}_c(\Psi) = \sum_{i=1}^k \sum_{j=1}^n z_{ij} \{\log \pi_i + \log f_i(y_j; \theta_i)\}$$

B.5 Expectation Maximization

Expectation Maximization (EM) algorithm is an iterative approach to solve the maximum likelihood problem of the finite mixture models. The EM algorithm treats the z_{ij} as missing data. It consists of two steps which runs iteratively, E-step (Expectation) and M-step (Maximization). Let $\Psi^{(0)}$ be the initial value specified for Ψ . On the first iteration of the EM algorithm, the E-step computes the conditional expectation of $\log \mathcal{L}_c(\Psi)$ given y , using $\Psi^{(0)}$ for Ψ :

$$Q(\Psi; \Psi^{(0)}) = E_{\Psi^{(0)}}\{\log \mathcal{L}_c(\Psi)|y\}$$

On the $(l + 1)$ -th iteration the E-step calculates $Q(\Psi; \Psi^{(l)})$, where $\Psi^{(l)}$ is the value of Ψ after the l th EM iteration. $\log \mathcal{L}_c(\Psi)$ is linear in the unobservable data z_{ij} and E-step simply requires the calculation of the current conditional expectation of Z_{ij} given the observed data y :

$$\begin{aligned} E_{\Psi^{(l)}}(Z_{ij}|y) &= pr_{\Psi^{(l)}}\{Z_{ij} = 1|y\} \\ &= \kappa_i(y_j; \Psi^{(l)}) \end{aligned}$$

where

$$\begin{aligned} \kappa_i(y_j; \Psi^{(l)}) &= \pi_i^{(l)} f_i(y_j; \theta_i^{(l)}) / f(y_j; \Psi^{(l)}) \\ &= \pi_i^{(l)} f_i(y_j; \theta_i^{(l)}) / \sum_{h=1}^k \pi_h^{(l)} f_h(y_j; \theta_h^{(l)}) \end{aligned}$$

for $i = 1, \dots, k; j = 1, \dots, n$. the quantity $\kappa_i(y_j; \Psi^{(k)})$ is the posterior probability that the j th member of the sample with observed value y_j belongs to the i th component of the mixture.. based on above equations the conditional expectation Q is:

$$Q(\Psi; \Psi^{(l)}) = \sum_{i=1}^k \sum_{j=1}^n \kappa_i(y_j; \Psi^{(l)}) \{\log \pi_i + \log f_i(y_j; \theta_i)\}$$

The M-step on the $(l+1)$ th iteration requires the global minimization of $Q(\Psi; \Psi^{(l)})$ with respect to Ψ all over parameter space to updated estimate $\Psi^{(k+1)}$. If the z_{ij} were observable, the the complete data maximum likelihood estimation of π_i would be given simply by

$$\widehat{\pi}_i = \sum_{j=1}^n z_{ij}/n \quad (i = 1, \dots, k)$$

As before, since z_{ij} is unknown, the values of z_{ij} are replace by the current values of the posterior conditional expectation $\kappa_i(y_j; \Psi^{(l)})$:

$$\pi_i^{(k+1)} = \sum_{j=1}^n \kappa_i(y_j; \Psi^{(l)})/n \quad (i = 1, \dots, k)$$

To update ξ on the M-step of the $(l+1)$ th iteration, it can be obtained as an appropriate root of:

$$\sum_{i=1}^k \sum_{j=1}^n \kappa_i(y_j; \Psi^{(l)}) \partial \log f_i(y_j; \theta_i) / \partial \xi = 0$$

The E- and M-steps are alternated repeatedly until the difference $\mathcal{L}(\Psi^{(l+1)}) - \mathcal{L}(\Psi^{(l)})$ changes by an arbitrarily small amount. The following algorithm shows the iterative procedure [25]:

```

initialization:  $\Psi^{(0)}, T, l = 0$ ;

repeat
   $i \leftarrow i + 1$ ;
  E-step: compute  $Q(\Psi^{(l)}; \Psi)$ ;
  M-step:  $\Psi^{(l+1)} \leftarrow \arg \max Q(\Psi^{(l)}; \Psi)$ ;
until  $\mathcal{L}(\Psi^{(l+1)}) - \mathcal{L}(\Psi^{(l)}) \geq T$ ;

```

Algorithm 1: Expectation Maximization

Bibliography

- [1] X. Bai, X. Yang, D. Yu, and L.J. Latecki. Skeleton Based Shape Classification Using Path Similarity. *International Journal of Pattern Recognition and Artificial Intelligence*, 22(4):733–746, 2008.
- [2] I. Bloch. On Links Between Mathematical Morphology and Rough Sets. *Pattern Recognition*, 33(9):1487–1496, 2000.
- [3] I. Bloch. Bipolar Fuzzy Mathematical Morphology for Spatial Reasoning. *Mathematical Morphology and Its Application to Signal and Image Processing*, pages 24–34, 2009.
- [4] I. Bloch and H. Maître. Fuzzy Mathematical Morphology. *Annals of Mathematics and Artificial Intelligence*, 10(1):55–84, 1994.
- [5] O. Boiman, E. Shechtman, and M. Irani. In Defense of Nearest Neighbor Based Image Classification. In *Computer Vision and Pattern Recognition, 2008. CVPR 2008. IEEE Conference on*, pages 1–8, 2008.
- [6] M. Borkowski and J.F. Peters. Matching 2D Image Segments with Genetic Algorithms and Approximation Spaces. *Transactions on Rough Sets*, V(LNAI 4100):63–101, 2006.
- [7] A.C. Bovik. *Handbook of Image and Video Processing*. Academic Press, 2005.
- [8] D.S. Broomhead and D. Lowe. Multivariable Functional Interpolation and Adaptive Networks. *Complex Systems*, 2:321–355, 1988.

- [9] T. Caliński and J. Harabasz. A Dendrite Method for Cluster Analysis. *Communications in Statistics-Simulation and Computation*, 3(1):1–27, 1974.
- [10] G. Carneiro, A. B. Chan, P. J. Moreno, and N. Vasconcelos. Supervised Learning of Semantic Classes for Image Annotation and Retrieval. *IEEE Transaction on Pattern Analysis and Machine Intelligence*, 29(3):394–410, 2007.
- [11] C. Carson, S. Belongie, H. Greenspan, and J. Malik. Blobworld: Image Segmentation using Expectation-Maximization and its Application to Image Querying. *IEEE Transactions on Pattern Analysis and Machine Intelligence*, 24:1026–1038, 2002.
- [12] R.H. Chan, C.W. Ho, and M. Nikolova. Salt and Pepper Noise Removal by Median Type Noise Detectors and Detail Preserving Regularization. *IEEE Transaction on Image Processing*, 14(10):1479–1485, 2005.
- [13] C.L. Chang. Fuzzy Topological Spaces. *Journal of Mathematical Analysis and Applications*, 24:182–190, 1968.
- [14] O. Chapelle, P. Haffner, and V. Vapnik. SVMs for Histogram Based Image Classification. *IEEE Transactions on Neural Networks*, 10(5):1055, 1999.
- [15] V. Chatzis and I. Pitas. A Generalized Fuzzy Mathematical Morphology and Its Application in Robust 2-D and 3-D Object Representation. *IEEE Transactions on Image Processing*, 9(10):1798–1810, 2000.
- [16] T. Chen and H.R. Wu. Space Variant Median Filters for the Restoration of Impulse Noise Corrupted Images. *IEEE Transactions on Circuits and Systems II: Analog and Digital Signal Processing*, 48(8):784–789, 2001.
- [17] C.K. Chow. An Optimum Character Recognition System Using Decision Functions. *IRE Transactions on Electronic Computers*, (4):247–254, 1957.
- [18] W.S. Cleveland. Robust Locally Weighted Regression and Smoothing Scatterplots. *Journal of the American Statistical Association*, pages 829–836, 1979.

- [19] D.L. Davies and D.W. Bouldin. A Cluster Separation Measure. *IEEE Transactions on Pattern Analysis and Machine Intelligence*, 1(2):224–227, 1979.
- [20] A.P. Dempster, N.M. Laird, D.B. Rubin, et al. Maximum Likelihood from Incomplete Data via the EM Algorithm. *Journal of the Royal Statistical Society. Series B (Methodological)*, 39(1):1–38, 1977.
- [21] J. Dombi. A General Class of Fuzzy Operators, the DeMorgan Class of Fuzzy Operators and Fuzziness Measures Induced by Fuzzy Operators. *Fuzzy Sets and Systems*, 8(2):149–163, 1982.
- [22] A. Dorado, D. Djordjevic, W. Pedrycz, and E. Izquierdo. Efficient Image Selection for Concept Learning. *IEE Proceedings on Vision, Image and Signal Processing*, 153(3):263 – 273, 8 2006.
- [23] E.R. Dougherty and R.A. Lotufo. *Hands on Morphological Image Processing*, volume 59. Society of Photo Optical, 2003.
- [24] D. Dubois and H.M. Prade. *Fuzzy Sets and Systems: Theory and Applications*. Academic Pr, 1980.
- [25] R.O. Duda, P.E. Hart, and D.G. Stork. *Pattern Classification and Scene Analysis*. Wiley, 2001.
- [26] J.C. Dunn. Well Separated Clusters and Optimal Fuzzy Partitions. *Cybernetics and Systems*, 4(1):95–104, 1974.
- [27] H. Fashandi and J. F. Peters. Mathematical Morphology and Rough Sets. In S. Pal and J. Peters, editors, *Rough Fuzzy Image Analysis. Foundations and Methodologies*, Chapman Hall/CRC Mathematical and Computational Imaging Sciences Series, part 4. CRC Press, Taylor Francis Group, 2010.
- [28] H. Fashandi and J. F. Peters. A Fuzzy Topological Framework for Classifying Image Databases. *International Journal of Intelligent Systems*, 26(7):621–635, 2011.

- [29] H. Fashandi and J.F. Peters. Crisp and Fuzzy Topological Interior and Closure Operators with Inclusion Degree. Theory and Applications. *Fundamenta Informaticae*. to appear.
- [30] H. Fashandi, J.F. Peters, and S. Ramanna. L2 Norm Length Based Image Similarity Measures: Concrescence of Image Feature Histogram Distances. In *Signal and Image Processing, Int. Assoc. of Science & Technology for Development*, pages 178–185, Honolulu, Hawaii, 2009.
- [31] J. Flusser and T. Suk. Rotation Moment Invariants for Recognition of Symmetric Objects. *IEEE Transactions on Image Processing*, 15(12):3784–3790, 2006.
- [32] M.C. Gemignani. *Elementary Topology*. Courier Dover Publications, 1990.
- [33] J.A. Goguen. L-Fuzzy Sets. *Journal of Mathematical Analysis and Applications*, 18:145–174, 1967.
- [34] J.A. Goguen. The Logic of Inexact Concepts. *Synthese*, 19(3):325–373, 1969.
- [35] K.S. Goh, E. Y. Chang, and B. Li. Using One-Class and Two-Class SVMs for Multiclass Image Annotation. *IEEE Transaction on Knowledge and Data Engineering*, 17(10):1333–1346, 2005.
- [36] R.C. Gonzalez and R.E. Woods. *Digital Image Processing*. Prentice-Hall, 2006.
- [37] A. Goshtasby. Description and Discrimination of Planar Shapes using Shape Matrices. *IEEE Transactions on Pattern Analysis and Machine Intelligence*, (6):738–743, 1985.
- [38] J. Goutsias and H. J. A. M. Heijmans. Fundamenta Morphologicae Mathematicae. *Fundamenta Informaticae*, 41(1-2):1–31, 2000.
- [39] V. Gregori and A. Vidal. Gradations of Openness and Chang’s Fuzzy Topologies. *Fuzzy Sets and Systems*, 109(2):233–244, 2000.

- [40] K. Haris, S.N. Efstratiadis, N. Maglaveras, and A.K. Katsaggelos. Hybrid Image Segmentation Using Watersheds and Fast Region Merging. *IEEE Transactions on Image Processing*, 7(12):1684–1699, 1998.
- [41] J.A. Hartigan. *Clustering Algorithms*. Wiley New York, 1975.
- [42] A.E. Hassanien, A. Abraham, J.F. Peters, G. Schaefer, and C Henry. Rough Sets and Near Sets in Medical Imaging: A Review. *IEEE Transaction on Information Technology in Biomedicine*, 13(6):955–968, 2009. doi: 10.1109/TITB.2009.2017017.
- [43] S. Haykin. *Neural Networks: a Comprehensive Foundation*. Prentice Hall, 1999.
- [44] R. N. Hazra, S. K. Samanta, and K. C. Chattopadhyay. Fuzzy topology redefined. *Fuzzy Sets and Systems.*, 45(1):79–82, 1992.
- [45] H.J.A.M. Heijmans. Theoretical Aspects of Gray-Level Morphology. *IEEE Transactions on Pattern Analysis and Machine Intelligence*, 13(6):568–582, 1991.
- [46] H.J.A.M. Heijmans. *Morphological Image Operators*. Academic Press, 1994.
- [47] U. Höhle et al. A General Theory of Fuzzy Topological Spaces. *Fuzzy Sets and Systems*, 73(1):131–149, 1995.
- [48] T. Huang, G. Yang, and G. Tang. A Fast Two Dimensional Median Filtering Algorithm. *IEEE Transactions on Acoustics, Speech and Signal Processing*, 27(1):13–18, 1979.
- [49] H. Hwang and R.A. Haddad. Adaptive Median Filters: New Algorithms and Results. *IEEE Transactions on Image Processing*, 4(4):499–502, 1995.
- [50] J. Järvinen. Set Operations for L-Fuzzy Sets. In Marzena Kryszkiewicz, James Peters, Henryk Rybinski, and Andrzej Skowron, editors, *Rough Sets and Intelligent Systems Paradigms*, volume 4585 of *Lecture Notes in Computer Science*, pages 221–229. Springer Berlin / Heidelberg, 2007.

- [51] K. Kawahara, T. Miyazaki, Y. Shidama, H. Yamaura, and H. Miyao. Fuzzy Image Processing with Topological Theory. In *TENCON'97. IEEE Region 10 Annual Conference. Speech and Image Technologies for Computing and Telecommunications., Proceedings of IEEE*, volume 1, 1997.
- [52] J.L. Kelley. General Topology, Volume 27 of Graduate Texts in Mathematics. 1955.
- [53] J. Kolodner. *Case Based Reasoning*. Morgan Kaufmann Publishers Inc., San Francisco, CA, USA, 1993.
- [54] B. Kosko. Fuzzy Entropy and Conditioning. *Information Sciences*, 40(2):165–174, 1986.
- [55] V. A. Kovalevsky. Finite Topology as Applied to Image Analysis. *Computer Vision, Graphics, and Image Processing*, 46(2):141–161, 1989.
- [56] W.J. Krzanowski and Y.T. Lai. A Criterion for Determining the Number of Groups in a Data Set Using Sum of Squares Clustering. *Biometrics*, 44(1):23–34, 1988.
- [57] L.J. Latecki and R. Lakamper. Shape Similarity Measure based on Correspondence of Visual Parts. *IEEE Transactions on Pattern Analysis and Machine Intelligence*, 22(10):1185 – 1190, oct 2000.
- [58] J. Li and J.Z. Wang. Automatic Linguistic Indexing of Pictures by a Statistical Modeling Approach. *IEEE Transactions on Pattern Analysis and Machine Intelligence*, 25(9):1075–1088, 2003.
- [59] S. X. Liao and M. Pawlak. On the Accuracy of Zernike Moments for Image Analysis. *IEEE Transactions on Pattern Analysis and Machine Intelligence*, 20(12):1358–1364, 1998.
- [60] S.X. Liao. *Image Analysis by Moments*. PhD thesis, University of Manitoba, Winnipeg, Manitoba, Canada, 1993.

- [61] S.X. Liao and M. Pawlak. On Image Analysis by Moments. *IEEE Transactions on Pattern Analysis and Machine Intelligence*, 18(3):254–266, 1996.
- [62] K. Liu and W. Shi. Computing the Fuzzy Topological Relations of Spatial Objects Based on Induced Fuzzy Topology. *International Journal of Geographical Information Science*, 20(8):857–883, 2006.
- [63] Y.M. Liu and M.K. Luo. *Fuzzy Topology, Advances in Fuzzy Systems Applications and Theory Vol. 9*. World Scientific, 1997.
- [64] S. Loncaric. A Survey of Shape Analysis Techniques. *Pattern Recognition*, 31(8):983–1001, 1998.
- [65] R. Lowen. Fuzzy Topological Spaces and Fuzzy Compactness. *Journal of Mathematical Analysis and Applications*, 56(3):621–633, 1976.
- [66] J. MacQueen et al. Some Methods for Classification and Analysis of Multivariate Observations. In *Proceedings of the Fifth Berkeley Symposium on Mathematical Statistics and Probability*, volume 1, page 14. California, USA, 1967.
- [67] G. Matheron. *Random Sets and Integral Geometry*. Wiley New York, 1975.
- [68] G.J. McLachlan and T. Krishnan. *The Em Algorithm and Extensions*. Wiley Series in Probability and Statistics. John Wiley & Sons, 2008.
- [69] G.J. McLachlan and D. Peel. *Finite Mixture Models*. Wiley-Interscience, 2000.
- [70] F. Meyer. Topographic Distance and Watershed Lines. *Signal Processing*, 38(1):113–125, 1994.
- [71] Y. Mingqiang, K. Kidiyo, and R. Joseph. A Survey of Shape Feature Extraction Techniques. In *Pattern Recognition Techniques, Technology and Applications*, volume 35, pages 978–953. I-Tech, Vienna, Austria, 2008.

- [72] T.M. Mitchell. *Machine Learning*. McGraw-Hill Series in Computer Science. McGraw-Hill, 1997.
- [73] F. Mokhtarian and A.K. Mackworth. A Theory of Multiscale, Curvature-based Shape Representation for Planar Curves. *IEEE Transactions on Pattern Analysis and Machine Intelligence*, 14(8):789–805, aug 1992.
- [74] T.K. Mondal and SK Samanta. On Intuitionistic Gradation of Openness. *Fuzzy Sets and Systems*, 131(3):323–336, 2002.
- [75] J. R. Munkres. *Topology*. Prentice Hall, 2000.
- [76] S.A. Naimpally and J.F. Peters. *Topology with Applications. Topological Spaces via Near and Far*. World Scientific, Singapore, 2012. , *in press*.
- [77] M. Nixon and A. Aguado. *Feature Extraction & Image Processing*. Academic Press. Academic, 2008.
- [78] N. Otsu. A Threshold Selection Method from Gray Level Histograms. *Automatica*, 11:285–296, 1975.
- [79] S.K. Pal and J.F. Peters. *Rough Fuzzy Image Analysis. Foundations and Methodologies*. London, UK, CRC Press, Taylor & Francis Group, Sept. 2010. ISBN 13:9781439803295, ISBN 10: 1439803293.
- [80] N. Palaniappan. *Fuzzy Topology*. Alpha Science International, Ltd, 2005.
- [81] E. Pascali and N. Ajmal. Fuzzy Topologies and a Type of Their Decomposition. *Rendiconti di Matematica, Serie VII*, 17:305–328, 1997.
- [82] E.A. Patrick and FP Fischer III. A Generalized k-Nearest Neighbor Rule. *Information and Control*, 16(2):128–152, 1970.
- [83] Z. Pawlak. Classification of objects by means of attributes. *Polish Academy of Sciences*, 429, 1981.

- [84] J.F. Peters and M. Borkowski. K-means Indiscernibility Relation Over Pixels. In S. Tsumoto, R. Slowinski, K. Komorowski, and J.W. Gryzmala-Busse, editors, *Lecture Notes in Computer Science 3066*, pages 580–585. Springer, Berlin, 2004.
- [85] J.F. Peters and S.A. Naimpally. Applications of near sets. *Amer. Math. Soc. Notices*, 59(4):536–542, 2012.
- [86] J.F. Peters and S Ramanna. Affinities Between Perceptual Granules: Foundations and Perspectives. In A. Bargiela and W. Pedrycz, editors, *Human-Centric Information Processing Through Granular Modelling SCI 182*, pages 49–66. Springer-Verlag, Berlin, 2009.
- [87] J.F. Peters and P Wasilewski. Foundations of Near Sets. *Information Sciences. An International Journal*, 179:3091–3109, 2009.
- [88] R.A. Peters et al. A New Algorithm for Image Noise Reduction Using Mathematical Morphology. *IEEE Transactions on Image Processing*, 4(5):554–568, 1995.
- [89] L. Polkowski. Approximate Mathematical Morphology. Rough Set Approach. *Rough Fuzzy Hybridization: A New Trend in Decision-Making*, pages 151–162, 1999.
- [90] M. Powell. Radial Basis Functions for Multivariable Interpolation: A Review. In *Algorithms for Approximation*, pages 143–167. Clarendon Press, 1987.
- [91] X. Qi and Y. Han. Incorporating Multiple SVMs for Automatic Image Annotation. *Pattern Recognition*, 40(2):728–741, 2007.
- [92] A.A. Ramadan, S.E. Abbas, and A.A. Abd El-Latif. Compactness in Intuitionistic Fuzzy Topological Spaces. *International Journal of Mathematics and Mathematical Sciences*, 2005(1):19–32, 2005.
- [93] S. Ramanna. Perceptually Near Pawlak Partitions. *Transactions on Rough Sets*, XII(LNCS 6190):170–192, 2010.

- [94] A. Rosenfeld. *Digital Picture Processing*. Academic Press, New York, 1982.
- [95] E. Şaykol, U. Gudukbay, and O. Ulusoy. A Histogram-based Approach for Object-based Query by Shape and Color in Image and Video Databases. *Image and Vision Computing*, 23(13):1170–1180, 2005.
- [96] T. Sebastian, Philip N. Klein, and B. Kimia. Recognition of Shapes by Editing Shock Graphs. In *Proceedings of 8th IEEE International Conference on Computer Vision, ICCV 2001*, volume 1, pages 755–762, 2001.
- [97] J. Serra. *Image Analysis and Mathematical Morphology*. Academic Press, Inc. Orlando, FL, USA, 1983.
- [98] J. Shi and J. Malik. Normalized Cuts and Image Segmentation. *IEEE Transaction on Pattern Analysis and Machine Intelligence*, pages 888–905, 2000.
- [99] W. Shi, L. Kimfung, and H. Changqing. A Fuzzy Topology-based Area Object Extraction Method. *IEEE transactions on geoscience and remote sensing*, 48(1):147–154, 2010.
- [100] W. Shi and K. Liu. A Fuzzy Topology for Computing the Interior, Boundary, and Exterior of Spatial Objects Quantitatively in GIS. *Computers & Geosciences*, 33(7):898–915, 2007.
- [101] D. Sinha and E. R. Dougherty. Fuzzification of Set Inclusion: Theory and Applications. *Fuzzy Sets and Systems*, 55(1):15–42, 1993.
- [102] A.P. Šostak. On a Fuzzy Topological Structure. *Proceedings of the 13th Winter School on Abstract Analysis*, 1985.
- [103] A.P. Šostak. Two Decades of Fuzzy Topology: Basic Ideas, Notions, and Results. *Russian Mathematical Surveys*, 44(6):125–186, 1989.

- [104] L.A. Steen and J.A. Seebach. *Counter Examples in Topology*. Courier Dover Publications, 1995.
- [105] J. Stell. Relations in Mathematical Morphology with Applications to Graphs and Rough Sets. *Spatial Information Theory*, pages 438–454, 2007.
- [106] M. Sugeno. Fuzzy Measures and Fuzzy Integrals: A Survey. *Fuzzy Automata and Decision Processes*, 78(33):89–102, 1977.
- [107] K.B. Sun and B.J. Super. Classification of Contour Shapes Using Class Segment Sets. In *Computer Vision and Pattern Recognition, 2005. CVPR 2005. IEEE Computer Society Conference on*, volume 2, pages 727–733, 2005.
- [108] Z.G. Sun, J. Chen, and G. Meng. A New Variable Precision Morphological Model for Eliminating Noises of Digital Images. In *Proceedings of the 2008 Congress on Image and Signal Processing*, volume 3 of *CISP '08*, pages 236–240, 2008.
- [109] X. Tang. Spatial Object Modeling in Fuzzy Topological Spaces. *PhD thesis, International Institute for Geo-Information Science and Earth Observation, Enschede, Netherland*, 2004.
- [110] M. Teshnehlab and K. Watanabe. *Intelligent Control based on Flexible Neural Networks*, volume 19. Springer Netherlands, 1999.
- [111] S. Tong and E. Chang. Support Vector Machine Active Learning for Image Retrieval. In *Multimedia '01: Proceedings of the ninth ACM international conference on Multimedia*, pages 107–118, New York, NY, USA, 2001.
- [112] J.W. Tukey. *Exploratory Data Analysis*. Reading, MA, 1977.
- [113] B. Wang, W. Shen, W.-Y. Liu, X.-G. You, and X. Bai. Shape Classification Using Tree-Unions. In *20th International Conference on Pattern Recognition (ICPR)*, pages 983–986, 2010.

- [114] J.Z. Wang, J. Li, and G. Wiederhold. SIMPLiCity: Semantics-Sensitive Integrated Matching for Picture Libraries. *IEEE Transactions on Pattern Analysis and Machine Intelligence*, 23(9):947–963, 2001.
- [115] L.X. Wang. *A Course in Fuzzy Systems and Control*. Prentice-Hall, Inc. Upper Saddle River, NJ, USA, 1996.
- [116] R. Yager. On Ordered Weighted Averaging Aggregation Operators in Multicriteria Decision Making. *IEEE Transactions on Systems, Man and Cybernetics*, 18(1):183–190, 1988.
- [117] X. Yang, X.Bai, D. Yu, and L. J. Latecki. Shape Classification Based on Skeleton Path Similarity. In *Proceedings of the 6th International Conference on Energy Minimization Methods in Computer Vision and Pattern Recognition*, pages 375–386, 2007.
- [118] V. R. Young. Fuzzy Subsethood. *Fuzzy Sets and Systems*, 77(3):371–384, 1996.
- [119] L. A. Zadeh. Fuzzy Sets. *Information and Control*, 8(3):338–353, 1965.
- [120] J. Zhang, F.G. Shi, and C.Y. Zheng. On L-Fuzzy Topological Spaces. *Fuzzy Sets and Systems*, 149(3):473–484, 2005.
- [121] R. Zhang and Z. Zhang. Image Database Classification Based on Concept Vector Model. *IEEE International Conference on Multimedia and Expo*, 0:93–96, 2005.
- [122] W. Ziarko. Variable Precision Rough Set Model. *Journal of Computer and System Sciences*, 46(1):39–59, 1993.

Author Index

- Šostak, A.P., 14, 105
- Aguado, A., 47
Ajmal, N., 23, 24
- Bai, X., 48, 63
Bloch, I., 49, 82
Bouldin, D. W., 68
Bovik, A.C., 93
Broomhead, D.S., 49
- Caliński, T., 68
Carneiro, G., 46
Carson, C., 69
Chan, R.H., 93
Chang, C.L., 14, 21, 31
Chapelle, O., 46
Chen, T., 94
Chow, C.K., 49
Cleveland, W.S., 49
- Davies, D.L., 68
Dempster, A.P., 65
Dombi, J., 17
Dorado, A., 46
Dougherty, E.R., 27, 82, 94
Dubois, D., 17, 27, 107
Duda, R. O., 113
Dunn, J.C., 68
- Fashandi, H., 26, 47, 52, 63, 82
Fischer III, F.P., 49
Flusser, J., 48
- Gemignani, M.C., 8, 36
Goguen, J.A., 14, 27, 28, 107
Gonzalez, R.C., 82, 93
Goshtasby, A., 93
Goutsias, J., 82
Gregori, V., 14
- Harabasz, J., 68
Haris, K., 65
Hartigan, J. A., 69
- Haykin, S., 49
Hazra, R.N, 14
Heijmans, H.J., 82
Huang, T., 94
Hwang, H., 94
- Järvinen, J., 107
- Kawahara, K., 48
Kelley, J., 9
Kolodner, J., 49
Kosko, B., 27, 28
Kovalevsky, V.A., 48
Krzanowski, W.J., 68
- Lai, Y.T., 68
Latckeri, L.J., 48
Li, J., 67, 71, 74
Liao, S.X, 48
Liu, K., 49
Liu, Y.M, 22
Loncaric, S, 93
Lotufo, R.A., 82
Lowe, D., 49
Lowen, R., 14, 104
Luo, M.K., 22
- Macqueen, J., 65, 67
Matheron, G., 1, 49, 82, 83
Mclachlan, G.J., 67, 109
Meyer, F., 65
Mingqiang, Y., 48, 93
Mitchel, T.M., 49
Mokhtarian, F., 48
Mondal T.K., 14
Munkres, J.R., 10
- Naimpally, S., 14
Nixon, S., 47
- Otsu, N., 65
- Pascali, E., 23, 24
Patrick, E.A., 49

Pawlak, M., 48
Pawlak, Z., 103
Peel, D., 109
Peters II, R.A., 94
Peters, J.F., 26, 47, 52, 63, 82
Polkowski, L., 11, 49
Powell, M., 49
Prade, H., 17

Qi, X., 46

Ramanna, S., 47, 52
Rosenfeld, A., 65

Saykol, E., 53, 54
Sebastain, T. B., 60
Seebach, J., 11
Serra, J., 1, 10, 49, 82
Shi, W., 49
Sinha, D., 27
Steen, L., 11
Stell, J., 49
Sugeno, M., 19
Sun, K.B., 48, 63
Sun, Z., 91, 95

Tang, X., 49
Teshnehlal, M., 49
Tong, S., 46
Tukey, J.W., 94

Wang, B., 48, 63
Wang, J.Z., 46, 71
Wang, J.Z., 67
Wang, Lie-Xin, 17
Wasilewski, P., 47
Woods, R.E., 82

Yager, R., 17–19
Yang, X., 48
Young, V.R., 27, 28

Zadeh, L.A., 14, 16, 31
Zhang, F.G., 107
Zhang, R., 46
Zirako, W., 103

Subject Index

- 2D hidden markov model, 46
- algebraic multiplication, 17
- algebraic sum, 16
- angle histogram, 52
- angle of view, 46
- artificial neural network, 48
- associativity, 15, 16
- basis, 10
- Bayesian Classifier, 47
- between classes similarity, 71
- boundary, 1, 11
- boundary condistion, 17
- boundary condition, 15, 16
- case base reasoning, 48
- CBIR, 45
- cellular complexes, 47
- center of mass, 52
- chord distribution, 55
 - chord angle distribution, 55
 - chord length distribution, 55
- classification accuracy, 71
- classifier, 45
- closed fuzzy set, 20
- closed set, 9
- closing, 81
- closure, 1, 11, 22
 - closure operator, 12
- closure operator with inclusion degree, 28
- cluster validation, 66
- cluster validation techniques
 - Calinski-Harabasz index, 67
 - Davis Bouldin index, 66
 - Dunn index, 67
 - Hartigan index, 67
 - Krzonowski-Lai index, 67
- collection of fuzzy sets, 35
- color features, 57
- color image database classification, 62
- color space
 - LUV, 45
 - RGB, 57
- commutativity, 15, 16
- connected component, 50
- content based image retrieval, 45
- continuity, 1
- convergence, 1
- COREL, 68
- COREL 10000 image database, 73
- crisp topology, 7
- decreasing, 13
- degree of openness, 103
- dilation, 80
- discrete topology, 10
- distance histogram, 52
- Dombi class, 16
- Dombi t-norm, 16
- drastic multiplication, 17
- drastic sum, 16
- dual operator, 11
- Dubois-Prade class, 16
- eager learner, 46, 48
- Einstein multiplication, 17
- Einstein sum, 16
- EM, 65
 - refer to *expectation maximization*, 65
 - see *expectation maximization*, 109
- erosion, 80
- Euclidean distance, 52
- Euclidean space, 1, 80
- expectation maximization, 65, 109, 110
- expectaton maximization, 65
- feature extraction, 45, 46, 51
- feature space, 49
- finite fuzzy topology, 47
- finite mixture models, 106
- fts
 - see *Fuzzy topological space*, 20
- fuzzy closure operator, 22

- Lowen's fuzzy closure operator, 102
- fuzzy closure operator with inclusion degree, 31
- fuzzy complement axioms, 17
- fuzzy complement, 18
 - Sugeno class, 18
 - Yager class, 18
- fuzzy interior operator, 22
 - Lowen's fuzzy interior operator, 102
 - Chang's fuzzy interior operator, 23
- fuzzy interior operator with inclusion degree, 30
- fuzzy intersection, 16
- fuzzy s-norm axioms, 15
- fuzzy subethood, 15
- fuzzy topological space, 13
 - Šostak's fuzzy topology, 102
 - Chang's fuzzy topology, 20
 - Goguen's fuzzy topology, 104
 - L-fuzzy topology, 104
 - Lowen's fuzzy topology, 101
- fuzzy union, 15
- fuzzy union axioms, 15

- Gaussian mixture model, 65, 107
- GIS, 48
- GMM, 65

- histogram thresholding, 65

- idempotent, 12
- identifiability, 46
- image category, 43
- image concept, 43
- image database, 44
- image database classification, 2, 43, 44
- image noise, 90
- image segment, 50
- image segmentation, 62
- impulse noise, 90
- inclusion degree, 1
- inclusion measure, 25
 - inclusion measure for crisp sets, 26
- inclusion measure for fuzzy sets, 27
 - Goguen's method, 27
 - inclusion from implication, 27
 - Kosko's method, 27
- increasing, 12
- initialization, 66
- instance based learner, 46, 48
- interior, 1, 11, 22
 - interior operator, 13
- interior fuzzy set, 22
- interior operator with inclusion degree, 28
- invariance, 46
 - occlusion, 46
 - rotation, 46, 52, 55
 - scale, 55
 - scale, 46, 52, 55
 - translation, 52, 55

- k-means, 65, 66
- k-nearest neighbor, 48
- Kimia database, 59
- Kimia image database, 55

- L-fuzzy sets, 13, 104
- lattice theory, 80
- lazy learner, 48
- leave one out method, 61
- likelihood, 65
- locally weighted regression, 48
- log likelihood, 65

- mathematical morphology, 1, 48, 80
 - dilation, 48
 - erosion, 48
- maximum likelihood, 65
- maximum likelihood estimation, 65, 107
- mean square error, 90, 91
- median filter, 92
- membership function, 13
- mixing parameters, 65
- MLE, 65
 - see *maximum likelihood estimation*, 107
- MM
 - see *mathematical morphology*, 48, 80
- monotonicity, 15–17
- morphological dilation with inclusion degree, 86
- morphological erosion with inclusion degree, 87

MSE
 see *means square error*, 90

naive Bayes, 48

nbd
 see *Neighborhood*, 21

nearest neighbor, 46

neighborhood, 1, 9, 21, 47

neighborhood system, 21

noise reduction, 90

noise resistance, 46

normalized inertia, 45

number of clusters, 66

OC
 see *open close sequence*, 92

OCCO
 see *open close close open sequence*, 92

open close open sequence, 92

open close close open sequence with inclusion degree, 93

open close sequence, 92

open close sequence with inclusion degree, 93

open fuzzy set, 20, 49

open set, 9

open-close noise reduction, 92

opening, 81

openness degree, 13

optical character reader, 90

optimum number of clusters, 66

partition topology, 10

peak signal to noise ratio, 90, 91

pixel vector, 52

power set, 7

pruned skeleton, 47

PSNR
 see *peak signal to noise ratio*, 90

quasi fuzzy topology, 101

radial basis function, 48

random functions, 80

region growing, 65

RGB, 57

rotation, 46

rotation invariant, 52

Rough sets, 100

s-norm, 15
 algebraic sum, 16
 Dombi class, 16
 drastic sum, 16
 Dubois-Prade class, 16
 Einstein sum, 16
 Yager class, 16

salt and pepper noise, 90

scale invariant, 52

SE
 see *structuring element*, 80

second moment, 52

semantic image annotation, 45

set theory, 80

shape classification, 2, 46, 57

shape database classification, 43

Shape features
 spatial features, 47

shape features, 47, 51
 angle histogram, 52
 distance histogram, 52
 moments, 47
 polynomial approximation, 47
 scale space methods, 47
 Shape transform domain, 47

shape tree, 47

shapes 216 database, 59

signal to noise ratio, 90, 91

SIMPLIcity image database, 59, 66

SNR
 see *signal to noise ratio*, 90

spatial distribution, 52

structuring element, 80

subspace topology, 10

Sugeno class, 18

support vector machine, 46

t-norm, 16
 algebraic multiplication, 17
 Dombi class, 16

- drastic multiplication, 17
- Dubois-Prade class, 16
- Einstein multiplication, 17
- Yager class, 17
- topological space, 1
- topology, 7, 80
 - discrete topology, 8, 10
 - indiscrete topology, 8
 - partition topology, 10
 - subspace topology, 10
- training instance, 49
- training set, 49
- translation, 46
- translation invariant, 52

- variable percision morphology, 88

- watershed, 65
- within class diversity, 71

- Yager class, 16–18